CA/DOH/AIHL/SP-34

DRY ACID DEPOSITION ON MATERIALS AND VEGETATION: CONCENTRATIONS IN AMBIENT AIR

FINAL REPORT
Prepared for the California Air Resources Board
Interagency Agreement A1-160-32

May, 1985

Walter John, Stephen M. Wall and Joseph L. Ondo
Air and Industrial Hygiene Laboratory
California Department of Health Services
2151 Berkeley Way
Berkeley, California 94704

Submitted to: John Holmes, Ph.D., Chief
Research Division
California Air Resources Board
P. O. Box 2815
Sacramento, California 95812

"The statements and conclusions in this report are those of the contractor and not necessarily those of the California Air Resources Board. The mention of commercial products, their source or their use in connection with material reported herein is not to be construed as either an actual or implied endorsement of such products."

CONTENTS

FIGURES (After page 53.)

TABLES

ABSTRACT

Ambient concentrations of acidic pollutants were measured in West Los Angeles and at Tanbark Flats. Alternative sampling methods for nitric acid, nitrate particles and other species were compared. Combined with data for Martinez, San Jose and the Kern River Canyon, the concentrations have systematic ratios. From these the approximate order of deposition fluxes is (decreasing): NO_x, SO_2, HNO_3 and H^+. The highest nitric acid and particulate strong acid were at Tanbark Flats, a vulnerable area downwind of Los Angeles.

Preliminary aerosol size distributions from a low pressure impactor show NH_4 and SO_4 with similar submicron size distributions but H^+ somewhat smaller. 51% of the nitrate at West L.A. was greater than 2.5 μm. The nitrate deposition velocity from washing leaves of japonicum was 0.22 cm/s at west L.A. and about half that on ovalifolium and a surrogate surface.

Evidence indicated that most of the sulfate on external leaf surfaces was due to SO_2, with a deposition velocity of 0.27 cm/s. Deposition velocities of SO_2 or SO_4 were less than 0.1 cm/s at Tanbark Flats. Exploratory measurements were made with a thin iron film detector for H_2SO_4 droplets and a surrogate Nuclepore "leaf" for SO_2.

I. INTRODUCTION

Significant acidity has been measured in California rain, fog water, atmospheric gases and suspended particles (1-4). Concern over the possible adverse effects from this acid led to the passage of the Kapiloff Acid Deposition Act of 1982, funding the investigation of the problem in California. The present work is part of the research program established by the Kapiloff Act.

The deposition of acidic particles and gases occurs continuously. In the absence of rain, it is called dry deposition. It has been estimated that, in California, considerably more acid is deposited by dry than by wet processes (1). Therefore, it is essential that dry deposition be included in the assessment of the acid impact in California. Unfortunately, this assessment is hampered by a lack of understanding of the details of the mechanisms of dry deposition and an associated lack of reliable methods to measure dry deposition (5).

The measurement techniques currently under study by various investigators can be grouped into three categories:

(1) Ambient concentration measurements coupled with estimated deposition velocities.

The ambient concentration of the species of interest is measured and multiplied by a parameter called the deposition velocity to obtain the deposition flux (7,8). The deposition velocity is taken from the literature, taking into account the topography, ground cover and meteorology.

(2) Micrometeorological techniques.

By modeling dry deposition as a heat or momentum transfer, it can be determined from micrometeorological variables. The gradient method combines the gradient of the pollutant concentration with certain meteorological parameters. The eddy correlation method involves separately sampling when the transport is downward and when it is upward to obtain the net transport to the surface (5).

(3) Collection on surfaces.

Particles may be collected on surrogate surfaces such as Teflon plates, filters or cups for subsequent analysis. Natural surfaces such as leaves may be washed to obtain the deposit.

Each of the above methods has some merits and some drawbacks. The concentration method has the advantage that techniques are available to measure all the pollutants of interest, although not all of the techniques are suitable for routine monitoring. Concentration data can be analyzed for trends and source apportionment. Ambient concentrations are also directly relevant to possible respiratory health effects. The main disadvantage is that the deposition velocities are not measured. This disadvantage might be partially offset by measuring the meteorological parameters upon which the deposition depends and then calculating the deposition velocities, presuming that current efforts to develop suitable theoretical relationships are successful. This approach is being developed (10).

The micrometeorological methods can be applied only if stringent site and atmospheric conditions are satisfied. The gradient technique requires measurement of the pollutant concentration at several heights to within 1%. The eddy correlation technique requires pollutant sensors with a time response of less than one second. It appears that the micrometeorological methods are suitable only for intensive research projects. However, these methods may provide data on deposition velocities needed for the concentration method.

Because particle deposition depends on the details of surface structure, it is difficult to interpret collection on surrogate surfaces. Nevertheless, this very practical method has some proponents (5). Recent work involving the washing of leaves has shown considerable promise (11,12).

On March 26, 1984, the California Air Resources Board Workshop on Dry Deposition was held in South San Francisco, CA. The majority of the prominent investigators from around the nation agreed that the concentration method, coupled with appropriate meteorological measurements, was the most practical approach to the monitoring of

dry acid deposition. A minority believed surface collectors to be important. These opinions paralleled those stated in the earlier U.S.E.P.A. workshop (5).

Program Objectives and Approach

The present report covers Phase II of a multiyear program whose objectives are:

1. To make baseline measurements of dry acid deposition at representative sites in California.

2. To develop measurement techniques suitable for long term monitoring of dry acid deposition.

3. To study the mechanisms of dry deposition in order to provide a better basis for monitoring methods.

Phase I

The ambient concentration method was selected for the development of monitoring techniques for dry acid deposition. All of the major acidic gas and particle species were sampled by methods designed to minimize artifacts, volatilization losses and interferences. Other pollutants and meteorological parameters were monitored. Sampling was conducted at Martinez, San Jose and Democrat Springs (Kern River canyon east of Bakersfield).

The results, which have been reported (4), established baseline values of ambient concentrations of acidic pollutants at these California locations and data on their diurnal variations. Redundant sampling and ion balances confirmed the quantitative accuracy of the sampling techniques.

Phase II

The objectives were to extend the baseline measurements of acidic pollutant concentrations to the important Los Angeles basin, to measure the size distribution of the ambient acidic particles and to explore several new techniques for sampling dry acid.

Acid droplets were detected by the holes they etch in a thin iron film. A new passive sampler (Nuclepore surrogate leaf) for sulfur dioxide, sulfate and nitrate was tested. Potted Ligustrum plants were exposed and the leaves washed for sulfate and nitrate deposits.

Phase III

The objective of this phase, currently underway, is to further develop and validate the techniques explored during Phase II. Additional measurements of acidic particle size distributions will be made and the low pressure impactor tested in the laboratory with the volatile ammonium nitrate. The iron film detector for acid droplets will be calibrated in the laboratory and the effects of sea salt investigated. Further measurements of acidic particle deposition on leaves and a surrogate surface will be made as well as further testing of the Nuclepore surrogate "leaf" for sulfur dioxide detection. Finally, an improved ammonium denuder will be developed.

Report on Phase II

This report presents in separate sections, measurements of ambient concentrations of acidic gases and particles in the South Coast Air Basin, a critique of sampling methodology for acidic pollutants, measurements of strong acid aerosol size distributions and acid deposition on leaves and surrogate surfaces.

II. AMBIENT CONCENTRATIONS OF ACIDIC GASES AND PARTICLES IN THE LOS ANGELES AIR BASIN

Experimental Methods

An AIHL laboratory van housed continuous monitors, a computer data system and facilities for sample processing. Meteorological instruments and samplers were deployed outside. Table 1 summarizes the environmental variables, the samplers or sensors and the methods of analysis. Details were given in our previous report (4). For the present work, monitors for sulfur dioxide and ozone were added. Measurements using several new techniques were made concurrently. These are described in following sections.

The data logger previously used was replaced by a microcomputer system with greater capacity and flexibility (Figure 1). Analog voltages from continuous monitors, meteorological instruments and flow sensors on samplers were input to an Analog Devices uMac-4000 Measurement and Control System which provided signal conditioning, A/D conversion and channel scanning. A command set in the uMac firmware allowed serial readout to an Apple II+ computer. A program was written in Basic to acquire the data in two tiers. Variables such as wind speed, wind direction and gas concentrations were read each minute. All variables were read every ten minutes. All data were recorded on flexible disks. Ten minute readings were displayed on a monitor and printed out. Selected variables were also monitored on an 8-channel chart recorder.

A total of 22 variables were monitored by the computer data system. A precision 5 volt D.C. power supply was connected to channel zero to check the overall accuracy of the system. Drift was typically $\pm$0.001 V over a one week period.

The filter sampling trains are shown schematically in Figure 2. The samplers were operated for periods of approximately 12 hours in order to sample day and night periods separately. Flow rates were set with a rotameter at the beginning of each run and audited at the end of the run.

Two dichotomous samplers provided fine fraction particulate (0-2.5 µm) and coarse fraction particulate (2.5-15 µm). Dichotomous sampler A was a Sierra Model 244 with a 15 µm Wedding inlet; dichotomous sampler B was the same except for the 15 µm Liu inlet. Both were operated with 2 µm pore size Teflon membrane filters.

Sampling Locations and Conditions

West Los Angeles

Sampling was conducted on the the campus of Los Angeles South West College approximately 13 km from the Pacific Coast (Figure 3). The site is downwind of refineries and power plants, major sources of SO_2. The sampling array was located on a largely vacant, paved parking lot near the corner of Imperial St. and Western Ave.

The sampling period, August 9-12, 1983, was preceeded by a tropical rain storm. Afterwards the weather remained hot and humid. The daily midday maximum was about 30°C and the nightly minimum was a warm 20°C; the relative humidity ranged from about 50 to 90% (Figure 5). During the first two daytime periods the wind direction ranged NW to S during the day and was easterly during the night. After 1200, Aug. 11, the winds remained westerly (Figure 7). Wind speeds had a regular pattern from a nightly minimum of 1 - 2 km/hr to an afternoon maximum of about 10 km/hr (Figure 6). Air pollution levels were light to moderate.

Tanbark Flats

Tanbark Flats is located in the mountains northeast of Los Angeles in the San Dimas Experimental Forest. The sampling site was a helicopter pad on a shelf in the side of San Dimas canyon at about 2500 ft. elevation. The site was a clearing surrounded by chapperal and stands of pine trees. A national network (NADP) and an ARB acid rain monitoring site is on the ridge adjacent to the helicopter pad.

Tanbark Flats is a receptor site, with daytime winds carrying pollutants up the canyon from the Los Angeles basin. The sampling period, August 21 - 24, 1983, was preceeded by light rains from a subtropical storm. The following period was clear with a warming trend accompanied by oxidant levels in the L.A. basin which went from low to moderately heavy.

During the sampling period, the wind came steadily from the SW (up canyon) except during 0600 - 0900 hours when it came from the east (Figure 29). The wind speed ranged from less than 4 km/hr at night to about 10 km/hr during the day (Figure 28). Temperatures were moderate during the day and cool at night when the relative humidity was high.

Results

All concentrations have been expressed in terms of equivalents to facilitate direct comparisons. (Equivalent weight = molecular weight/valence). Time series for the measured variables are shown in Figures 4 to 47, grouped by sampling site. NO_x and SO_2 concentrations from the continuous monitors and meteorological variables are

plotted as hourly averages. Because of the large volume of data, a concise summary of the means and ranges of the variables is given in Table 2. For comparison, previous results (4) for Martinez, San Jose and Kern are included. The results for each species are discussed below.

NO_x

Concentrations at West Los Angeles averaged 53 ppb, which was the highest of the five locations sampled. The strong daytime peaks were probably from local traffic as evidenced by the relatively large NO component. At Tanbark, NO_x concentrations were next to the lowest, averaging 15 ppb. The pattern was strongly diurnal with afternoon peaks reflecting transport up the canyon from the L.A. basin. NO_x was primarily NO_2 at Tanbark indicating the absence of local combustion sources.

HNO_3

Peak daytime nitric acid concentration reached 5 ppb at West Los Angeles which is twice the level previously seen in San Jose, another auto emission-dominated urban site. At all sites, the pattern was strongly diurnal with very low nighttime minima. The highest concentrations occured at Tanbark Flats, where daytime levels reached 8 ppb on two consecutive days when ozone exceeded 0.1 ppm. A strong diurnal correlation between nitric acid and ozone was seen at both South Coast Air basin sites as expected from their common dependence on photochemical acitivity. A higher mean nitric acid concentration at Tanbark (2.7 ppb vs 1.7 ppb for West Los Angeles) was associated with a higher average ozone concentration (56 ppb vs. 27 ppb for West Los Angeles) over the 4 day sampling periods.

NO_3

Fine fraction nitrate values were substantially higher at West Los Angeles than any other site, with daytime peaks which sometimes exceeded nitric acid levels. Nighttime levels of nitrate were low. At Tanbark Flats, nitrate concentrations were about half those at Los Angeles, with a strong diurnal variation shaped by the canyon air flow. Again, daytime levels were the highest, but at Tanbark nitrate was consistently less

than half the nitric acid concentration. At night fine nitrate predominated, since nitric acid approached near-zero levels after sundown.

SO_2

Sulfur dioxide concentrations at West L.A. were the highest observed, averaging four times those at Kern, with a diurnal pattern decreasing to about half at night. At Tanbark, SO_2 concentrations, although lower than at West L.A., were still comparable to those at Kern. There was a fairly strong diurnal pattern, with low nighttime values, attributable to a lack of local sources.

SO_4

At West L.A., sulfate concentrations were two to three times those previously seen. The pattern was weakly diurnal. Sulfate levels were lower at Tanbark with not much variation. The dichotomous sampler results indicate that almost all the sulfate was in the fine fraction ($<2.5\mu m$) at West L.A. and at Tanbark.

In Figure 11, the sulfate measured at west L.A. on the prefilters of sampling trains Nos. 1, 2 and 3 are plotted. The close agreement confirms the precision of the flow rates and the sulfate analysis. A similar plot for Tanbark Flats is shown in Figure 33.

Particulate Strong Acid

At West L.A., particulate strong acid concentrations were about double those at Martinez or San Jose and had an irregular time dependence. Tanbark acid levels were the highest seen, nearly twice that at West L.A. There was no diurnal pattern, but a trend upward over the sampling period. Sulfate was the only other species to show a somewhat similar pattern. This suggests that sulfuric acid derivatives were the main components of the particulate strong acid.

NH_4

Ammonium ion concentrations at West Los Angeles and Tanbark Flats were about triple

those at previous locations outside the South Coast Air basin. Daytime peaks occured at both sites but West Los Angeles levels were higher. A strong similarity to sulfate in both concentration and time dependence indicates the presence of ammonium sulfate salts. Ammonium and sulfate diurnal patterns were well correlated at all previous sites as well.

After correction for volatile loss during sampling, a strong diurnal correlation with nitrate suggested the presence of the less stable ammonium nitrate at both South Coast sites.

NH_3

Peak ammonia concentrations at West Los Angeles were slightly higher than at Martinez and much higher than at other locations. At all sites the time dependence was irregular and unrelated to that of any other pollutants. At Tanbark, the ammonia concentrations were lower than at any other site except Kern. Ammonia exceeded ammonium ion concentrations at all sites except Tanbark Flats.

O_3

Ozone peaked daily in the afternoon at West L.A., reaching a maximum of 100 ppb. A strong diurnal pattern was also seen at Tanbark, peaking at 1700-1800 hrs. A maximum of 190 ppb was seen, typical of the high oxidant concentrations seen towards the eastern part of the L.A. basin. Nighttime concentrations were very low.

Particulate Mass

At West L.A., the fine (0-2.5 μm) and coarse (2.5-15 μm) mass fractions were comparable, with no pattern evident. At Tanbark the fine fraction was about twice the coarse with a slight diurnal variation.

Discussion

Ion Balance

In Figure 48, the sum of the major anions, sulfate and nitrate, is plotted vs. the sum of the major cations, ammonium and particulate strong acid, at West L.A. Although the data fit a straight line well (r=0.99), the slope is 0.76 rather than 1.0 and there is a significant positive intercept. Similar ion balance plots for Martinez, San Jose and Kern had unit slopes and zero intercepts, showing that all major ions were accounted for and that the sampling techniques were quantitative.

The major sampling difficulty stems from the volatility of ammonium nitrate. As explained previously (4), our ammonium ion concentrations obtained from the strong acid sampling train are corrected for volatility based on the nitrate data from the parallel nitrate sampling trains. If the present data were plotted without the correction, the slope of the ion balance line would be 1.14 with a nearly zero intercept, i.e., the correction changes the slope from 1.14 to 0.76. Some of the deviation of the slope from unity could be due to an overcorrection. On the basis of previous experience it appears likely that some of the deviation is also due to the presence in the air of ions which were not included in the analysis, e.g. chloride. Moreover, the ion balance obtained from our impactor measurements (Section IV) shows a similar inbalance. Additional negative ions such as Cl could have been contributed by sea salt aerosol due to the coastal location.

Further inland at Tanbark, the ion balance plot (Figure 49) has a slope not significantly different from one, although there is a negative intercept which is marginally significant.

Relative Concentrations

The data for acidic pollutant concentrations can be examined for variations with location. For this purpose, relative concentrations are more useful than absolute concentrations because the relative values are less dependent on atmospheric conditions and general air quality during the sampling period. The present data are based on a limited number of days in the July-September period. The primary pollutants NO_x or SO_2 are the logical choices for normalization variable; pollutant concentrations at each site have been normalized arbitrarily to SO_2 at that site because the resulting spread of the variables is somewhat less than if NO_x were used. Probably NO_x levels are affected by local automobile sources. The relative concentrations are plotted in Figure 50.

For the gases, NO_x has the highest relative concentrations, followed by SO_2 and HNO_3, decreasing by almost an order of magnitude from NO_x to SO_2 and from SO_2 to HNO_3. The mean concentrations lie close to a straight line on the semilog plot. In calculating the mean for HNO_3, the value for Tanbark was excluded as an outlier. For the other four sites, the mean $[HNO_3] / [SO_2]$ was 0.12 $\pm$ 0.01. The standard deviation is remarkably small; there is no obvious explanation for this. The concentration ratio is approx. 7 times higher for Tanbark. Tanbark has unusually high nitric acid levels which is important since it is representative of vulnerable forested mountain areas downwind of the Los Angeles air basin. Pollutants arrive during the day via up-canyon air flows from the Los Angeles basin, an area of high photochemical activity. Kern is also a receptor site, but in a less photochemically active basin and it does not show a high $[HNO_3]/[SO_2]$ ratio. The Kern site has SO_2 sources located at the mouth of the canyon so there is less time for oxidation of SO_2 to SO_4. The $[SO_4]/[SO_2]$ ratios are 0.26 for Kern and 0.69 for Tanbark. The latter is higher than any listed for the U.S. and Canada by Altshuler (22).

The relative concentrations for particulate species decrease in the order SO_4, NO_3 and H^+ (particulate strong acid), where the decrease is less than a factor of 2 from SO_4 to NO_3 and from NO_3 to H^+. The means again lie close to a straight line. The average $[NO_3] / [H^+]$ ratio for Martinez, San Jose and L.A. is 3.7 $\pm$ 0.6 whereas the same ratio averaged over Kern and Tanbark is 0.9$\pm$ 0.1. Again, Kern and Tanbark are both receptor sites, a characteristic evidently favoring high particulate strong acid.

Ammonia has the potential to neutralize the acidic species. The ratio $[NH_3] / [SO_2]$ for all sites except Martinez averages 0.8$\pm$ 0.2. The Martinez sampling site was adjacent to a strong source of ammonia. Thus for most sites, the average ammonia concentration was comparable to that of SO_2, although it should be emphasized that the time dependences are quite different.

Deposition Fluxes

The regularities in the concentrations of the acidic pollutants, evident in Figure 50, make possible some discussion of deposition fluxes, even in the absence of quantitative knowledge of deposition velocities. Deposition velocities for ambient gases are of the order of 1 cm/sec, with most published values varying within a factor of 2 or 3 (7,8).

Deposition velocities for ambient particles are smaller and also more uncertain. The acidic particles are in the 0.1 - 1.0 μm size range (Section IV), i.e., in the minimum of the deposition velocity vs. particle diameter curve. Current theories predict deposition velocities in the range 0.01 - 0.1 cm/sec (33). Some measurements imply higher values, but the evidence is not definitive. For the present discussion, it will be assumed that the deposition velocity for particles is 1/10 that for gases. In Figure 50, the dashed line is the relative concentrations for particles multiplied by 1/10. Then the solid line for gases and the dashed line for particles approximates the relative deposition fluxes. Because of the uncertainties, only orders of magnitude can be considered significant. Within this limitation, the figure shows that deposition fluxes decrease by a factor of 10 successively in going from NO_x to SO_2, HNO_3 and H^+.

The deposition fluxes of the primary pollutants NO_x and SO_2 are higher than those of their secondary products. However, the degree of acidification produced by direct deposition depends upon the complex physical, chemical and biological processes which take place subsequent to deposition on a surface, and is specific to each type of surface. For example, although particulate strong acid has the lowest deposition flux, an acid particle can deliver a concentrated dose, initiating a spot of damage on a surface. Therefore, to further examine the consequences of direct deposition would necessitate focussing on a particular target and would require detailed knowledge of subsequent processes. Nevertheless, because the deposition fluxes of the primary species are much greater than those of the secondary products, it is possible that the acid impact on a particular target is greater from the primary species.

III. CRITIQUE OF SAMPLING METHODOLOGY FOR AMBIENT CONCENTRATIONS OF ACIDIC POLLUTANTS

The many parallel samplers and multiple chemical analyses employed in the present project afford considerable data on sampler performance. It is possible to make quantitative comparisons between the results from the denuder difference method, filter packs and dichotomous samplers. Information was also obtained on the effect of an ammonium denuder on the amount of particulate strong acid sampled.

Nitrogen Compounds

Of all the acidic species, nitrogen compounds present the greatest sampling challenge because of the volatility of ammonium nitrate. In the atmosphere, solid NH_4NO_3 is in equilibrium with its gas phase precursors:

$$NH_3(g) + HNO_3\ (g) \rightleftarrows NH_4NO_3(s)$$

The NH_4NO_3 dissociation constant is affected by temperature, relative humidity and the presence of other chemical species, particularly sulfate. Sampling the aerosol onto a filter can disturb the equilibrium, especially if conditions change over the sampling period.

Denuder Difference Method for NO_3 and HNO_3

The denuder difference method (Figure 2, sampling trains No. 2 and 3) is believed to be the best available method for particulate nitrate and nitric acid (13). The Teflon filter medium minimizes positive artifact from conversion of NO_2 and SO_2 to NO_3 and SO_4, respectively. Volatilized NH_4NO_3 produces HNO_3 which is retained on the the second, Whatman 41 - NaCl filter, thus accounting for negative artifact. The filter assembly alone, referred to as a filter pack, has been used by some investigators (14). The nitrate on the first filter is interpreted as particulate and the nitrate on the second filter as gaseous nitric acid. Volatilization of NH_4NO_3 on the first filter will lead to an overestimate of HNO_3. The magnitude of this error can be derived from a plot of our data from Tanbark and L.A., as shown in Figure 52 and similarly from San Jose and Kern in Figure 51. From the slopes of the regression lines, the overestimates for Tanbark, San Jose and Kern are 17, 18 and 19% respectively, and 56% for West L.A. The earlier intercomparison study at Claremont (in the L.A. basin not far from Tanbark) found filter packs to overestimate HNO_3 by an average of about 16%.

The dichotomous sampler NO_3 is plotted against denuder NO_3 (sampling train No. 2) in Figure 53 for western L.A. and in Figure 54 for Tanbark. At both sites the slopes of the regression lines are not significantly different at the 95% confidence level, indicating that less than half of the nitrate is sampled by a dichotomous sampler.

Another interesting aspect of the dichotomous sampler is revealed by comparing dichotomous sampler nitrate to that on the Teflon filter which is protected by a nitric acid denuder (sampling train No. 2). These data are shown in Figure 55 for western L.A. and in Figure 56 for Tanbark. In both cases the agreement is quite good, implying that most of the HNO_3 is adsorbed onto the surfaces of the dichotomous sampler upstream of the filter. Such affinity of nitric acid for aluminum surfaces is not unexpected; indeed, we have constructed the inlets for sampling train Nos. 1, 2 and 3 from pyrex, the material found to minimize HNO_3 losses. Additionally, the internal surfaces of the cyclones are Teflon coated.

The use of the cyclones with cutpoints of 2.5 μm in sampling trains 2 and 3 prevents the loss of coarse NO_3 particles in the acid denuder. Forrest, et al. (13) found no significant losses of particles smaller than 3 μm in a similar denuder. Such losses would produce a positive error in the HNO_3 measurement by the denuder difference method. Another possible error might be volatilization of ammonium nitrate particles during their passage through the denuder because the equilibrium with HNO_3 is disturbed. However, Forrest, et al., found this error to be negligible in laboratory experiments.

While the denuder difference method is labor-intensive, the foregoing discussion shows that short cuts produce unacceptable errors. Also, at present there are no continuous monitors available which have been proven to have the sensitivity and specificity required for nitric acid sampling. The denuder difference method can be simplified by replacing the filter packs with a single filter of nylon or NaCl-impregnated cellulose. In the present work, the multiple filters afforded the data for evaluation of the alternate methods.

NH_4 Sampling

Ammonium was determined from the Teflon filter on sampling train No. 1, corrected for NH_4NO_3 volatilization by the NO_3 data from the filters of sampling train No. 2. The correction to NH_4 for volatilization is considerably smaller than in the case of NO_3 because only 20 or 30% of the NH_4 is in the form of NH_4NO_3, the remainder being in non-volatile sulfate compounds. This probably accounts for the relatively good agreement of the fine fraction NH_4 from the dichotomous samplers with the corrected NH_4 from the sampling train.

NH_3 Sampling

NH_3 was determined with sampling train No. 5 which utilizes a quartz prefilter to remove particles. Quartz was selected rather than Teflon because it was believed (there is no rigorous justification) that coarse alkaline particles would be deposited nearer the front surface of the filter than the fine NH_4NO_3 particles and thus reduce the interaction of the two types of particles. Alkaline conditions could release artifact ammonia from the NH_4NO_3 particles. In most but not all cases the resulting error is not serious since ambient NH_3 levels tend to be considerably higher than the upper limit of the artifact ammonia.

The oxalic acid-impregnated filters were changed in a glove box under an Argon atmosphere to prevent contamination by ambient ammonia. This cumbersome handling procedure is time-consuming but necessary to ensure low and reproducible blank levels.

A denuder difference method for ammonia would be artifact-free. This could be accomplished by adding to sampling train No. 1 a NaCl-Whatman 41 filter followed by a pair of oxalic acid-impregnated glass fiber filters and adding a pair of the oxalic acid filters to sampling train No. 3. Sampling train No. 5 would be eliminated. As discussed in the preceeding section, precautions would have to be taken to ensure that the Teflon filter used for particulate strong acid analysis would not be contaminated with oxalic acid.

The continuous monitor for nitrogen gases (Teco 14T) has an ammonia channel. However, no useful data were obtained because the low concentrations encountered require more rigorous calibration and intensive care than was possible to provide.

Dissociation Constant

The theory of the dissociation of ammonium nitrate provides a basis for understanding the observed concentrations of nitrogen compounds and emphasizes the importance of accounting for volatility losses in sampling. The dissociation constant is quite sensitive to temperature and also, above the deliquescence point, to relative humidity. Figure 57 shows the dissociation constant for pure NH_4NO_3 predicted by Stelson, et al. (16). A complication is that the presence of other ions, i.e. SO_4, is expected to depress the dissociation constant from that of pure NH_4NO_3.

In Figure 57, measured values of the product $[NH_3]$ $[HNO_3]$ are shown for West Los Angeles and Tanbark Flats. The points naturally cluster into daytime and nighttime regimes. Most of the points are in agreement with theory; the most notable exceptions are two 12^oC points near 90% R.H. Time series plots of the dissociation constant are shown in Figures 58 and 59.

Near-quantitative agreement with the calculated dissociation constant has also been reported by Hildeman, et al. (15), for sites in the South Coast Air Basin. At humidities above the deliquescence point agreement is <u>not</u> expected, since in solution SO_4 should depress the dissociation. At both L.A. and Tanbark the dissociation constant should have been depressed by about a factor of 5 according to theory. Instead most of the points agree, within experimental error, with the equilibrum value; moreover, the two points in disagreement lie well above, not below the calculated value. These shortcomings of the theory have been noted before by Stelson (16).

It is instructive to examine the concentrations of NH_3 and HNO_3 at West Los Angeles and Tanbark, plotted in Figures 60 and 61. If the NH_3 and HNO_3 were due solely to dissociation of NH_4NO_3, the concentrations of the two gases would be equal. At Western L.A., NH_3 concentrations far exceed those of HNO_3, while the two are more comparable at Tanbark Flats. Thus at Western L.A., NH_3 from local sources suppresses the dissociation of NH_4NO_3 and hence the concentration of HNO_3. Additionally, the oxidation of NO_2 to HNO_3 has less time to proceed than in the eastern end of the Air Basin where Tanbark is located. At Tanbark these factors act to enhance the HNO_3 level, as observed. In the absence of significant local NH_3 sources, HNO_3 dominates the daytime dissociation. Since HNO_3 is a pollutant of great concern for acid deposition, these effects have serious implications for receptor sites like Tanbark Flats.

Sampling artifacts produced during daylight hours are largely responsible for the disagreements between methods for nitrogen compounds. This is consistent with the greater dissociation during the day as shown in Figures 60 and 61. At Western L.A., the average temperature was 8^oC higher than at Tanbark, which can account for the significantly poorer performance of the filter pack for HNO_3 at this site.

Nighttime conditions of lower temperature and higher humidity depress dissociation, reducing the magnitude of sampling artifacts. Consequently the agreement between nitric acid determined by filter pack and by denuder difference method is substantially better for nighttime values, which are clustered near the origin in Figure 57. Similar conditions which could suppress artifact formation exist during winter months.

Particulate Strong Acid - Ammonia Denuder

The purpose of the ammonia denuder (sampling train No. 1, Figure 2) is to prevent neutralization of the particulate strong acid which has been collected on the filter by ambient ammonia. Previously, in the laboratory, the ammonia denuder was shown to have an efficiency > 96% for concentrations as low as 16 ppb. The functioning of the denuder in the field can be examined by comparison of the particulate strong acid measured without the denuder (sampling train No. 3, Teflon filter) to that measured with the denuder (sampling train No. 1). The (no denuder)/(ammonia denuder) particulate strong acid ratio was calculated for all five locations sampled. The weighted average is 0.98 ± 0.02.

The data were further examined by plotting regressions of the above ratio minus one vs. the ammonia concentration. If the denuder were affecting the results, a negative slop would be expected. Instead, only the plot for Kern, where the ammonia concentrations were low, showed a significant negative slope.

A visual comparison between the particulate strong acid values measured at West L.A. on the prefilters of sampling train Nos. 1, 2 and 3 is afforded by Figure 10. It is apparent that the points from the ammonia denuder-protected filter are not significantly higher than the others. A similar conclusion is reached for the measurements at Tanbark Flats, shown in Figure 32.

It is therefore concluded that the ammonia denuder had little effect during the sampling at the five locations with ammonia levels ranging up to about 1000 nequiv/m^3. The ammonia denuder is very labor-intensive to prepare and to operate. At the western L.A. site, a severe problem developed because of the high ambient relative humidity. Sufficient moisture collected in some of the tubes to create a blockage, necessitating frequent changes of phosphorous acid coated denuder tubes. The concern is that

bursting bubbles could create an acid aerosol capable of contaminating the filter. However, in that event, the phosphorous acid would deposit phosphate on the filter. Such phosphate was not detected in the ion chromatograms.

The foregoing suggests that unless ambient ammonia levels are unusually high, it is not necessary to use an ammonia denuder. If it were necessary, a denuder which is less hygroscopic would be desirable.

The sampling data provide another informative comparison, namely that between the particulate strong acid sampled without a denuder (sampling train No. 3) to that sampled with an acid denuder (sampling train No. 2). For the five locations, the weighted average for the ratio (no denuder)/(acid denuder) particulate strong acid is 1.12 ± 0.01. This result suggests that gaseous acid (probably nitric acid) is deposited on the Teflon filter and titrated with the particulate acid. This would presumably also occur on sampling train No. 1, producing an overestimate of particulate strong acid. The magnitude of the potential error would not be serious in most cases, averaging less than 20%.

IV. STRONG ACID AEROSOL SIZE DISTRIBUTIONS IN THE LOS ANGELES AIR BASIN

Dry deposition is difficult to measure directly in a manner representative of the large variety of natural surfaces (5). Direct measurement of acid aerosol deposition is subject to the additional problems of interferences from the adsorption of acid and basic gases and neutralization by alkaline soil particles. Estimation of acid particle deposition flux can be made from a knowledge of deposition velocities and particulate strong acid concentrations near ground level. Since deposition velocity is a strong function of particle size (8), the acidic particle size distribution must be measured. The size distribution of acidic particles is not known, except that they are predominately in the fine fraction.

Preliminary measurements have been made using a new low pressure cascade impactor from the University of Vienna. Sufficient sample was obtained in the Los Angeles basin to allow acid micro-titration and chemical analysis of major ions on each stage.

Experimental Methods

The size selective aerosol sampling system employed for all measurements is shown in Figure 62. The Berner low pressure impactor (17) was preceeded by an ammonia denuder and a cyclone. The sampler inlet was 1.3 meters above ground level, and the connection pipes were 50 mm ID Pyrex. Acidic particles collected were protected from ammonia neutralization by the denuder and from alkaline soil particles by the cyclone. The cyclone was developed at AIHL (18) and is Teflon coated on the internal surfaces. Operated at the impactor flow rate of 26 L/min, the cyclone provided a 50% cutpoint of 2.1 μm to exclude coarse alkaline soil particles which could bounce through to the submicron impactor stages. The ammonia denuder consisted of multiple glass tubes in parallel which were coated inside with phosphorus acid. The denuder efficiency was designed to be 99.9% based on the Gormley-Kennedy diffusion equation (19) and a diffusion coefficient of 2.36×10^{-5} m^2/sec for ammonia (20). Laboratory evaluations using a permeation tube to generate ammonia concentrations less than 16 ppb showed acceptable removal efficiencies of greater than 96%.

The aerosol impactor was designed to collect particles in evenly spaced logarithmic size intervals over the range 0.06 to 16 μm as shown in Table 3. The cyclone inlet restricted the impactor deposits to the five reduced pressure stages which encompass the submicron size range. Each impaction stage consists of a ring of equally spaced acceleration nozzles, and a circular impaction surface with a central hole to allow passage of uncollected particles to the next stage. This design minimizes wall losses and the possibility of particle bounce contaminating subsequent stage deposits. The impaction stages were covered with a 0.05 mm thick Tedlar foil, which provided a flat, rigid and chemically inert collection substrate. Clean Tedlar foils were kept under inert argon atmosphere and exposed foils were immediately transferred to individual containers for storage under dry ice.

Impactor samples were removed from dry ice storage just prior to extraction in 40 ml polypropylene centrifuge tubes. The extraction volume was minimized by curling the foil to lie flat against the interior surface of the centrifuge tube. Samples could then be extracted in only 5 ml of double glass-distilled water which was continuously washed over the foil deposit by axial rotation of the tubes in a circular rack for one hour. Recovery of all major cation and anions by this extraction method was determined

to exceed 98%. All sample preparation and extraction was performed under inert argon atmosphere to inhibit ammonia contamination.

The same water extracts were used for all the chemical analysis to maximize analytical sensitivity. Analysis for strong acid and ammonia were performed immediately after extraction. Nitrate and sulfate were sufficiently stable under refrigerated storage to allow analysis the next day. Strong acid was determined by microtration under Argon atmosphere employing an Autoburette AB12 (Radiometer of Denmark). Gran's plots (21) of hydrogen ion concentration against the volume of titrant (NaOH) added were used to distinguish strong acid ($PK_a < 4$) from weaker organic acids. Extrapolation of the linear portion of the curve to the base line provided a means for quantifying the strong acid present. The acid determination limit was 0.2 µg/ml (as H_2SO_4) with a reproducibility of 10%.

Extracts were analyzed for ammonia under Argon by specific ion electrode. A determination limit of 0.2 µg/ml was achieved with a reproducibility of 20%. Nitrate and sulfate analysis by ion chromatography (Dionex) provided a determination limit of 0.5 µg/ml and reproducibility of 10%. Based on 24 hours of sampling at 26 L/min the determination limits in nequiv/m^3 were: strong acid 0.5, ammonium 3, sulfate 0.6 and nitrate 1.

Sampling periods of several days were required to collect sufficient sample for strong acid determinations on each impactor stage. Sampling was conducted during August 1983 at the sites in West Los Angeles and Tanbark Flats (see Section II).

Experimental Results

Particle size distributions for Los Angeles during the period August 9-12, 1983 are shown in Figure 63 and at Tanbark Flats for the period August 21-25, 1983 in Figure 64. All concentrations are expressed in terms of equivalents to allow direct comparisons between chemical species (equivalent weight = molecular weight/valence). Size distributions have been plotted as the concentration determined for each stage normalized by the logarithm of the particle size range collected.

Size Distributions

At both sampling sites the size distribution of strong acid was much different than that for sulfate, which would preclude the estimation of acid particle size or concentration from the more easily obtainable sulfate measurements. Sulfate consistently peaked on impactor stage 4 with mean diameter 0.71 μm while strong acid was distributed toward smaller particle size. The very strong correlation in size distribution for ammonium and sulfate ions is consistent with the presence of ammonium sulfate salts. Levels of ammonium, sulfate and nitrate were significantly higher at the coastal, source-dominated Los Angeles site; however, the highest strong acid levels were observed further inland at Tanbark Flats. At Los Angeles, the mass median diameter (MMD) for strong acid (0.27 - 0.45 μm) and sulfate (0.31 - 0.47 μm) were similar, while the strong acid MMD (0.23 μm) was significantly less than sulfate (0.30 - 0.38 μm) at Tanbark Flats.

A nitrate peak was absent in the submicron range, except for the first sampling period at Tanbark Flats which was preceeded by a summer rain storm. For the remaining sampling episodes, nitrate concentration increased with particle size with a peak diameter greater than 1 μm. This is consistent with the data from the denuder sampling train for fine nitrate and the dichotomous sampler for coarse nitrate, which show that 51% of the nitrate at West L.A. and 40% at Tanbark Flats was above 2.5 μm (see discussion in Section V.).

In Figure 65, the sum of the anions sulfate and nitrate on each impactor stage is plotted vs. the sum of the cations, particulate strong acid and ammonium for each sampling period at both sampling locations. The Stage numbers correspond to those given in Table 3. If ionic balance was obtained, the points would lie along a 45^{o} line through the origin. This provides an indication of whether the major ionic species have been determined. An ion balance was most closely approached at Tanbark Flats, the more inland site. The intercepts of the regression lines are not significantly different from zero at the 95% confidence limit and the slopes differ from unity by less than the error in the measurements. Failure to achieve as complete an ion balance on many of the impactor stages for Los Angeles samples has no definite explanation. The western Los Angeles site represents a multiplicity of strong, nearby sources and

a background of marine aerosol which could have contributed an unaccounted for anion, perhaps chloride.

Strong Acid Distributions

Particulate acid size distributions, plotted from concentrations determined on each impactor stage, are shown in Figure 66. All distributions were broad and reached a maximum on the third impactor stage (mean diameter 0.35 μm) with one exception at Los Angeles which was displaced toward larger particle size (0.71 μm). Submicron strong acid levels were somewhat higher at Tanbark Flats. The total strong acid as the sum of the levels on the impactor stages ranged from 0.6 to 0.9 $\mu g/m^3$ (as H_2SO_4) at Los Angeles and 1.2 to 1.4 $\mu g/m^3$ at Tanbark Flats.

These results must be considered preliminary since the reduced pressure on the last three stages of the impactor increases the possibility of volatility losses of ammonium nitrate and an undersizing of the particles. A potential for particle growth also exists due to the temperature drop from the jet expansion, which could condense moisture on the particles. There is presently insufficient knowledge of these effects to permit reliable estimates of their magnitudes. We have laboratory experiments underway to investigate these effects.

V. ACID DEPOSITION ON SURFACES

Measurement of Acid Droplets with Thin Iron Film Detectors

The direct measurement of acidic particle deposition on surfaces avoids the difficulties associated with the determination of deposition velocities. A reaction spot technique employing thin metal films is under development for this purpose. The Thin Film Acid Detector is an extension of laboratory work elsewhere which demonstrated that micron size sulfuric acid droplets etch into a thin layer of iron on glass producing a hole representative of the size of the airborne droplet (34). During August 1983, iron films were exposed to ambient air at the West Los Angeles site for one to two day periods as a feasibility study.

Film preparation

The iron film was vacuum-evaporated onto formvar-coated electron microscope finder grids, 3 mm in diameter, from ultra-pure iron wire (99.999%). Specially prepared ceramic-coated tungsten filaments and a carefully controlled heating procedure were used to produce a homogeneous film. Film thickness was monitored with a piezoceramic mass loading detector calibrated for deposited Fe by X-ray fluorescence. Optimum coatings were 10 nm thick, providing the best morphological identification of acid droplet reaction sites.

Films were stored in a desiccator under Argon before and after exposures. Exposed films stored for periods exceeding one year show no apparent changes in the reaction site.

Exposures

The films, supported on 3 mm electron microscope grids, were mounted on a 10 cm diameter, 3 mm thick Delrin disk mounted horizontally at elevations of 2-3 meters. Delrin is a rigid fluorocarbon which can be machined flat without the warpage problem inherent with Teflon. The disk edges were rounded and the films mounted 2 cm from the edge to reduce artifact turbulent deposition.

Analysis

Reaction spots were formed in sufficient surface concentration for automated scanning electron microscope (ASEM) analysis, which was capable of locating and sizing the etched holes under computer control. This was carried out in the AIHL Center for Automatic Particle Analysis. Figure 67 shows the dark circular reaction spots which could be easily distinguished from defects in the thin film which appear as linear cracks. The presence of an acid-etched reaction spot was confirmed by the detection of sulfur in the X-ray fluorescence spectrum, which was automatically acquired for each canidate reaction site. A preliminary site distribution for the acid is shown in Figure 68.

Method Assessment and Future Development

The feasibility of detecting reaction sites with thin films has been demonstrated for urban exposures of 24 hours. Laboratory studies are currently under way to determine a transforming factor to equate reaction spot size and airborne submicron sulfuric acid droplet diameter. Previous work elsewhere has demonstrated that, unlike other metallic films, Fe has the advantage of a constant transformation factor for most droplet acid levels (34). Acid droplet diameters as small as 0.06 μm have been detected with Fe films (35).

A potential interferent in the method could be NaCl aerosol, which might attack the Fe surfaces. Reaction spots involving chloride can be automatically identified from their X-ray fluorescence spectrum during ASEM analysis. However, it will be necessary to use laboratory-generated NaCl aerosol to assess the full extent of the problem.

Deposition of Acidic Particles and Gases on External Surfaces of Leaves and a Surrogate Surface

Deposition of acidic particles and gases onto the exterior surfaces of leaves can be measured by washing off the deposit and analyzing the extract. This direct measurement automatically includes the effects of micrometeorology and the surface structure of the leaves. If the ambient concentrations of the acidic pollutants are measured simultaneously, deposition velocities can be obtained. We have chosen to use Ligustrum, an ornamental shrub, following promising results reported by Sickles, et al. (12). These plants can be transported in pots, making possible measurements of deposition onto the same plants at different locations.

Ligustrum is an ornamental shrub of the olive family. We have used two species, L. ovalifolium - the California privet, and L. japonicum - the Japanese or waxleaf privet. Both are small, hardy shrubs which grow well in 19 liter pots. The leaves, which range in length from 2 to 7 cm, have stomata presented on their lower surfaces. The japonicum leaf is slightly larger than that of the ovalifolium and has a waxy surface.

The interior of the Ligustrum leaves contain large amounts of sulfate and nitrate, making it impossible to determine the uptake of these materials through the stomata.

To obtain information on the stomatal uptake, we have developed a surrogate "leaf", which is discussed in the next section. The outer surfaces of the surrogate leaf were extracted to obtain the exterior deposit for comparison of the surrogate surface to that of Ligustrum.

Experimental Methods

For each exposure three plants of each species are first washed well with tap water then glass-distilled water. A given number of leaves, usually eight from each plant, are harvested from random locations for controls. At the end of the exposure eight more leaves from each plant are harvested, samples and controls are immediately extracted in 50 mL of glass-distilled water by gentle agitation for one minute, then the water is poured off into a glass flask for transportation to the lab. The leaves are dried, then photocopied to determine their area. The extract, after filtration, can be directly analyzed by ion chromatography for sulfate and nitrate. Normalized to leaf area, the detection limits were 0.1 $\mu g/cm^2$ SO_4 and 0.02 $\mu g/cm^2$ NO_3. Extracts above the detection limit had an accuracy of 10%.

Others have extracted the leaves in water from 3 to 30 minutes (32). We have found that most of the particulate deposit is extracted in the first minute (Figure 69). Extended extraction produced no appreciable increase in sulfate or nitrate, indicating that there was no leaching of material from the interior. Extracts of crushed leaves showed sulfate and nitrate concentrations ten to fifty times greater. An experiment was done in Berkeley to see if any of the interior material was extracted through the stomatal pores. The plants were covered with either clear or dark plastic bags then flushed with carbon dioxide (3% in air) for thirty minutes. This should have the effect of tightly closing the stomata (28). As can be seen from Figure 70, there was no significant differences in extracted concentrations between the four conditions. It should also be noted that the leaves of the japonicum collected particles at approximately twice the rate as of the ovalifolium. This may be due to the waxy surface of the japonicum leaf, which, under the microscope, has a rougher appearance than that of ovalifolium.

Field experiments at Western Los Angeles and Tanbark Flats

In August, 1983, exposures were made at two sites in the South Coast Air Basin during sampling for acidic particles and gases (see Section II). The Ligustrum and the surrogate leaves were put out for four days of sampling at each site. The surrogate leaves were held on ring stands with surfaces horizontal approximately 50 cm above the ground. At the Western Los Angeles site, the Ligustrum plants and surrogate leaves were placed next to a low hedge on the edge of a grass lawn adjacent to the parking lot where the sampling trains were located. At Tanbark, the Ligustrum and surrogate leaves were placed on the edge of the sampling site amongst some natural plants of roughly the same height. Additional surrogate leaves were placed in nearby Pine and Cypress canopies, affixed to trees at about 2 meters above the ground.

The Ligustrum leaves were washed, then eight leaves were picked from each plant as controls. Eight leaves were harvested after one to four days. All extract solutions were refrigerated until analysis. The surrogate leaves of 8 μm pore size were put out in duplicate sets, with one set being left out for two days and another for four days. When these leaves were "harvested" they were taken into the mobile lab and split apart. The component parts (Figure 72) were put into separate tubes and placed on dry ice until analysis. A control set of leaves were charged with water and placed in a desiccator flushed with dry Argon as blanks.

Results

Comparison of the extracts from exposures of varying duration (Table 4) reveals considerable deviations from proportionality to exposure time. Part of the deviation may be due to varying airborne concentrations and atmospheric conditions, but most of it is probably attributable to the relatively small deposits. Further discussion will be based on the four day results (Figure 71) which should be the most reliable.

The entries of Table 4 were obtained by dividing the extract (including both top and bottom surfaces) by twice the area of one side. The values obtained are thus the average of the fluxes to both sides. For the surrogate leaf only, it was possible to extract the top and bottom separately. At Western L.A., in four day exposures, the nitrate flux to the top surface was eight times that to the bottom. By contrast,

essentially all of the sulfate was found on the top surface. At Tanbark Flats, the nitrate flux to the top surface was twice that to the bottom. No sulfate was detectable on top or bottom. Presumably the deposition fluxes to the real leaves were also much greater to the top than to the bottom surfaces. In that case, the deposition velocities to the top surfaces would be nearly double the average values listed in the following section.

NO_3 Deposition

Deposition velocities were computed for the nitrate deposits, assuming it to be mainly due to particles. For the airborne concentrations the denuder NO_3 was used for the fine (< 2.5 μm) fraction and the dichotomous sampler coarse NO_3 (> 2.5 μm) for the coarse fraction. While the fine fraction includes the correction for NH_4NO_3 volatility, no direct data is available to make a correction for coarse nitrate. However, coarse nitrate is expected to be associated with compounds of low volatility. On this basis, the fine NO_3 at western Los Angeles was 49% of the total and 60% at Tanbark.

The calculated deposition velocities for NO_3 particles are listed in Table 5. The results for the two sites are remarkably close. The deposition velocity on japonicum is about twice that on ovalifolium, as seen previously in Berkeley. Deposition velocities for the surrogate surface are about the same as ovalifolium.

Deposition velocities on the surrogate surfaces in the Pine and Cypress canopies are comparable or smaller than those in the clearing, but are based on limited data.

It is necessary to consider the possibility that NO_x might deposit on the surfaces. The total NO_3 to NO_x ratio at Western L.A. was 0.09 and at Tanbark 0.11. Since these ratios are nearly equal the dependence of the deposition with location cannot be used to detect NO_x deposition. However, if NO_x deposition were appreciable, one would expect considerably higher deposition on the natural leaves than on the surrogate surface because of the larger effective surface areas on the leaves due to microstructure. We conclude that there is no evidence for deposition of NO_x. Nitric acid is another gaseous species to be considered. The ratio of the measured flux of nitrate to L. japonicum at L.A. to that at Tanbark was 2.5. The ratio of total nitrate concentrations (L.A./Tanbark) was 2.8. The ratio of nitric acid concentrations (L.A./Tanbark) was

0.6. This implies that most of the deposition was due to nitrate. HNO_3 deposition would be expected to increase the deposition velocities on natural leaves relative to the surrogate surface, but this is not observed. Deposition of nitrate was considerably greater on the top of the surrogate leaf than on the bottom. This also favors nitrate particle deposition over gaseous nitric acid. However, the top to bottom ratio was less at Tanbark Flats where nitric acid had high concentrations which suggests some nitric acid deposition. To summarize, the evidence favors the interpretation that particulate nitrate accounted for most of the deposition, but it is not possible to rule out some contribution from nitric acid.

The nitrate deposition velocities are somewhat higher than the 0.1 cm/sec maximum theoretically predicted value for submicron particles. However, since the nitrate particles have a substantial fraction above one micron, the deposition velocities appear to be reasonable due to the rapid increase with particle size above one micron.

Sulfur Deposition

There is strong evidence based on the present data that SO_2 deposition occurs as well as SO_4 particle deposition. For example, if the deposition velocities to japonicum were calculated considering SO_4 particle deposition only, the results would be 1.25 cm/sec for West L.A. and 0.14 cm/sec for Tanbark Flats. These values are unreasonable, first, because they are very different for the two sites whereas this is not the case for NO_3 particles and second, the value for Western L.A. is much larger than that for nitrate particles. The reverse is expected from the particle size distributions. As discussed previously, the NO_3 particles have a significant coarse fraction. By contrast, at Western L.A., 81% of the SO_4 particle mass is in the fine fraction and at Tanbark Flats 90% is in the fine fraction.

The flux of sulfur to the surrogate surface is much less than that to the Ligustrum leaves (Table 4). The larger effective surface area of the natural leaves would adsorb more SO_2. The natural leaves would also be expected to collect more sulfate particles, but probably not by such a large factor.

At each site, the flux to a surface is given by:

(1) $C_p v_p + C_G v_G = F$

where C_p and C_G are the airborne concentrations of SO_4 particles and SO_2 gas, respectively. v_p and v_G are the deposition velocities of particles and gas respectively, and F is the total sulfur flux to the surface. At Tanbark, Equation (1) reduces to:

(2) $4.56\ v_p + 6.58\ v_G = 0.65$

where v_p and v_G are in units of cm/sec. Applying the condition that v_p and v_G must be positive, equation (2) yields the conditions:

$0 \leq v_p \leq 0.14$ cm/sec, $0 \leq v_G \leq 0.10$ cm/sec. The upper limits are equivalent to assuming that all of the flux is due solely to particles or gas. Even though it is not possible to obtain separate deposition velocities, the upper limits are small enough to constitute important information.

The equation for the deposition velocities at West L.A. is:

(3) $6.24\ v_p + 2.61\ v_G = 7.77$

Here the relatively high $[SO_2]$ to $[SO_4]$ ratio requires a different approach. We will arbitrarily set $v_p = 0.1$ cm/sec, a value near the upper theoretical limit for submicron particles. Then from Equation (3), $v_G = 0.27$ cm/sec. This value is near the upper limit of 0.30 cm/sec which results from attributing all of the sulfur flux to SO_2.

The calculations were repeated for the other surfaces and tabulated in Table 6. The deposition velocity for SO_2 at West L.A. on ovalifolium is nearly the same as on japonicum and much less on the surrogate surface. The surrogate surface is Tedlar, chemically similar to Teflon which has low affinity for SO_2, also, the Tedlar is very slightly acidic.

To reiterate, the requirement that the SO_4 particle deposition velocity be of the order of 0.1 cm/sec implies that SO_2 has a deposition velocity of about 0.3

cm/sec on Ligustrum leaves at the West L.A. site. It is likely that the humid conditions during the sampling period were conducive to SO_2 deposition to the external surfaces of the leaves. Although it has been suggested before that SO_2 might deposit on external surfaces of leaves, we are unaware of any data on the deposition velocity. Experiments with various surrogate surfaces have suggested that SO_2 deposition is significant, particularly to glass fiber filters (23).

Passive Sampling of Sulfur Dioxide with a Surrogate Nuclepore "Leaf"

Sulfur dioxide is very important to the understanding of injury to plants by air pollution because the stomata openings enlarge in the presence of a low concentration of sulfur dioxide, allowing the uptake of harmful gases or bacterial and fungal agents (29).

A surrogate leaf has been constructed with a Nuclepore filter membrane simulating the stomatal openings of a leaf. Nuclepore filters consist of polycarbonate film with circular pores penetrating straight through the plastic. A moist filter is placed inside the "leaf" to absorb sulfur dioxide and other acidic gases diffusing through the Nuclepore pores. After exposure the exterior surfaces are washed to extract any dry particulate, and the interior filter is analyzed for dissolved acidic gases. The "leaf" is small enough to be placed in the canopy in field studies. An advantage of the surrogate leaf is that it is a dynamic system. The evaporation of water out of the leaf and the diffusion of gases into the leaf simulate the respiration and transpiration which occur in the natural leaf.

A 2 x 2 inch plastic film slide holder is attached by a short tube to a water reservoir. The "leaf" is a sandwich (Figure 72) contained in the slide holder consisting of, from top to bottom, Tedlar film, aluminum foil (as a sun screen), Tedlar film, cellulose filter (with a wick to a water reservoir), Teflon screen (with 0.4 mm openings, to keep the Nuclepore filter from wetting) and the Nuclepore filter membrane. The wick of cellulose filter passes through a short Teflon tube and into the reservoir which is filled with glass-distilled water. The whole unit is sealed with the only opening to ambient air being through the pores in the Nuclepore filter. Care had to be taken to use only inert material in the construction of the leaf. In earlier models there was a

contamination problem due to nitrates and sulfates absorbed on black rubber stoppers which are now no longer used.

A reservoir of water is necessary to keep the interior of the "leaf" moist. At first we tried using various buffer systems to approximate the conditions in the interior of natural leaves, but this was dropped in favor of glass-distilled water. The main problem with buffers was that as evaporation took place at the surface of the Nuclepore filter, the buffer salts would encrust on the filter and block the pores. Distilled water presents no such problem. Also distilled water, in equilibrium with CO_2, has a pH of approximately 5.6, which is similar to that which is found in the interior of the leaf of the Ligustrum (30). The amount of distilled water in the reservoir must be balanced between having as little as possible in order to make the analysis more sensitive, and enough to allow for evaporation. In the spring in Berkeley water loss was about 0.7 mL per day; in Los Angeles, the loss rate was 4 mL per day and at the cooler Tanbark Flats, 2 mL evaporated per day.

The surrogate leaves are assembled in the lab, then placed, with reservoirs dry, in plastic bags to be transported to the field. There the reservoirs are filled with glass-distilled water and the leaves deployed. After exposure the leaves are returned to the plastic bags and brought back to the laboratory for analysis. The top and bottom surfaces are extracted with distilled water. The fluid remaining in the reservoir is measured. The cellulose filter and wick are placed in a tube for extraction with glass-distilled water. All of these extracts are analyzed for sulfate and nitrate by ion chromatography. The reservoir and internal filter are combined to determine total gaseous absorption.

A concern in the construction of the Nuclepore leaf is deciding on a pore size to simulate the stomatal openings of the natural leaf. Stomata are found on lower surfaces of the Ligustrum leaf with a pore density of $1 \times 10^4/cm^2$. The size of the stomatal guard cells is about 22 x 17 μm, with the pore size roughly one half of that when fully open (31). One of our leaves uses a Nuclepore membrane with a pore size of 8 μm, which approximates the natural pores. We have constructed a second leaf using two Nuclepore filters in series, separated by a second Teflon screen. The outside filter has 0.03 μm pores and the inner one has 0.05 μm pores resulting in a higher

pore resistance. The two types of leaves were set out side by side in the Los Angeles Air Basin. They were placed in open, exposed locations and within the local canopy, as discussed above.

Results and Discussion

The measured internal deposition of nitrate and sulfate are listed in Table 7. Comparison of the deposition for various numbers of days shows considerable variability, partly attributable to the short exposure periods. Further discussion will involve the four day exposures only.

The comparison of the results to theory is based on Fick's Law of diffusion:

$$dm/dt = -AD \ \delta C/\delta Z$$

where dm/dt is the rate of mass transfer per unit area, A the area across which the molecules are diffusing, D the diffusion coefficient and $\delta C/\delta Z$ the concentration gradient. The rate of mass transfer across a unit area of the Nuclepore leaf will then be given by:

$$\frac{dm}{dt} = \frac{DAC}{L}$$

where C is the airborne concentration just outside the leaf and L is the distance from the entrance to the wet cellulose filter surface where the concentration is taken to be zero. The area A is:

$$A = \frac{fN\pi d^2}{4}$$

where N is the number of pores/cm^2 and d the pore diameter. The parameters N and d for 8 μm pore size filters are taken from John, et al. (24) and from the Nuclepore Corp. brochure for 0.03 and 0.05 μm pore sizes. The factor f is the fraction of open area of the Teflon screen, which is 0.35. For the second version of the leaf using

0.03 and 0.05 μm pore size filters, the diffusional resistances were combined in series. The diffusion coefficient for NO_2 is 0.154 cm^2/sec (25). The same value is adopted for SO_2 in the absence of available data. (It is not expected to be much different.)

The ratios of measured to calculated internal depositions are listed in Table 8. For SO_2 diffusing into the 8 μm pore size leaf, the measured values are higher than calculated. A possible explanation is that the Teflon screen was partially wetted by contact with the cellulose filter decreasing the effective diffusion distance L. Also, water vapor is continually diffusing out of the leaf. The lack of similar effect for NO_x would be explained by the lower solubility of NO_x so that the gas would diffuse to the much greater area presented by the wet cellulose filter. For NO_3 there is an uncertainty as to which gases to include. In Table 8, the calculation is made for several combinations. The results are mainly dependent on NO_x which dominates the concentrations.

For the nitrogen species there is rough agreement with theory for the 8 μm pore size.

All of the results for the 0.03 + 0.05 μm pore size are in disagreement with theory. We cannot account for such large discrepancies. In future work, we will adopt the 8 μm pore size which approximates stomatal sizes in real leaves.

The above calculations do not include the boundary layer resistance. Friedlander (26) has estimated a boundary layer thickness of 0.05 cm at a point 2 cm from the leading edge of a leaf in a wind speed of 5 miles/hr. Such a layer would present only 1% as much diffusional resistance as the 8 μm pore size leaf. In real leaves the stomatal resistance is also greater than the boundary layer resistance (27). A real leaf has a smaller pore area because the pore density is much smaller than for a Nuclepore filter. However, the diffusion distance inside may be less than for the surrogate leaf.

VI. SUMMARY AND CONCLUSIONS

This report covers Phase II of a multiyear program to study dry acid deposition in California including the development of measurement techniques, collection of baseline data and investigation of deposition mechanisms.

Ambient Concentrations and Deposition Fluxes

Measurements of ambient concentrations of acidic gases and particles, similar to those done in Martinez, San Jose and the Kern River Canyon during Phase I were carried out at two new sites in the South Coast Air Basin, Western Los Angeles and Tanbark Flats (in the mountains to the northeast). All of the major acidic species were determined in 12 hour time periods over four days with techniques designed to minimize sampling artifacts. Redundant sampling afforded comparisons of alternative sampling methods. New developments included measurement of strong acid aerosol size distributions and exploratory work with a new thin iron film detector for acid droplets. Acidic species were collected on leaves of Ligustrum plants and on a surrogate surface. Acidic gases were sampled with a new surrogate Nuclepore "leaf".

The pollutants SO_2, NO_x, NO_3, SO_4 and NH_4 all had higher concentrations at West Los Angeles than at the other four sites. Nitric acid and particulate strong acid were highest at Tanbark Flats followed by West L.A. At Tanbark Flats, the high levels of HNO_3 and H^+, coupled with low NH_3 levels, raise concern for this vulnerable forested mountain area downwind of Los Angeles. Nitric acid has a strong diurnal pattern, nearly zero at night and correlating with ozone. Sulfur dioxide also varied diurnally but was appreciable at night, particularly at West L.A.

The particle ion balance was fairly good at Tanbark but at West L.A. negative ions were missing. The concentration ratio (concentrations in equivalents) $[SO_4]/[SO_2]$ was 0.24 at west L.A. and 0.69 at Tanbark Flats, the latter being an unusually high ratio. Several ratios are notably consistent from site to site: $[HNO_3]/[SO_2] = 0.12 \pm 0.01$ for four sites not including Tanbark Flats; $[NO_3]/[H^+]$ is 3.7 ± 0.6 for Martinez, San Jose and West L.A. but is 0.9 ± 0.1 for the receptor sites Kern and Tanbark Flats; $[NH_3]/[SO_2] = 0.8 \pm 0.2$ for four sites not including Martinez.

Because the observed concentrations span orders of magnitude, it is possible to order the deposition fluxes with a fair degree of confidence even in the absence of quantitative deposition velocities. The descending order is: NO_x, SO_2, HNO_3 and H^+. NO_3 and SO_4 are probably between HNO_3 and H^+. Significantly, the deposition fluxes of the primary species NO_x and SO_2 are greatest so that they may also have the greatest

total acid impact, but specific damage also depends on the characteristics of the acid species.

Sampling Methodology

To understand one of the major sampling problems, namely, that arising from the volatilization of NH_4NO_3, the data were compared to the theory of dissociation. Good agreement was obtained except at 12°C and 90% R.H. The predicted lowering of the dissociation above the deliquesence point by the effect of SO_4 on the ion fraction was not observed. At West L.A., ammonia from local sources probably suppresses the dissociation and the resulting nitric acid.

Compared to the denuder difference method, the simple filter pack overestimated HNO_3 by 56% at West L.A. The dichotomous sampler collected less than half of the fine particle NO_3 at West L.A. because of volatility losses. Virtually no HNO_3 reaches the filter in the dichotomous sampler, apparently because of adsorption on surfaces.

The ammonia denuder used to protect the filter used for particulate strong acid had no significant effect at the five sampling sites. The weighted average ratio of H^+, (no denuder)/(denuder) was 0.98 $\pm$ 0.02. Also, H^+ was not anti-correlated to NH_3. Therefore, there is ordinarily no need for the denuder. Moreover, the phosphorous acid-coated denuder presented severe problems in the high humidity at West L.A.

Strong Acid Aerosol Size Distributions

Because deposition velocities depend strongly on particle size, size distributions were measured with a low pressure cascade impactor, preceeded by a cyclone and an ammonia denuder. Stage deposits were analyzed for strong acid, sulfate, nitrate and ammonium ion.

The NH_4 and SO_4 size distributions were very similar, the mass median diameters (MMD) at West L.A. being 0.3 - 0.5 µm and 0.3 - 0.4 µm at Tanbark Flats. Three out of the four distributions showed a smaller MMD for strong acid, which was 0.3 -0.5 µm at West L.A. and 0.2 µm at Tanbark. A NO_3 peak was not seen, it being above 1 µm except for the first period at Tanbark Flats. This is consistent with

dichotomous sampler data showing 51% of the total NO_3 above 2.5 μm at West L.A. and 40% at Tanbark Flats, whereas SO_4 was predominately in the fine fraction at both sites.

The observed differences in the size distributions show the need for such measurements. The present measurements which include strong acid are believed to be the only data available. However, these results should be considered preliminary because of possible instrumental effects from the low pressure which are currently under investigation.

Thin Film Detectors for Acid Droplets

A reaction spot technique has been explored for the detection of sulfuric acid droplets by the holes etched in thin iron films. The sizes of the reaction spots can be used to infer the sizes of the airborne droplets. Reaction spots in films exposed at West L.A. were found to have sufficient surface concentration for analysis by automated scanning electron microscope in the AIHL Center for Automatic Particle Analysis. The X-ray spectra confirmed the presence of sulfur in the reaction spots.

Additional work will be necessary to calibrate the method and to determine possible effects of salt aerosol.

Collection of Acidic Particles and Gases on Leaves of Ligustrum and a Surrogate Surface

The direct measurement of the deposition of acidic species on the surfaces of leaves obviates the necessity to determine the complicated effects of micrometeorology and surface structure. We have used two species of Ligustrum, japonicum and ovalifolium in pots, allowing transport to different sites. The deposits are recovered by leaf washing and the results combined with data on airborne concentrations to obtain deposition velocities. Preliminary experiments demonstrated that the exterior leaf surfaces could be extracted without leaching material from the interior.

Surrogate surfaces (Tedlar top, polycarbonate bottom) were also used for comparison. Nitrate deposition to the top surface was eight times that on the bottom at West

L.A., and twice at Tanbark Flats. At West L.A. all of the sulfate was on the top; none was detected on the bottom at L.A. or on any surface at Tanbark Flats.

Comparison of exposures from one to four days showed that four days is minimal for measurements on Ligustrum. For nitrate particles (some contribution from nitric acid is possible) the deposition velocity (average over top and bottom) was 0.22 $\pm$ 0.03 cm/sec for japonicum at West L.A. and 0.26 $\pm$ 0.04 at Tanbark. On ovalifolium and on the surrogate surface the nitrate particle deposition velocity was about half that on japonicum. Japonicum has a waxy leaf which appears rough under the microscope. Surrogate surfaces yielded deposition velocities somewhat reduced under Pine and Cypress canopies. The measured deposition velocities are reasonable considering that about half of the nitrate particle mass is above 2.5 μm and the rapid increase of deposition velocities above 1 μm.

The results for sulfate on Ligustrum at West L.A. provide strong evidence that most of the deposition was due to SO_2. If, for example, the SO_4 deposit were attributed to SO_4 particles, the deposition velocity would be six times that measured for NO_3 particles. This is unreasonable since the SO_4 particles were predominately submicron. Also the deposition velocity for SO_4 particles at West L.A. would be nine times that at Tanbark, whereas the NO_3 particle deposition velocities were the same at both sites. Further evidence is the approx. 10 times lower sulfur flux to the surrogate surface, which has less surface area than a real leaf. Based on the above reasoning, the deposition velocity for SO_2 on japoncium was 0.27 $\pm$ 0.04 cm/sec and on ovalifolium, 0.25 $\pm$ 0.04 cm/sec at West L.A. Deposition velocities for SO_2 or SO_4 on any surface were generally less than 0.1 cm/sec at Tanbark Flats even assuming all of the sulfur is either in SO_2 or SO_4. The high SO_2 concentrations and humid conditions at West L.A. were conducive to SO_2 deposition.

Passive Sampling for Sulfur Dioxide with a Surrogate Nuclepore "Leaf"

A surrogate leaf was constructed with the pores of a Nuclepore filter simulating leaf stomata. After diffusing through the pores, acidic gases are absorbed on a wet cellulose filter which can be extracted for analysis. Surrogate leaves were deployed as a trial during the West L.A. and Tanbark sampling.

Compared to theoretical calculations, the internal absorbtion of NO_x was in rough agreement for an 8 µm pore surrogate leaf. The observed deposition of SO_2 was higher than expected, possibly due to some wetting of internal surfaces. For a second version of the leaf using 0.03 and 0.05 µm pores, agreement with theory was very poor.

The 8 µm pore size surrogate leaf shows some promise. The pore size approximates that of plant stomata and the diffusional resistance is greater than the boundary layer resistance, as in real plants. The surrogate leaf could be deployed for several weeks to determine SO_2 levels in plant canopies. Additional development work will be necessary to validate the technique.

VII. RECOMMENDATIONS

The present work completed a comprehensive sampling of acidic pollutants at five California locations. These baseline data afford useful systematics of relative concentrations of acidic species, diurnal variations and location dependences. However, the sampling represents only four days at each location in the July - September period. Therefore, it is desireable to obtain sampling data throughout the year on a more sustained basis in order to better assess the magnitude of dry acid deposition. This would require a simplified sampling scheme.

The relatively high levels of nitric acid and particulate strong acid observed at Tanbark Flats indicates that this and similar areas representing the vulnerable, forested mountain receptor sites downwind of Los Angeles, deserve special monitoring and study of possible dry acid damage.

Performance data were obtained on samplers for acidic gases and particles which reemphasize the unacceptable errors incurred by shortcut methods for nitric acid and nitrate particles. However, the present results provide a basis for designing a simplified but rigorous sampling scheme for routine monitoring of dry acid deposition by the concentration method.

For example, consider the following samplers:

(1) A dichotomous sampler with the Teflon fine fraction filter backed by a Nylon filter, for particulate strong acid, ammonium, sulfate and nitrate.

(2) A Teflon-coated cyclone followed by a Teflon filter backed by a Nylon filter, for total fine nitrate. Nitric acid is obtained by subtracting the particulate nitrate found in (1).

(3) A bubbler for sulfur dioxide.

This preliminary design (shown in Figure 73) is based on the present results which showed that an ammonia denuder was unnecessary at all the sites visited and that nitric acid does not reach the filter of the dichotomous sampler. The sampler's internal surfaces apparently functioned as a nitric acid denuder. The use of the Nylon backing filter in (1) and (2) is mandatory to overcome the problem of dissociation of ammonium nitrate. Fine particulate ammonium concentrations would be corrected as in the present work (Pg. 10). The validation of a simplified sampling scheme, such as the example given, is a logical next step in the development of a dry acid monitoring network.

Several promising new sampling methods for direct measurement of deposition were introduced during Phase II. Some of the additional development work necessary to explore the potential of these methods and provide validation are currently underway in Phase III. Further exposures of Ligustrum plants have been made in Oildale, a site of high SO_2 and low relative humidity, providing a new test of the real and surrogate surface collectors. Work is also planned to calibrate the thin iron film detectors with sulfuric acid aerosol and to investigate the effect of sea salt. The cascade impactor is being calibrated in the laboratory and experiments planned to study the effects of low pressure on volatile materials. This information is needed to validate the unique data on the size distributions of acidic particles obtained during Phase II.

Dry deposition is still the most difficult aspect of acid deposition assessment. Theoretical and experimental knowledge of deposition velocities is inadequate. A continuing research effort is warranted because of the importance of dry deposition, especially in California.

VIII. ACKNOWLEDGEMENTS

The field sampling was made possible by the kind cooperation of Dr. Mary Borell, Los Angeles Southwest College and Chuck Colver, San Dimas Experimental Forrest. Dr. Paul Miller also lent assistance. We thank Dr. Axel Berner, University of Vienna, for providing his new low pressure impactor. Dr. Evaldo Kothny was responsible for the strong acid analysis. We thank Lurance Weber for his assistance in the AIHL Center for Automatic Particle Analysis. We appreciate the encouragement from Dr. Jerome J. Wesolowski.

This report was submitted in fulfillment of Interagency Agreement No. A1-160-32 by the California Department of Health Services under the sponsorship of the California Air Resources Board. Work was completed as of February 15, 1985.

IX. REFERENCES

1. Liljestrand, H.M. and Morgan, J.J., Environ. Sci. and Technol. 15, 333-338 (1981). Spatial Variations of Acid Precipitation in Southern California.

2. McColl, J.G., (1980), A Survey of Acid Precipitation in Northern California, Final Report, California Air Resources Board, Contract A7-149-30.

3. Waldman, J.M., Munger, J.W., Jacob, D.J., Flagan, R.C., Morgan J.J. and Hoffman, M.R., Science 218, 678-680 (1982). Chemical Composition of Acid Fog.

4. John, W., Wall, S.M., Wesolowski, J.J., Assessment of Dry Acid Deposition in California, Final Report, Interagency Agreement ARB No. A1-053-32, Air and Industrial Hygiene Laboratory Report CA/DOH/AIHL/SP-31, California Dept. of Health Services, June 1984.

5. Hicks, B.B., Wesely, M.L. and Durham, J.L., Critique of Methods to Measure Dry Deposition, Workshop Summary, EPA-600/9-80-050, Environmental Sciences Research Laboratory, U.S. Environmental Protection Agency, Research Triangle Park, North Carolina, October 1980. Available from NTIS, Report No. PB81-126443.

6. Davidson, C.I. and Friedlander, S.K., J. Geophys. Res. 83, 2343-2352 (1978). A filtration model for aerosol dry deposition: application to trace metal deposition from the atmosphere.

7. McMahon, T.A. and Denison, P.J., Atmos. Environ. 13, 571-585 (1979). Empirical Atmospheric Deposition Parameters - A Survey.

8. Sehmel, G.A., Atmos. Environ. 14, 983-1011 (1980). Particle and Gas Dry Deposition: A Review.

9. Shepherd, J.G., Atmos. Environ. 8, 69-74 (1974), Measurements of the Direct Deposition of Sulphur Dioxide onto Grass and Water by the Profile Method.

10. Hicks, B. Presentation at California Air Resources Board Workshop on Dry Acid Deposition, South San Francisco, CA, March 26, 1984.

11. Lindberg, S.E., Shriner, D.S. and Hoffman, W.A., Jr., The Interaction of Wet and Dry Deposition with the Forest Canopy. CONF-810464-1, Oak Ridge National Laboratory.

12. Sickles, J.E., Bach, W.D. and Spiller, L.L. Comparison of Several Techniques for Determining Dry Deposition Flux. In Precipitation Scavenging, Dry Deposition, and Resuspension, Vol. 2, Proceedings of the Fourth International Conference, Santa Monica, CA, 29 Nov. - 3 Dec., 1982, Pruppacher, H.R., Semonin, R.G. and Slinn, W.G.N., coordinators, Elsevier Science Pub. Co., Inc., N.Y., p. 979.

13. Forrest, J., Spandau, D.J., Tanner, R.L. and Newman, L., Determination of Atmospheric Nitrate and Nitric Acid Employing a Diffusion Denuder with a Filter Pack. Atmos. Environ. 16, 1473-1485 (1982).

14. Spicer, C.W., Howes, J.E., Jr., Bishop, T.A., Arnold, L.H. and Stevens, R.K. Nitric Acid Measurement Methods: An Intercomparison. Atmos. Environ. 16, 1487-1500 (1982).

15. Hildemann, L.M., Russell, A.G. and Cass, G.R. Ammonia and Nitric Acid Concentrations in Equilibrium with Atmospheric Aerosols: Experiment vs. Theory. Atmos. Environ. 18, 1737-1750 (1984).

16. Stelson, A.W. and Seinfeld, J.H. Relative Humidity and Temperature Dependence of the Ammonium Nitrate Dissociation Constant. Atmos. Environ. 16, 983-992 (1982).

17. Berner, A., Lurzer, C.H., Pohl, F., Preining O. and Wagner, P., The size distribution of the urban aerosol in Vienna. Science of the Total Environment 13, 245-261 (1979).

18. John, W. and Reischl, G., A cyclone for size-selective sampling of ambient air. J. Air Pollut. Contr. Assoc. 30, 872 (1980).

19. Gormley P.G. and Kennedy, M., Proc. R. Ir. Acad. 52, 163 (1949).

20. Coulson, J.M. and Richardson, J.F., Chemical Engineering, Vol. 1, Pergamon Press, Oxford, 1954. p. 239.

21. Askne, C. Method of determining strong acid in precipitation based on coulometric titration with application of Gran's plot. IVL Publication B 152 (1973).

22. Altshuler, A.P. Atmospheric Particle Sulfur and Sulfur Dioxide Relationships at Urban and Nonurban Locations. Atmos. Environ. 18, 1421-1431 (1984).

23. Dasch, J.M. A Comparison of Surrogate Surfaces for Dry Deposition Collection. In Precipitation Scavenging, Dry Deposition, and Resuspension, Vol. 2, Proceedings of the Fourth International Conference, Santa Monica, CA, 29 Nov. - 3 Dec., 1982, Pruppacher, H.R., Semonin, R.G. and Slinn, W.G.N. coordinators, Elsevier Science Pub. Co., Inc., N.Y., p. 883.

24. John, W., Hering, S., Reischl, G., Sasaki, G. and Goren, S. Characteristics of Nuclepore Filters with Large Pore Size - I. Physical Properties. Atmos. Environ. 17, 115-119 (1983).

25. Palmes, E.D., Gunnison, A.F., DiMattio, J. and Tomczyk, C. Personal Sampler for Nitrogen Dioxide. Am. Ind. Hyg. Assoc. J. 37, 570-577 (1976).

26. Friedlander, S.K. In Smoke, Dust and Haze, Friedlander, S.K., John Wiley & Sons, N.Y. (1977), p. 70.

27. Zelitch, I. In Photosynthesis, Photo respiration, and Plant Production, Academic Press, N.Y. (1971), pp. 216-238.

28. Raschlee, K. Stomatal Action. Ann. Rev. Plant Physiol. 26, 309-340 (1975).

29. Unsworth, M.H., Biscoe, P.U. and Pinckney, H.R. Stomatal Responses to Sulfur Dioxide. Nature 239, 458-459 (1972).

30. Fluckiger-Keller, H., Fluckiger, W., and Oertli, J.J. Changed pH-Values on the Vegetation Along a Motorway. Water, Air, and Soil Pollution 11, 153-157 (1979).

31. Srivastava, K. Epidermal Studies in Some Member of Oleaceae. Current Science 48, (2) 79-80. (1979).

32. Lindberg, S.E. and Lovett, G.M. Application of Surrogate Surface and Leaf Extraction Methods to Estimation of Dry Deposition to Plant Canopies. In Precipitation Scavenging, Dry Deposition, and Resuspension, Vol. 2, Proceedings of the Fourth International Conference, Santa Monica, CA, 29 Nov. - 2 Dec., 1982, Pruppacher, H.R., Semonin, R.G. and Slinn, W.G.N., coordinators, Elsevier Science Pub. Co., Inc., N.Y., p. 837.

33. Slinn, W.G.N. Predictions for Particle Deposition to Vegetative Canopies. Atmos. Environ. 16, 1787-1794 (1982).

34. Hayashi, H., Koshi, S. and Sakable, H. Determination of Mist Size by Metal Coated Glass Slide. Bull. Nat. Inst. Indust. Health 6, 35-42 (1961).

35. Hortsman, S.W., Jr., Wagman, J. Am. Ind. Hyg. Assoc. J. 28, 523-529 (1967).

TABLE 1. Summary of Environmental Variables, Samplers and Methods of Analysis

Variable	Sampler or Sensor	Analysis
Particulate strong acid	Cyclone NH_3 Denuder Teflon filter	Acid titration
SO_4	"	Ion chromatography
NH_4	"	Ion selective electrode
NO_3	Cyclone, acid denuder, Teflon and Whatman 41-NaCl filters	Ion chromatography
HNO_3	Denuder difference method	Ion chromatography
SO_2	H_2O_2 bubbler	Ion chromatography
NH_3	Quartz prefilter, acid-washed glass fiber filters w/oxalic acid	Ion selective electrode
Nitrogen oxides	TECO 14 T monitor	---
Sulfur dioxide	Monitor Labs 8450	---
Ozone	Dasibi 1003-AH	---
Fine particulate mass	Cyclone, NH_3 denuder Teflon filter	Microbalance
Fine and coarse particulate mass, SO_4, NO_3 and NH_4	Sierra 244 Dichotomous Sampler, 15 µm inlet, Teflon filters	Microbalance
Temperature	Platinum RTD in aspirated radiation shield	---
Dew point (for relative humidity)	LiCl-RTD in aspirated radiation shield	---
Wind direction wind speed	Met One 010 assembly	---

TABLE 2. Summary of the Mean and Range of the Variables. Concentrations in nequiv/m^3.

Species	Martinez	San Jose	Kern	West Los Angeles	Tanbark
SO_2	125, 56-157	154, 30-330	172, 0-450	543, 314-877	137, 28-284
Particulate strong acid	10, 0-23	6, 0-26	17, 6-22	20, 14-35	43, 24-65
SO_4	46, 13-69	19, 0-52	45, 10-78	130, 66-208	95, 64-144
NH_4	50, 22-80	36, 12-65	55, 15-93	200, 86-336	143, 85-202
NH_3	554, 140-875	145, 25-247	108, 72-153	450, 145-1155	84, 65-161
HNO_3	14, 0-68	18, 0-100	20, 1-50	71, 10-191	112, 16-315
NO_x*	1370, 600-2190	1740, 712-3840	448, 370-510	2160, 1500-3200	614, 303-1226
NO_3	35, 22-85	23, 10-63	14, 10-20	93, 46-200	40, 13-110
O_3	- -	- -	- -	1092, 343-2235	2280, 550-4760
Fine particulate mass	- -	18, 12-30**	17, 8-28	33, 22-73	26, 13-40
Wind direction	30°, NNW	Northerly, westerly at times	NE daytime, SW night	270°, W afternoon, variable night	220° SW except E. early morning
Wind speed*	7, 6-21km/hr	6, 0-15km/hr	5, 3-8km/hr	5, 3-8km/hr	5, 1-6km/hr
Temperature*	19, 12-30°C	19, 13-29°C	19, 12-25°C	24, 20-27°C	16, 8-22°C
Relative humidity*	59, 26-82%	63, 32-85%	50, 30-70%	71, 55-88%	75, 54-88%

*Ranges refer to averages of instrument reading over sampling period (6-12hr.).

**From cyclone, all other fine particulate masses from dichotomous sampler.

TABLE 3. Impactor Characteristics, from Ref. 17.

Stage	Separation diameter (μm)	Mean particle diameter on stage (μm)	No. of holes	Hole diam. (mm)	Pressure p/p_o	Velocity U (m/s)
9	16.0	--	1	16.6	1.000	2.31
8	8.0	11.3	7	5.5	1.000	3.01
7	4.0	5.7	13	2.8	1.000	6.25
6	2.0	2.8	26	1.4	0.995	12.5
		Cyclone precut				
5	1.0	1.4	50	0.75	0.991	26.0
4	0.50	0.71	30	0.60	0.954	64.0
3	0.25	0.35	22	0.50	0.814	153
2	0.125	0.17	30	0.40	0.485	227
1	0.06	0.087	130	0.25	0.324	227

TABLE 4. Deposition Fluxes to External Surfaces of Ligustrum and Surrogate Leaves.

	Total $\mu g/cm^2/day$ extracted by washing (blank corrected)					
	L. japonicum		L. ovalifolium		Surrogate	
	Nitrate	Sulfate	Nitrate	Sulfate	Nitrate	Sulfate
West Los Angeles						
2 day exposure	0.22	1.23	0.03	0.96	0.16, 0.08	0.08, 0.08
4 day	0.24	0.69	0.15	0.64	0.14, 0.09	0.07, 0.06
Tanbark Flats						
1 day	0.05	0.17	0.03	0.16	0.09, 0.06	<0.1, <0.05
2 day	0.10	0.07	0.02	0.20	0.11, 0.08	<0.05, <0.03
3 day	0.12	0.09	0.05	0.02	0.06, 0.11	<0.03, <0.02
4 day	0.10	0.06	0.06	0.03	0.07, 0.08	<0.03, <0.01
Tanbark Canopies						
Pine, 4 day	-	-	-	-	0.02, 0.06	<0.03, <0.03
Cypress, 4 day	-	-	-	-	0.02, 0.04	<0.03, <0.03

TABLE 5. Deposition velocities (cm/sec) for Nitrate Particles on External Surfaces of Leaves.*

Location	Japonicum	Ovalifolium	Surrogate**
West Los Angeles	0.22 ± 0.03	0.14 ± 0.02	0.13 ± 0.02
Tanbark Flats	0.26 ± 0.04	0.13 ± 0.02	0.18 ± 0.03
Tanbark, Pine Canopy	-	-	0.04 ± 0.01 0.16 ± 0.02
Tanbark, Cypress Canopy	-	-	0.04 ± 0.01 0.11 ± 0.02

*Averaged over top and bottom surfaces

**Upper surface Tedlar, bottom surface polycarbonate.

TABLE 6. Deposition Velocities (cm/sec) for SO_2 and SO_4 on External Surfaces of Leaves.*

Surface	Location	Velocity SO_2	Velocity SO_4
Japonicum	West Los Angeles	0.27 ± 0.04	-
	Tanbark Flats	<0.10	<0.14
Ovalifolium	West Los Angeles	0.25 ± 0.04	-
	Tanbark	<0.04	<0.06
Surrogate	West Los Angeles	<0.03	<0.1
	Tanbark	<0.05	<0.05

*See footnotes on Table 5.

TABLE 7. Internal Deposition Fluxes to Surrogate Leaf. $\mu g/cm^2/day$

	8μm pore		0.03 + 0.05μm pore	
	Nitrate	Sulfate	Nitrate	Sulfate
West Los Angeles				
2 day exposure	0.15	0.66	-	-
4 day	0.20	0.35	-	-
Tanbark Flats				
1 day	0.02	<0.04	0.11	0.16
2 day	0.11	0.21	0.05	0.17
3 day	0.17	0.18	0.02	0.14
4 day	0.16	0.13	0.07	0.13
Tanbark Flats, Canopies, 4 days				
Pine	0.10	0.09	0.04	0.19
Cypress	0.20	0.31	0.02	0.09

TABLE 8. Ratio of Measured to Theoretical Internal Deposition for Surrogate Leaf.

Location	Species	8 μm pore	0.03 + 0.05 μm pore
West Los Angeles	SO_2	4.1	-
Tanbark	SO_2	6.6	100
West Los Angeles	NO_x	0.47	-
	$NO_x + HNO_3$	0.46	-
	$NO_x + HNO_3 + NH_3$	0.38	-
Tanbark	NO_x	1.38	8.1
	$NO_x + HNO_3$	1.17	6.9
	$NO_x + HNO_3 + NH_3$	1.05	6.1

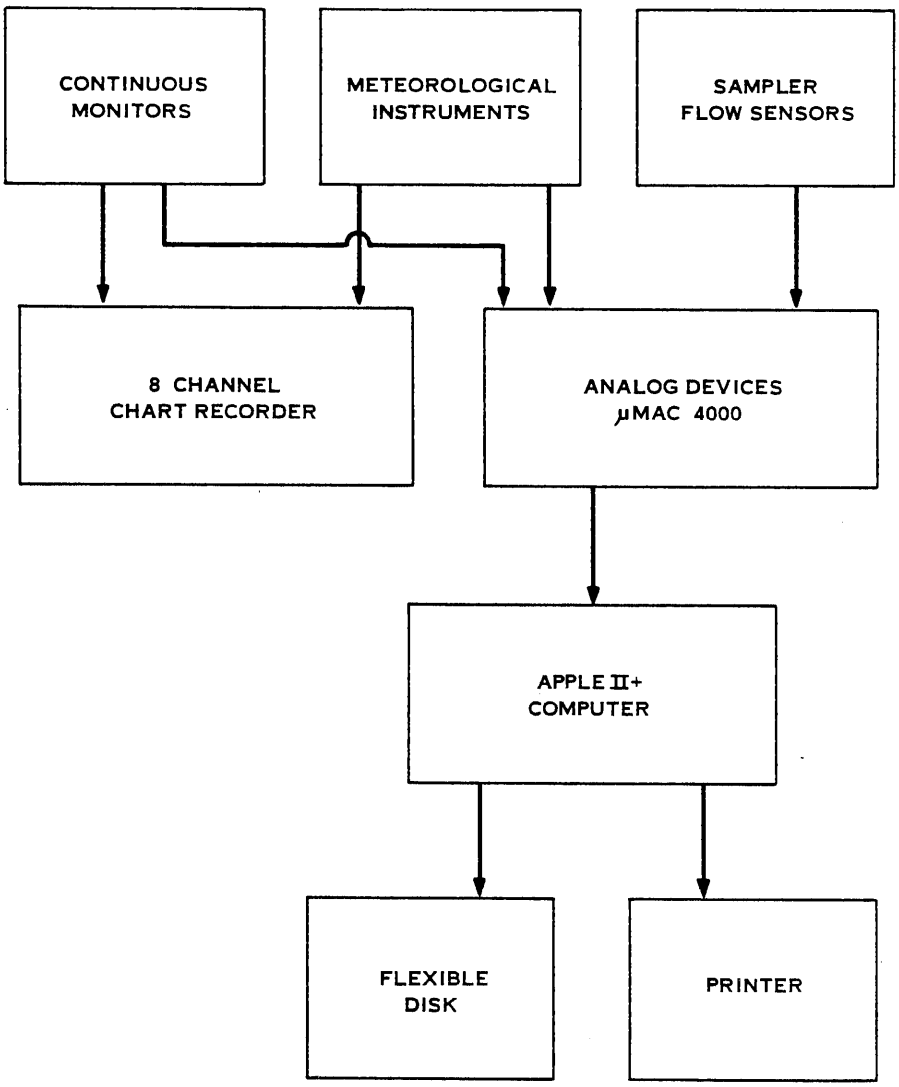

Figure 1. Data acquisition system.

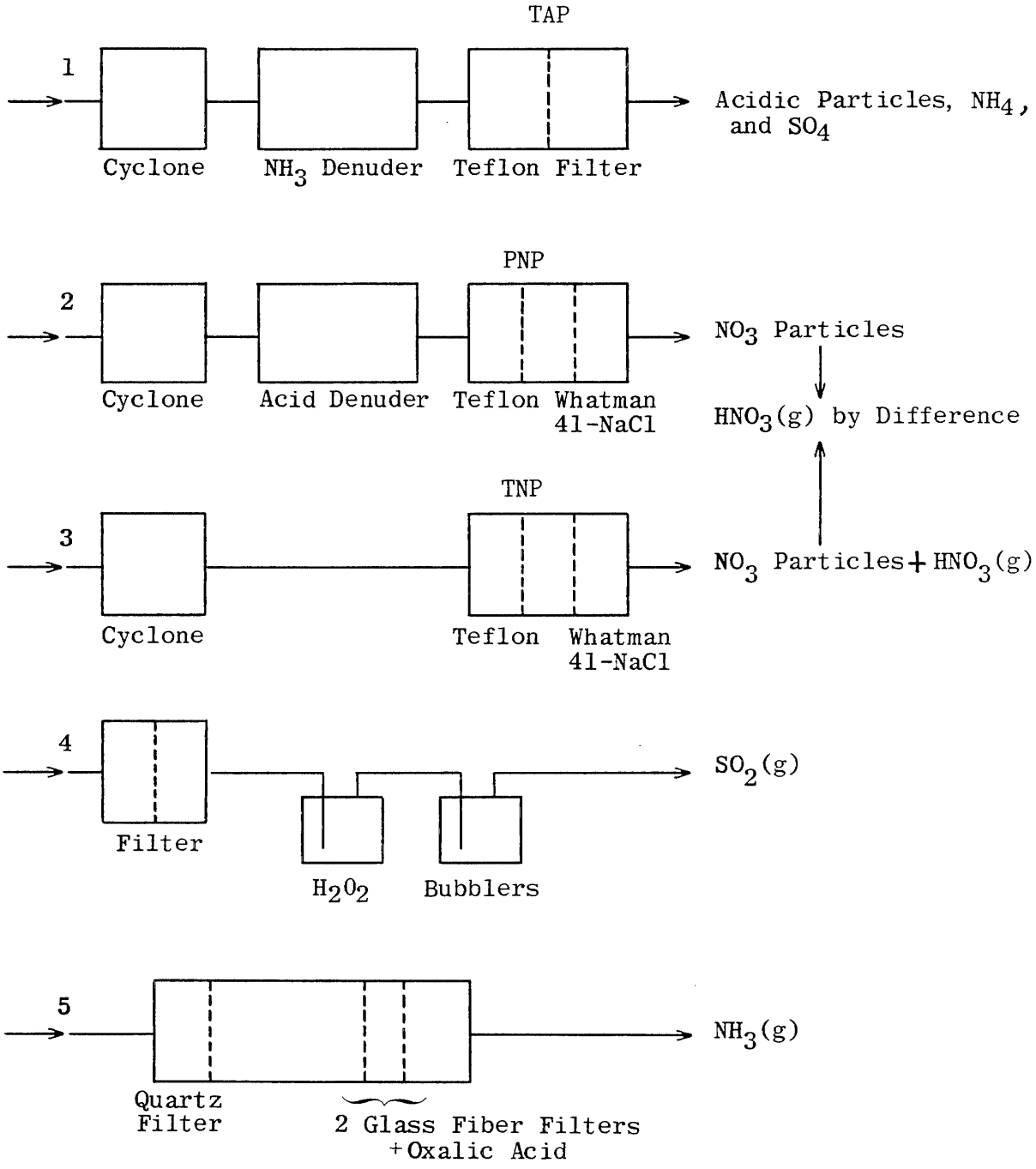

Figure 2. Schematic drawing of filter sampling trains.

Filter designations referred to above and in subsequent plots are TAP, total strong acid prefilter; PNP, particulate nitrate prefilter and TNP, total nitrate prefilter.

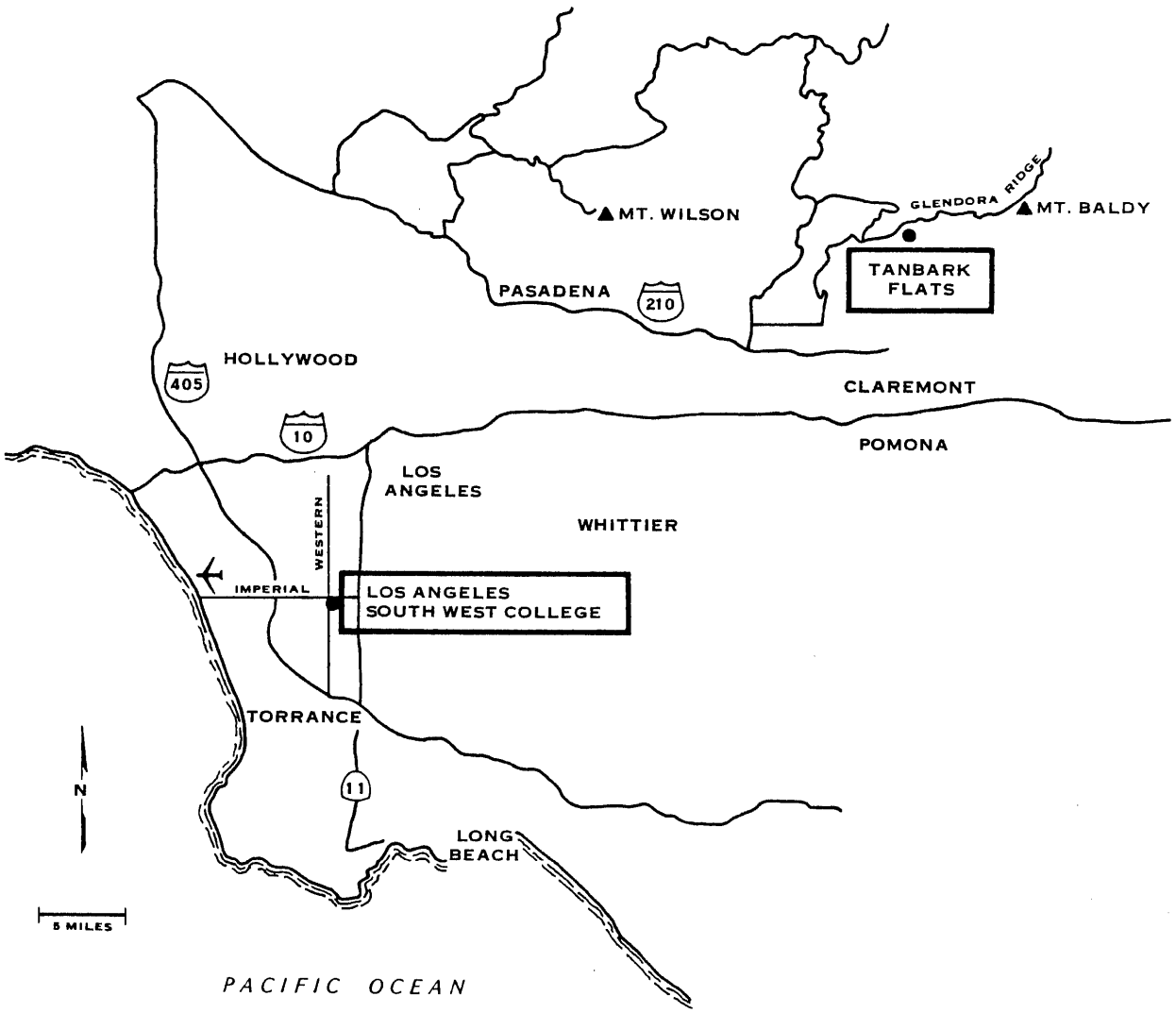

Figure 3. Sampling locations in the South Coast Air Basin.

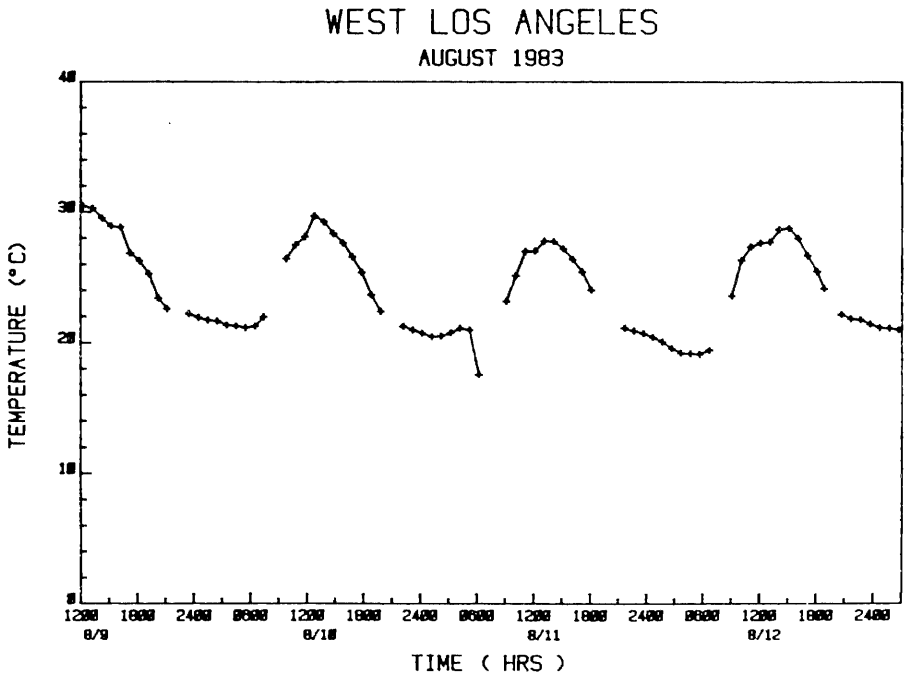

Figure 4. Temperature vs. time at West Los Angeles.

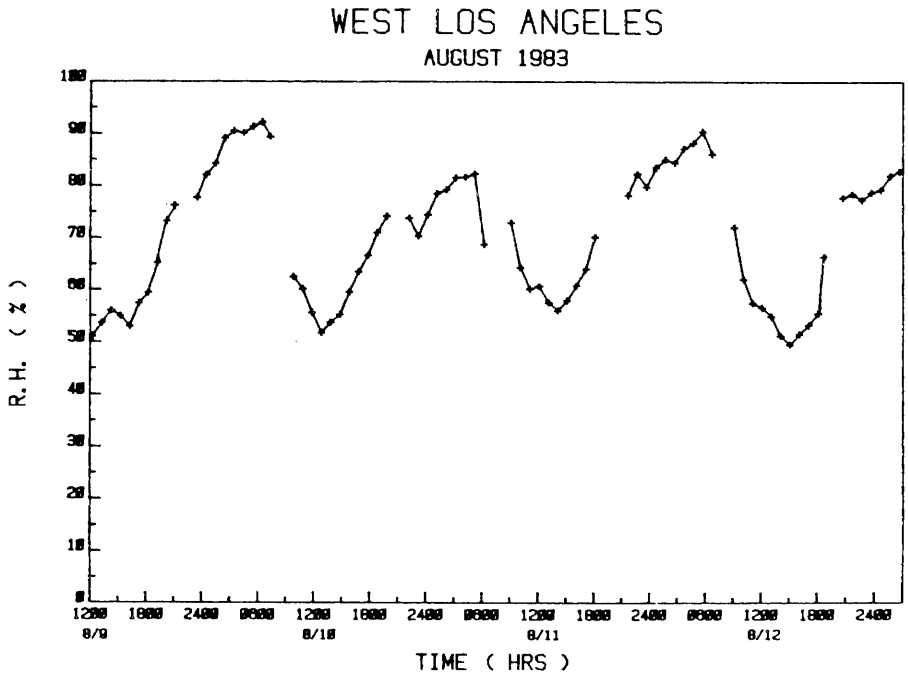

Figure 5. Relative humidity vs. time at West Los Angeles.

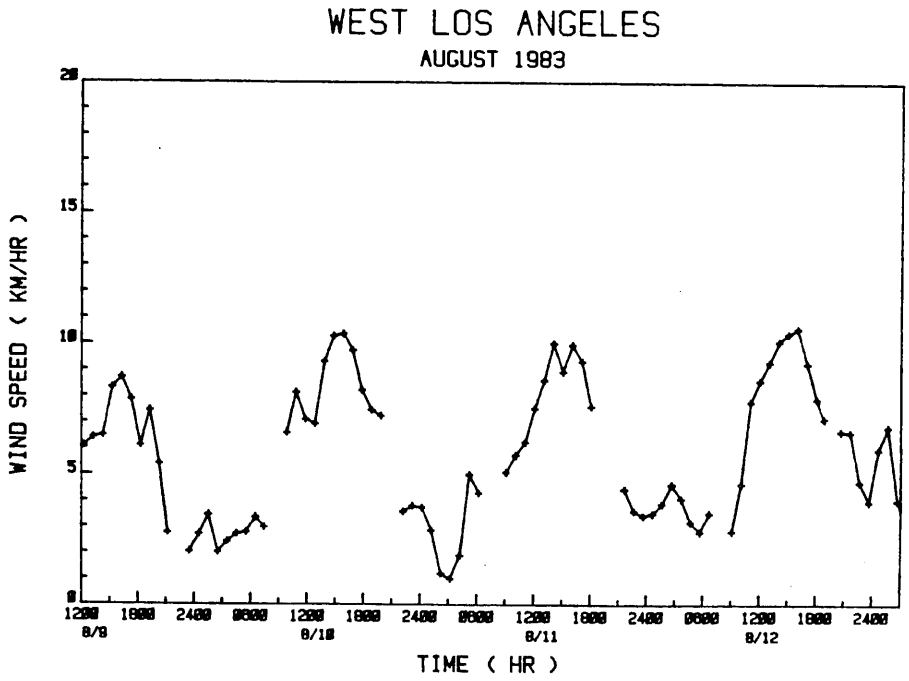

Figure 6. Wind speed vs. time at West Los Angeles.

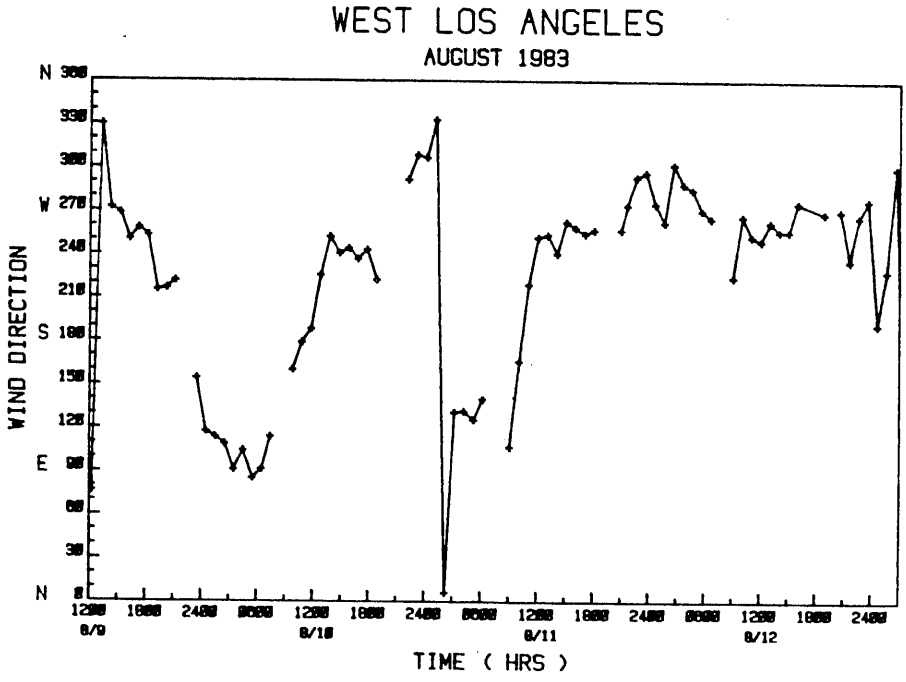

Figure 7. Wind direction vs. time at West Los Angeles.

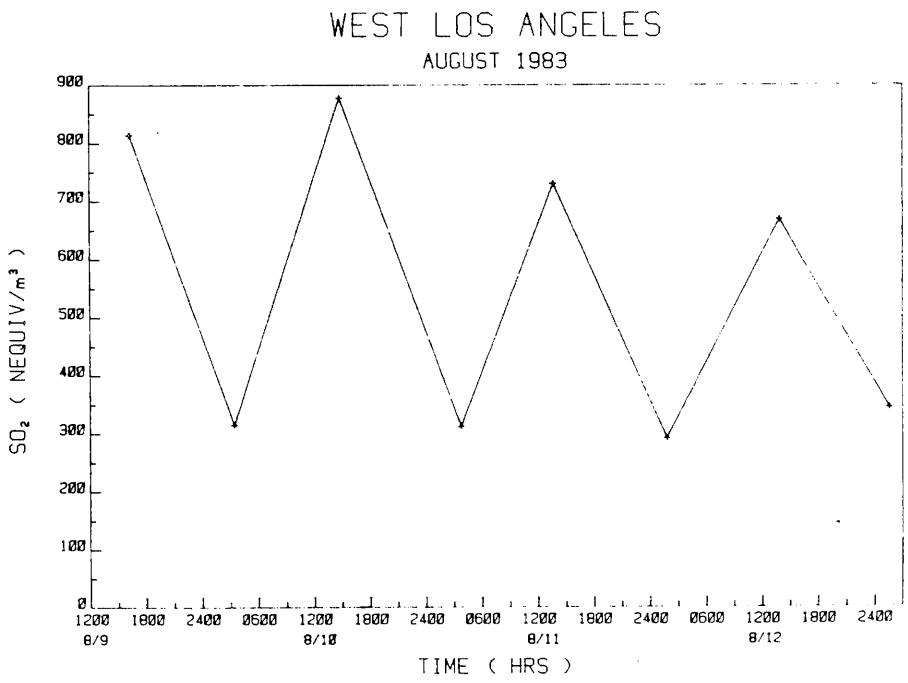

Figure 8. Sulfur dioxide concentration vs. time at West Los Angeles.

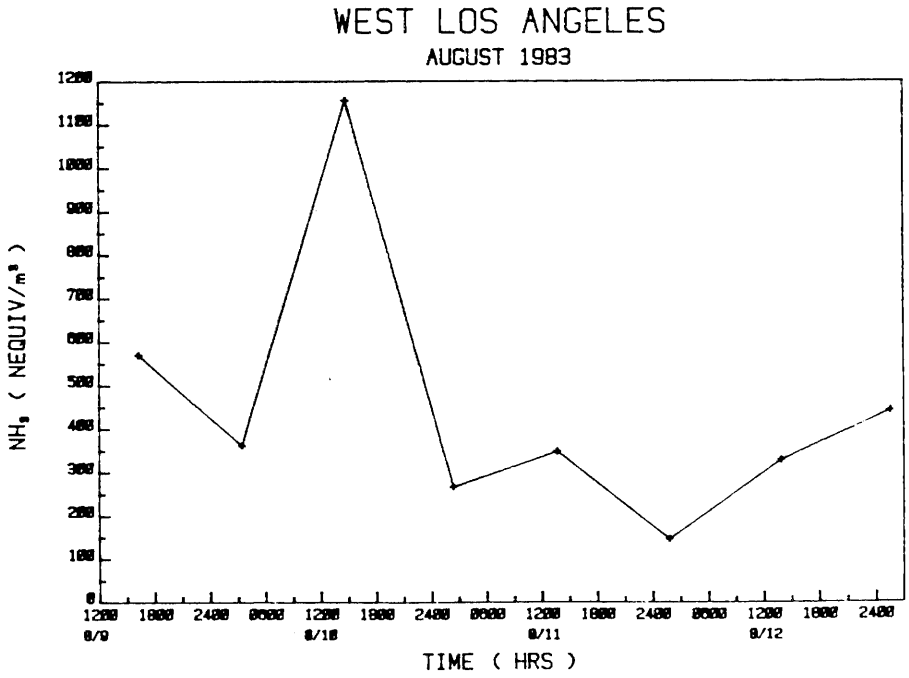

Figure 9. Ammonia concentration vs. time at West Los Angeles.

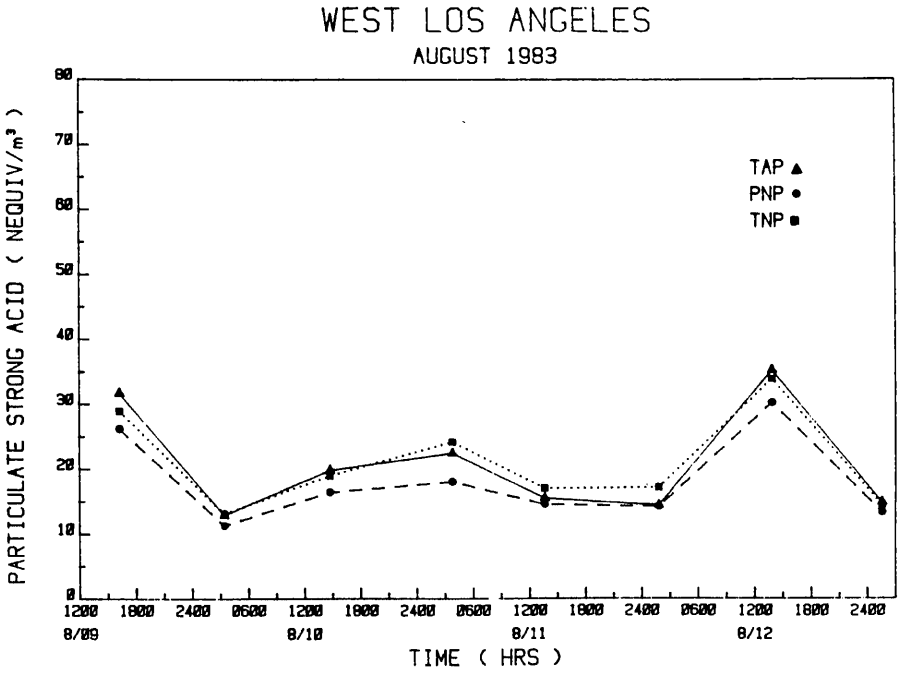

Figure 10. Particulate strong acid vs. time at West Los Angeles. TAP, PNP and TNP refer to the Teflon filters on sampling trains nos. 1, 2 and 3 respectively. See Fig.2 for filter designations.

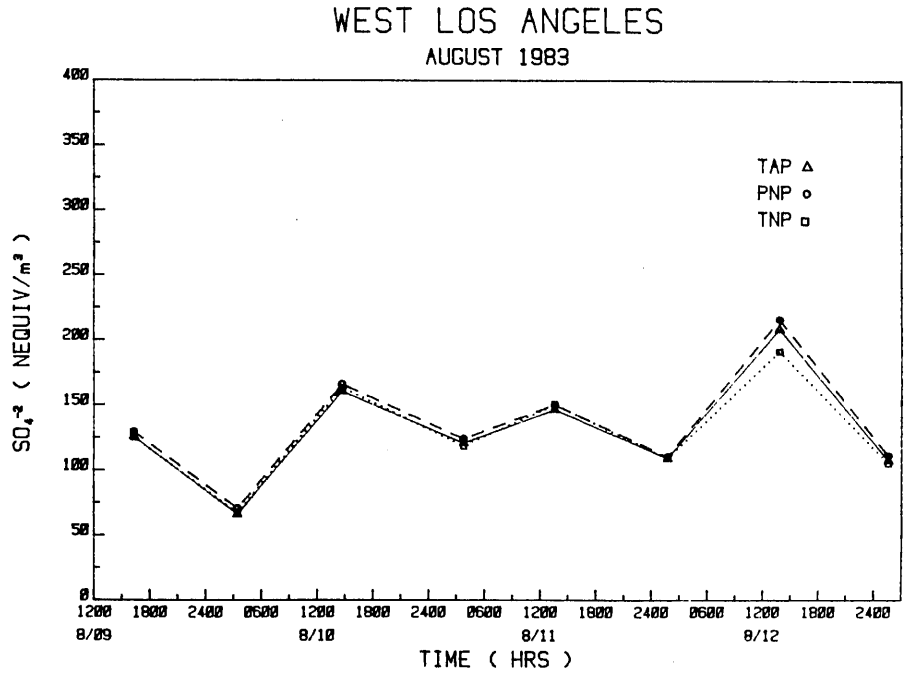

Figure 11. Fine particulate sulfate vs. time at West Los Angeles. See Fig.2 for filter designations.

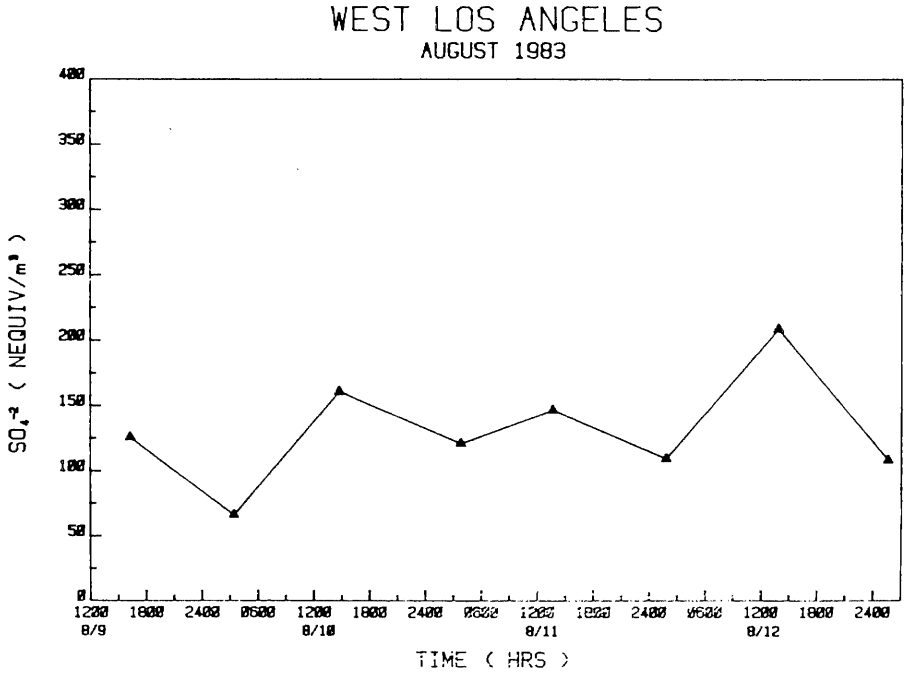

Figure 12. Fine particulate sulfate vs. time at West Los Angeles.

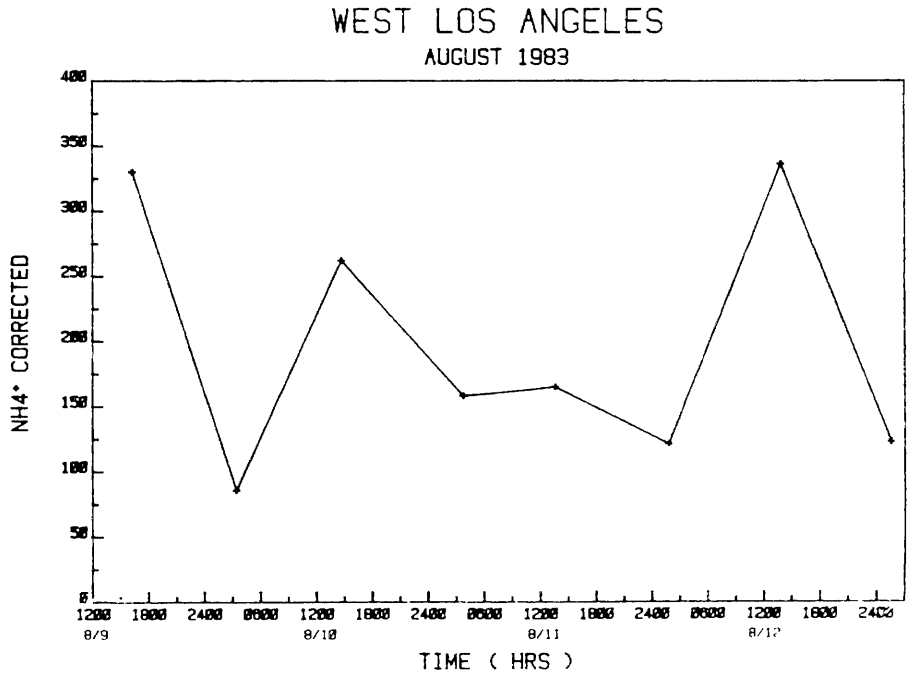

Figure 13. Fine particulate ammonium concentration vs. time at West Los Angeles.

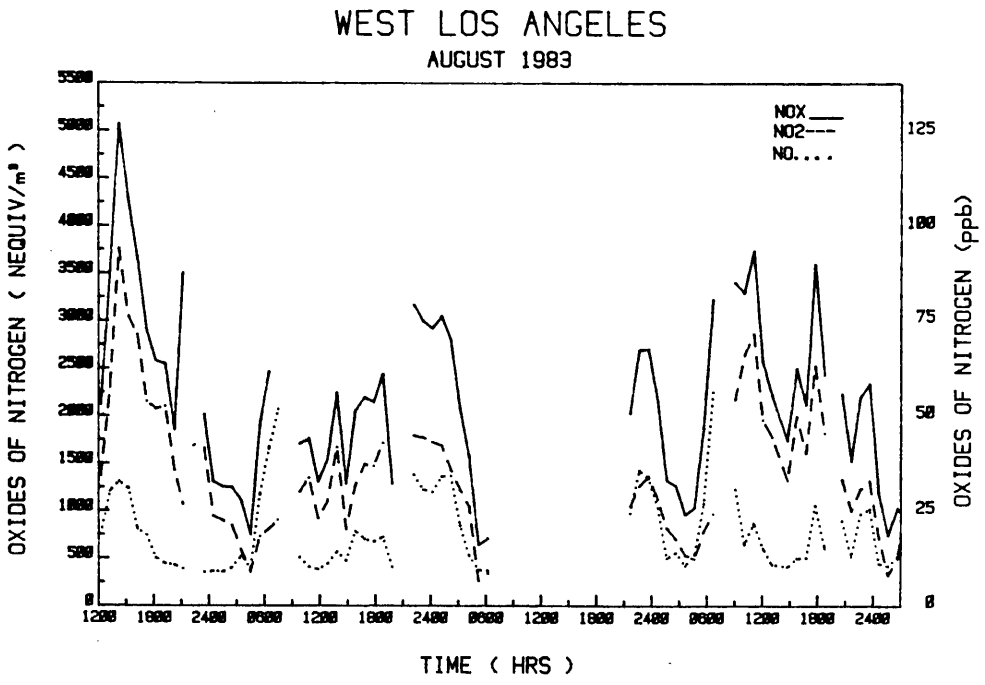

Figure 14. Concentration of oxides of nitrogen vs. time at West L. A.

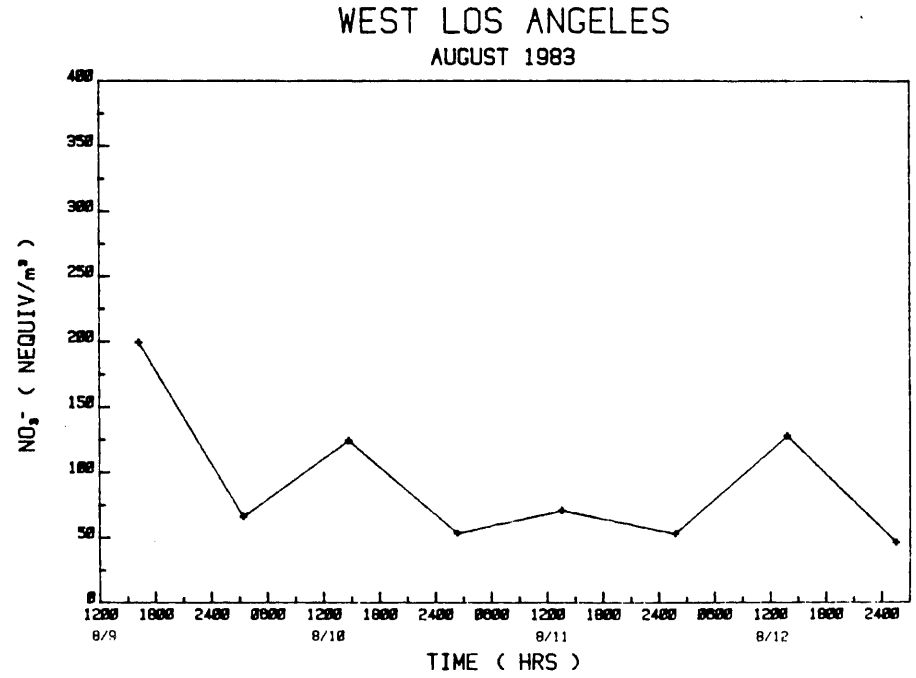

Figure 15. Fine particulate nitrate vs. time at West Los Angeles.

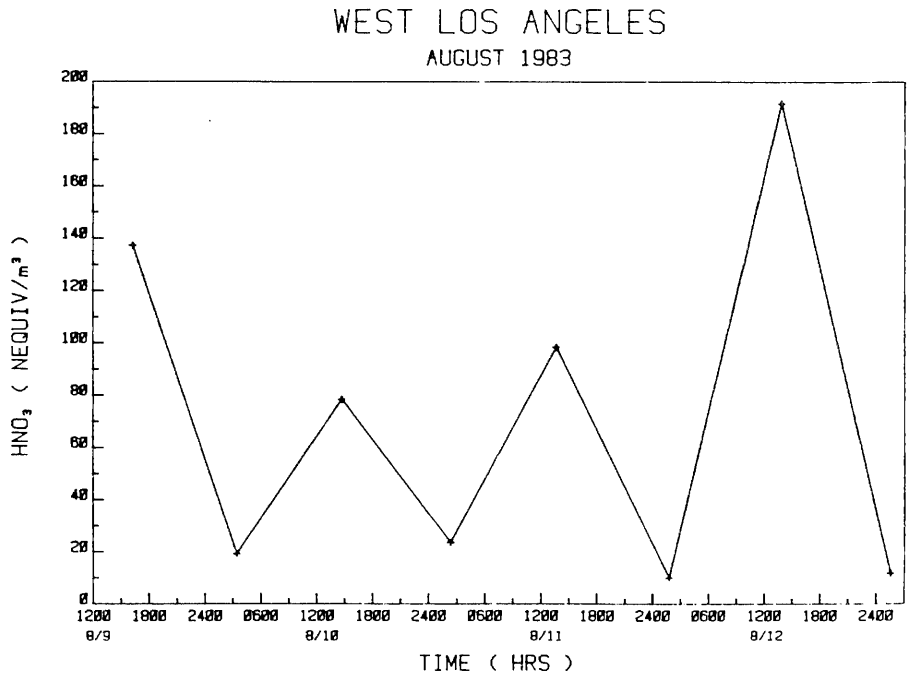

Figure 16. Nitric acid concentration vs. time at West Los Angeles.

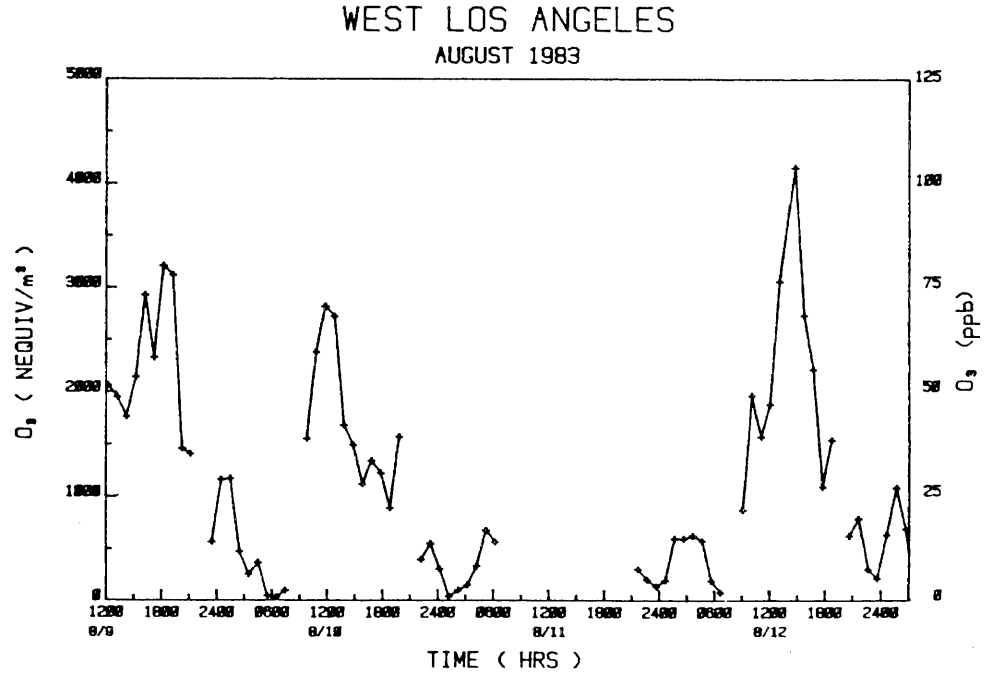

Figure 17. Ozone concentration vs. time at West Los Angeles.

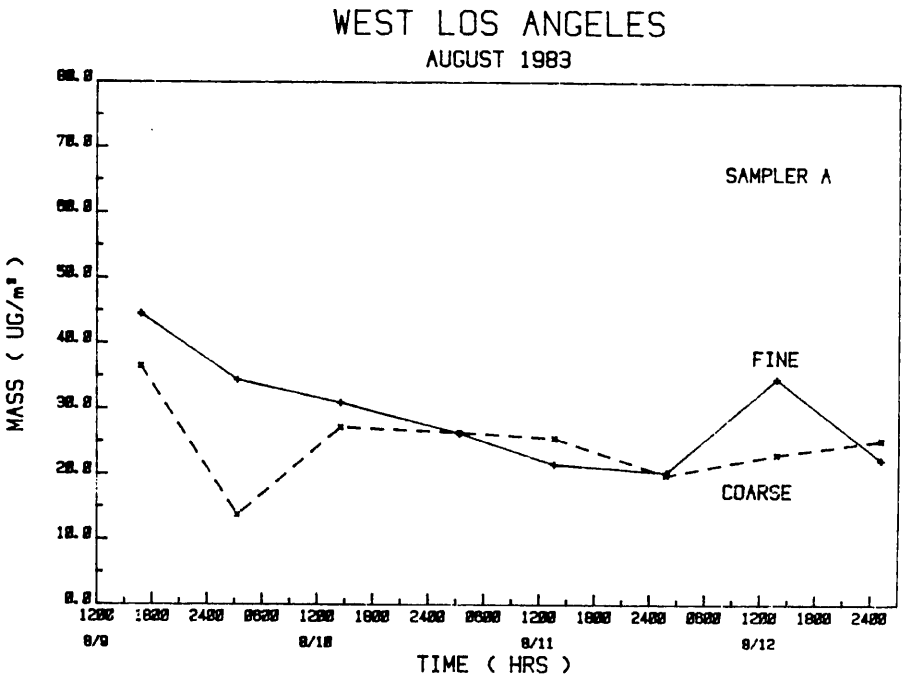

Figure 18. Fine and coarse particulate concentrations at West L. A.

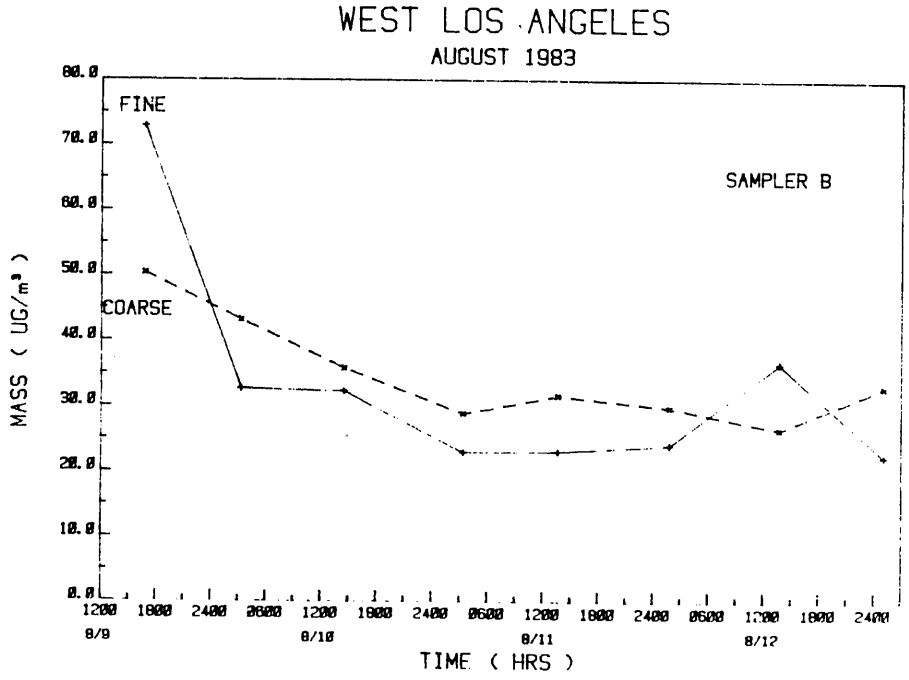

Figure 19. Same as Fig. 18 but for dichotomous sampler B.

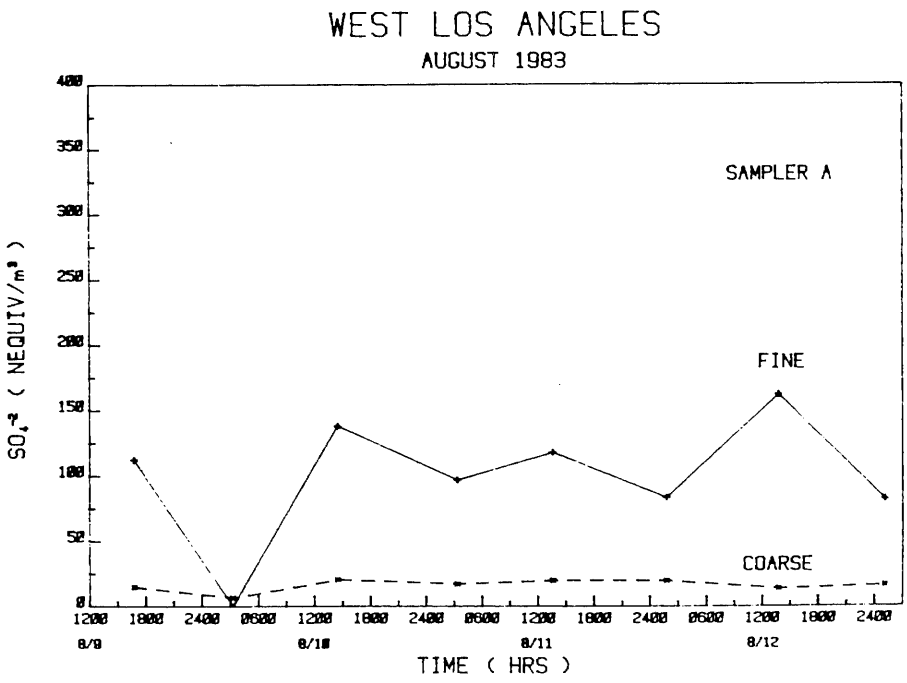

Figure 20. Fine and coarse sulfate concentrations at West L. A.

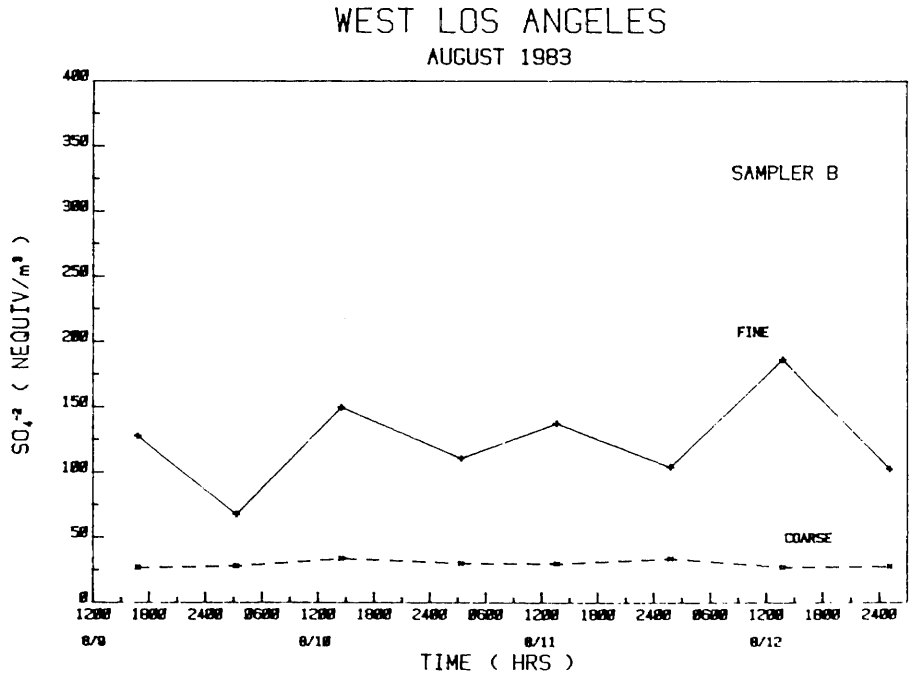

Figure 21. Same as Fig. 20 but for dichotomous sampler B.

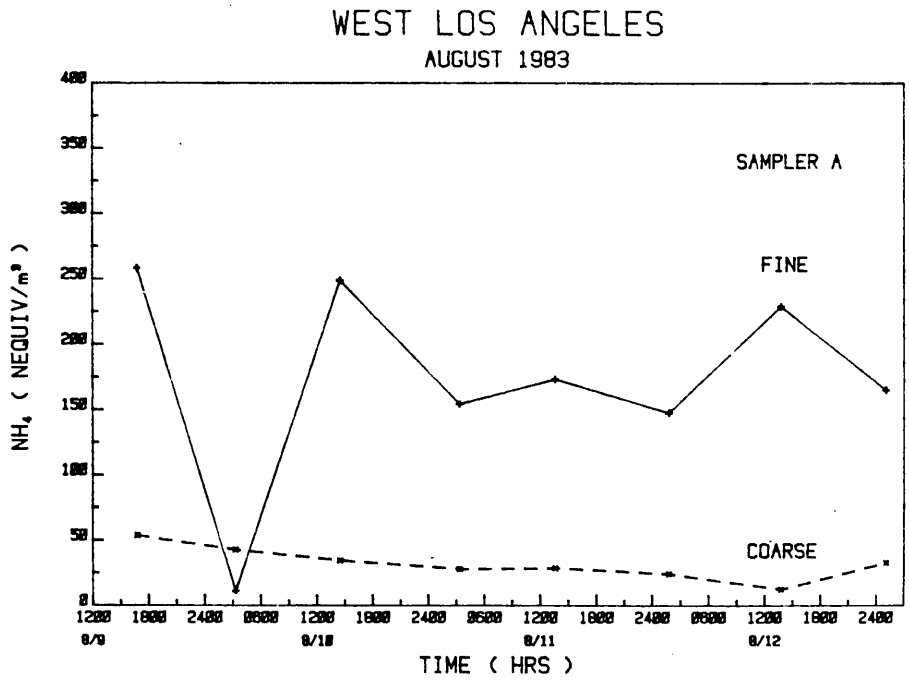

Figure 22. Fine and coarse ammonium concentrations at West L. A.

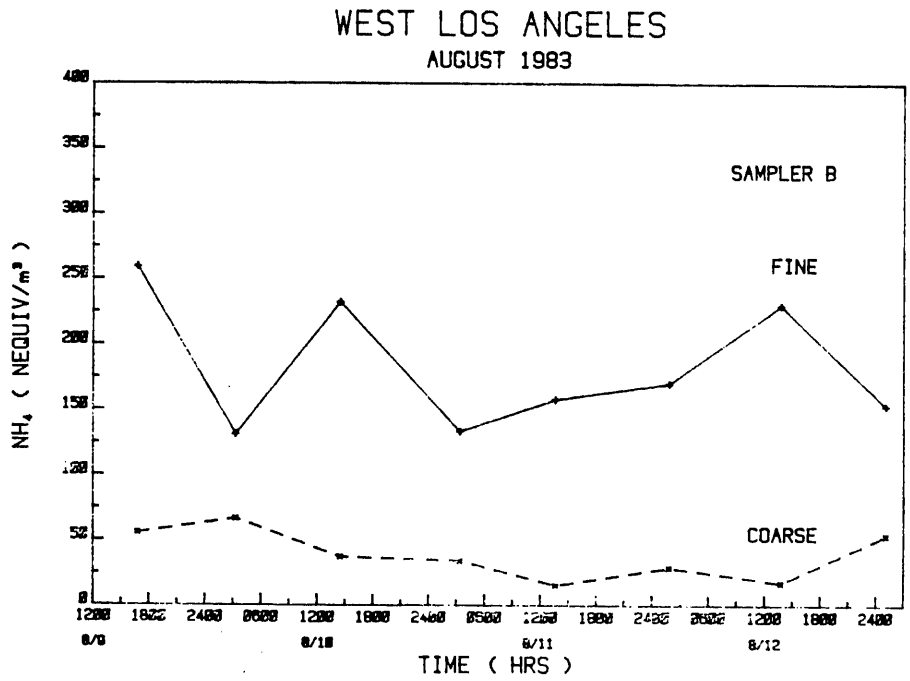

Figure 23. Same as Fig. 22 but for dichotomous sampler B.

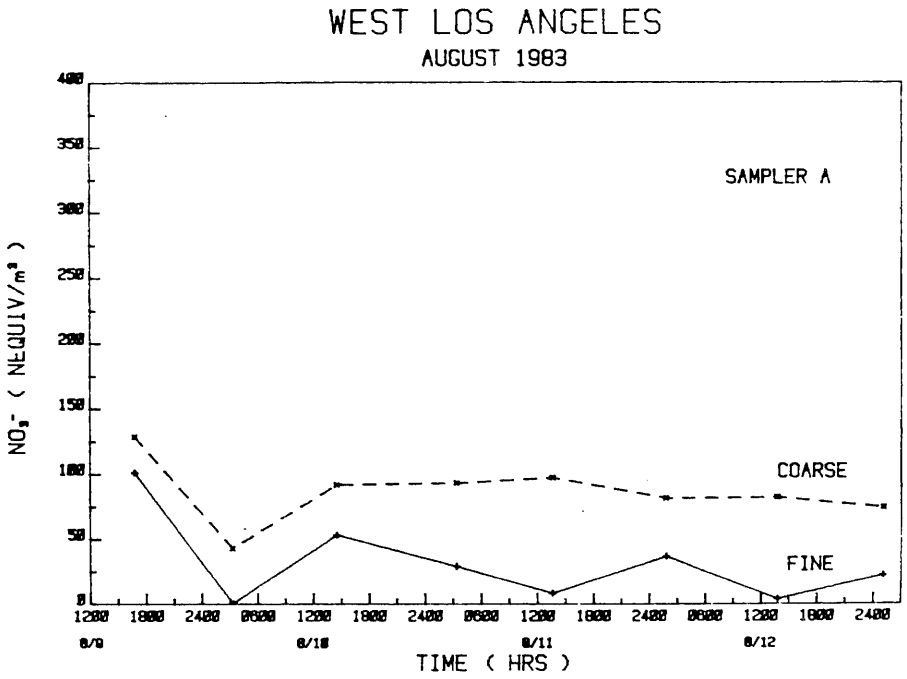

Figure 24. Fine and coarse nitrate concentrations at West L. A.

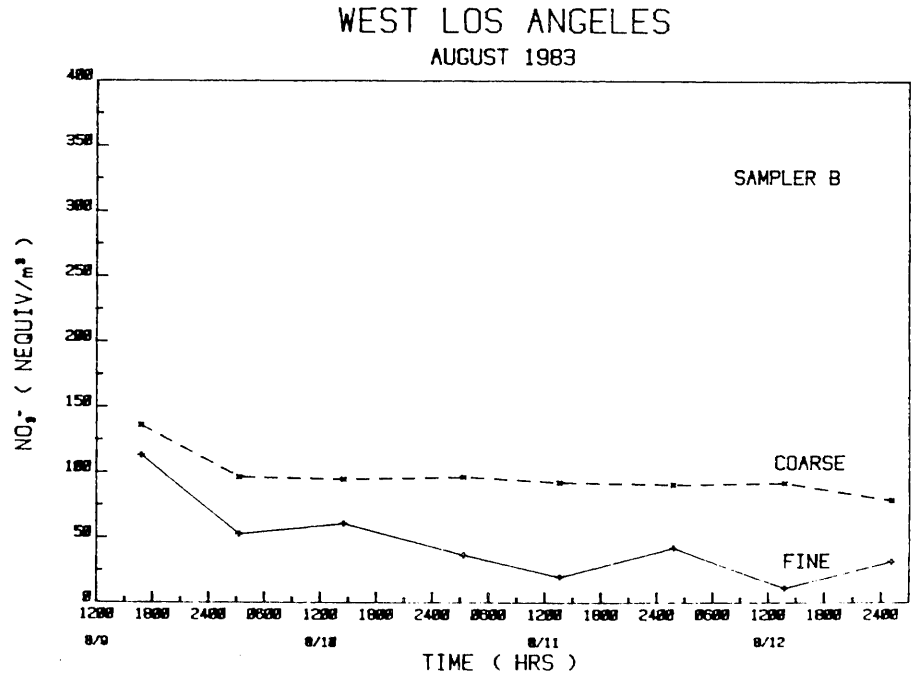

Figure 25. Same as Fig. 24 but for dichotomous sampler B.

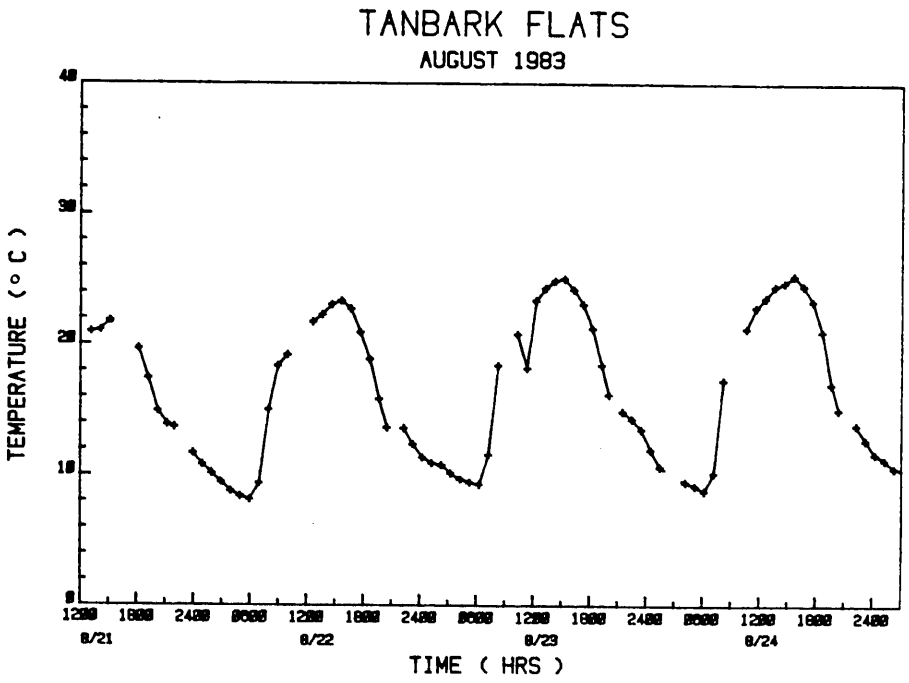

Figure 26. Temperature vs. time at Tanbark Flats.

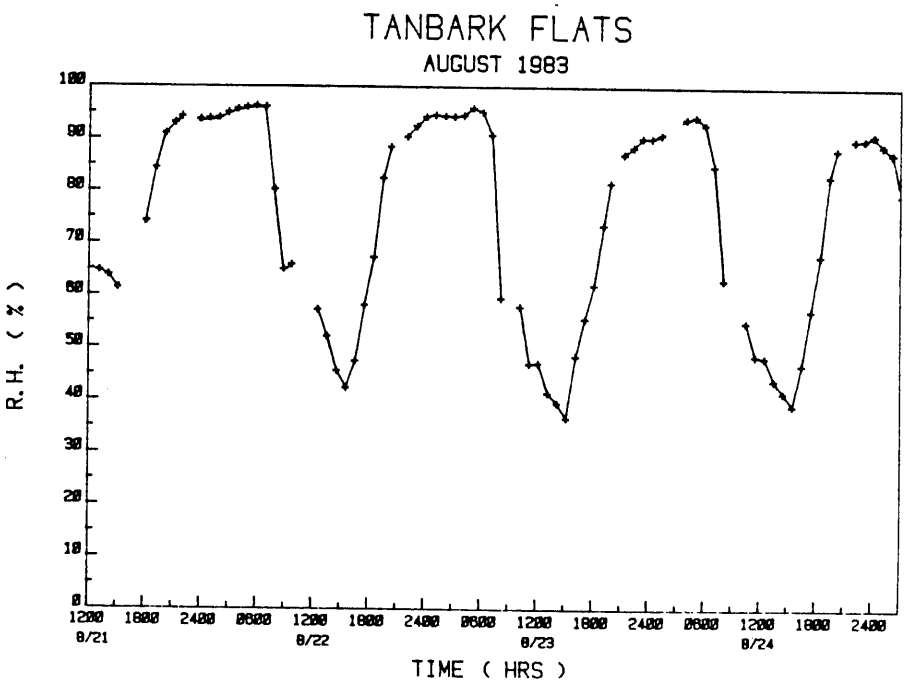

Figure 27. Relative humidity vs. time at Tanbark Flats.

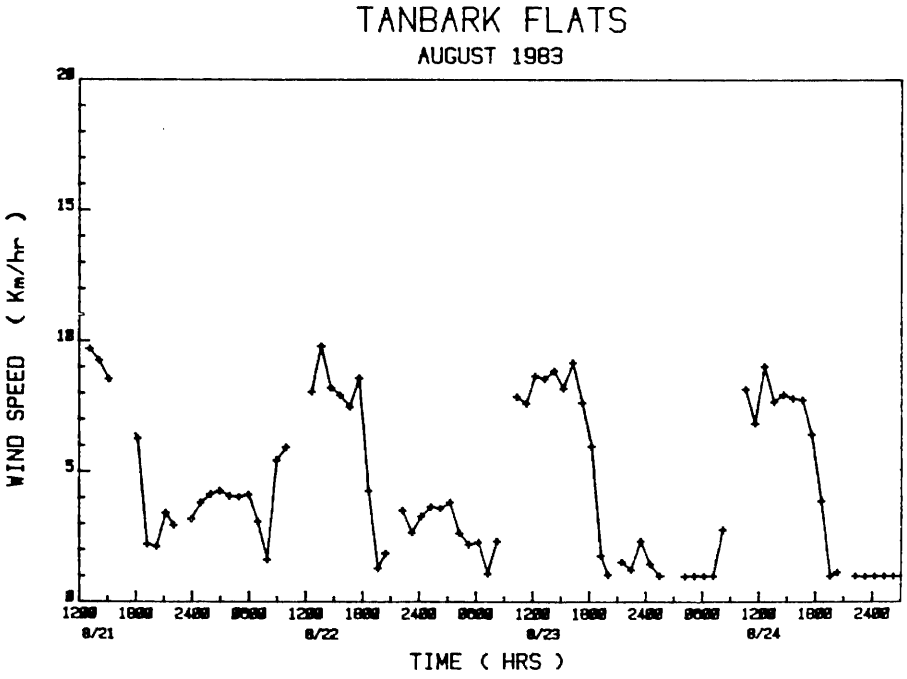

Figure 28. Wind speed vs. time at Tanbark Flats.

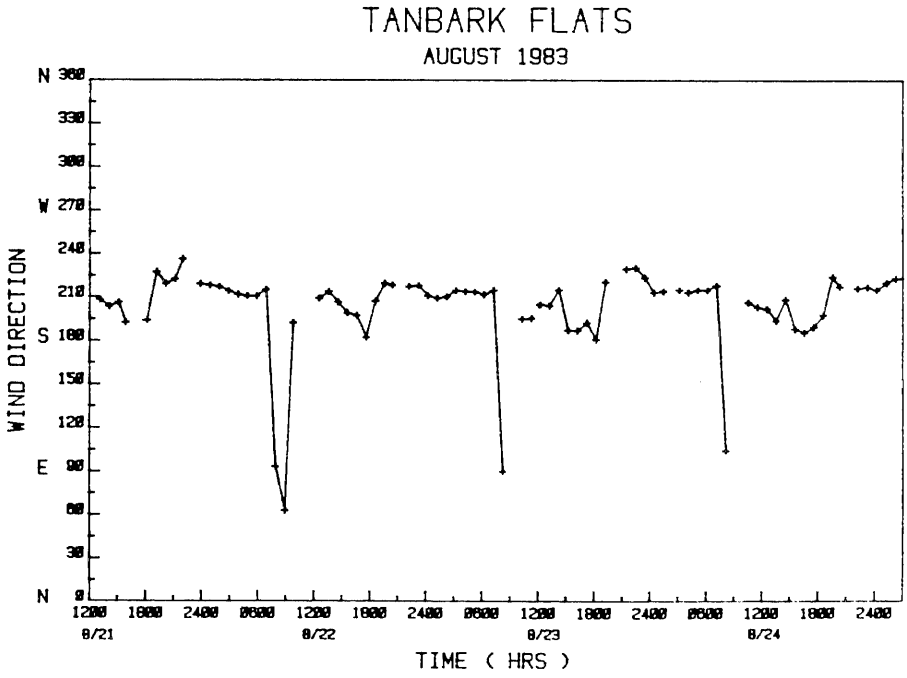

Figure 29. Wind direction vs. time at Tanbark Flats.

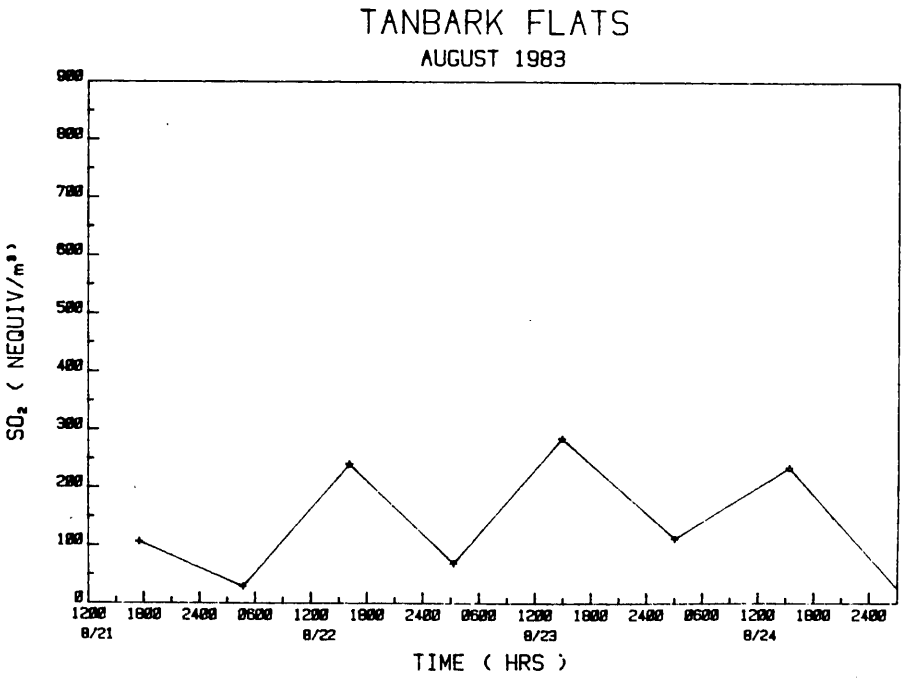

Figure 30. Sulfur dioxide concentration vs. time at Tanbark Flats.

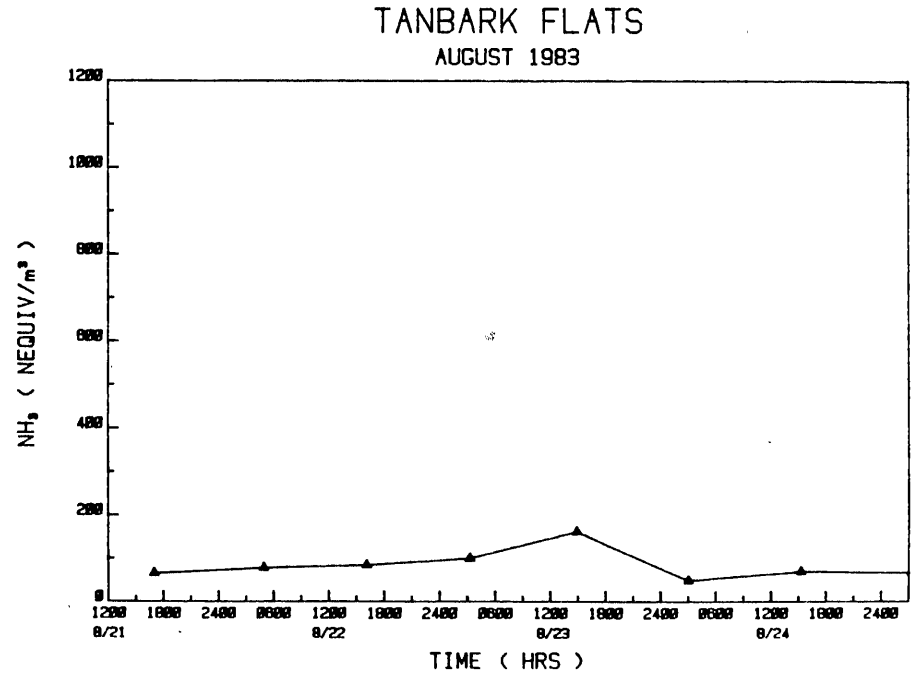

Figure 31. Ammonia concentration vs. time at Tanbark Flats.

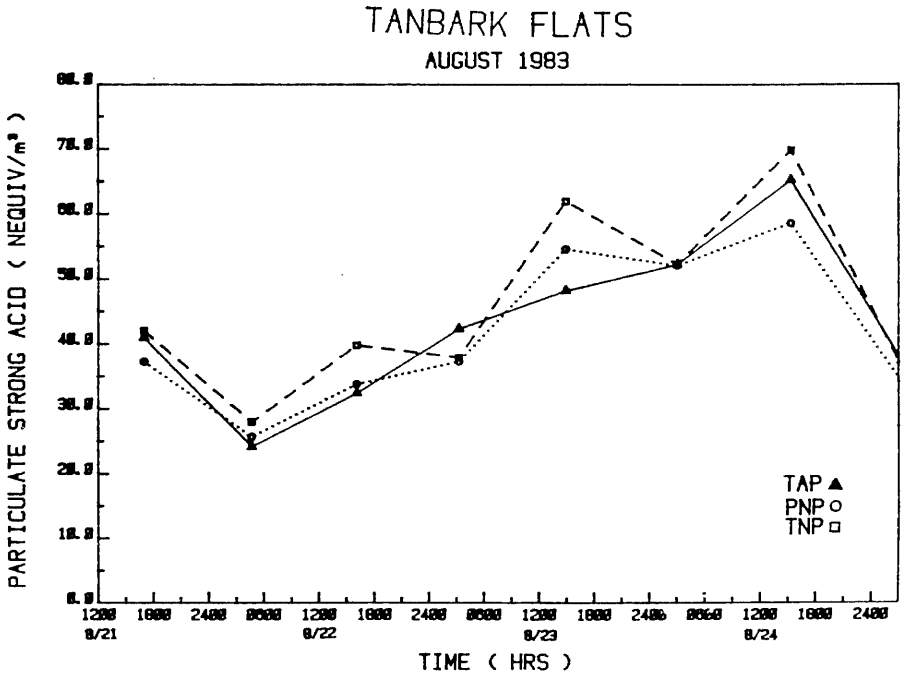

Figure 32. Particulate strong acid vs. time at Tanbark Flats. TAP, PNP and TNP refer to the Teflon filters on sampling train nos. 1,2 and 3 respectively. See Fig.2 for filter designations.

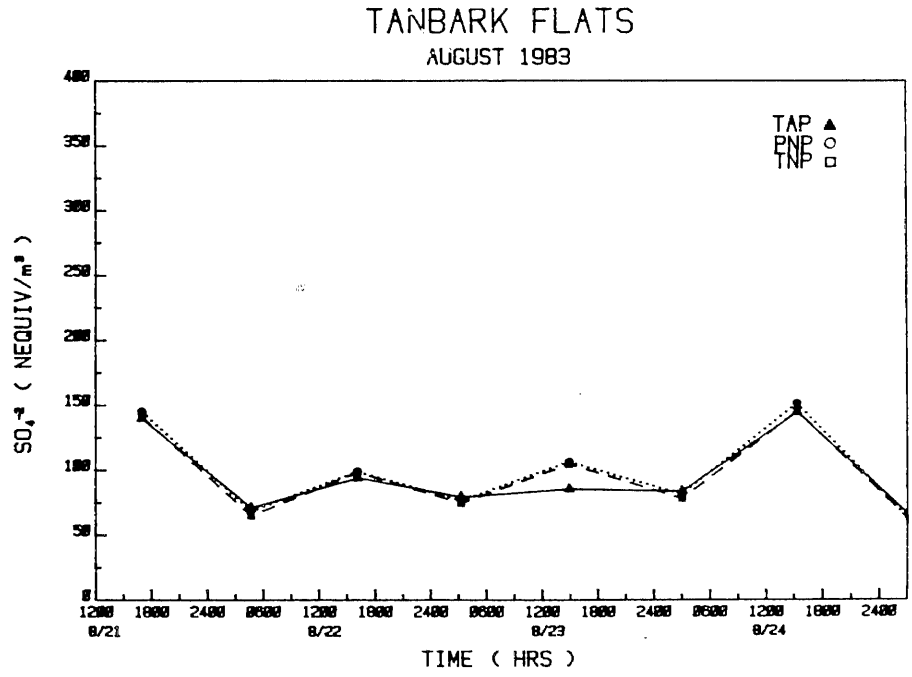

Figure 33. Fine particulate sulfate vs. time at Tanbark Flats. See Fig.2 for filter designations.

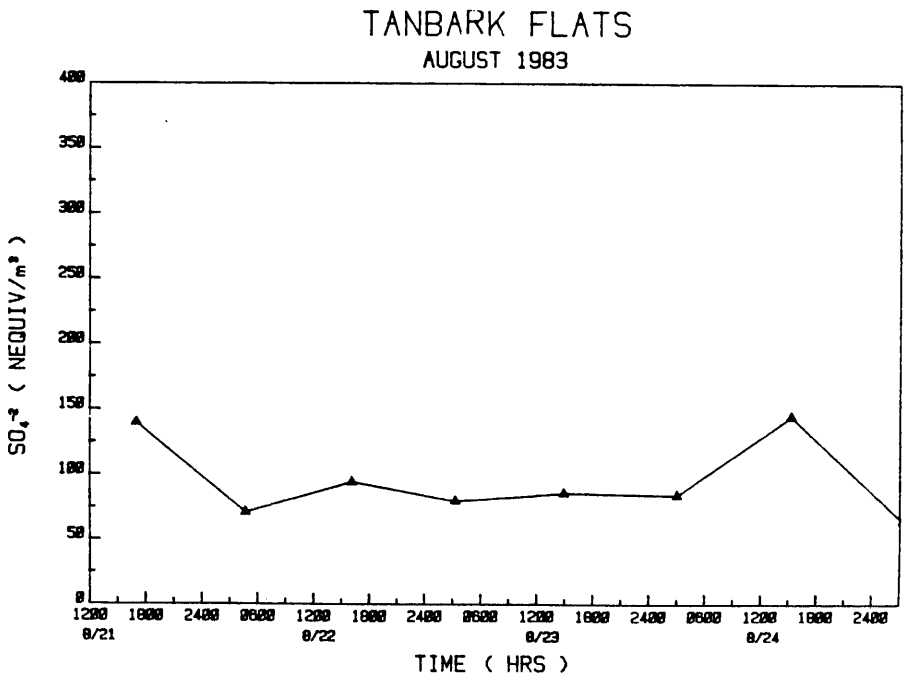

Figure 34. Fine particulate sulfate vs. time at Tanbark Flats.

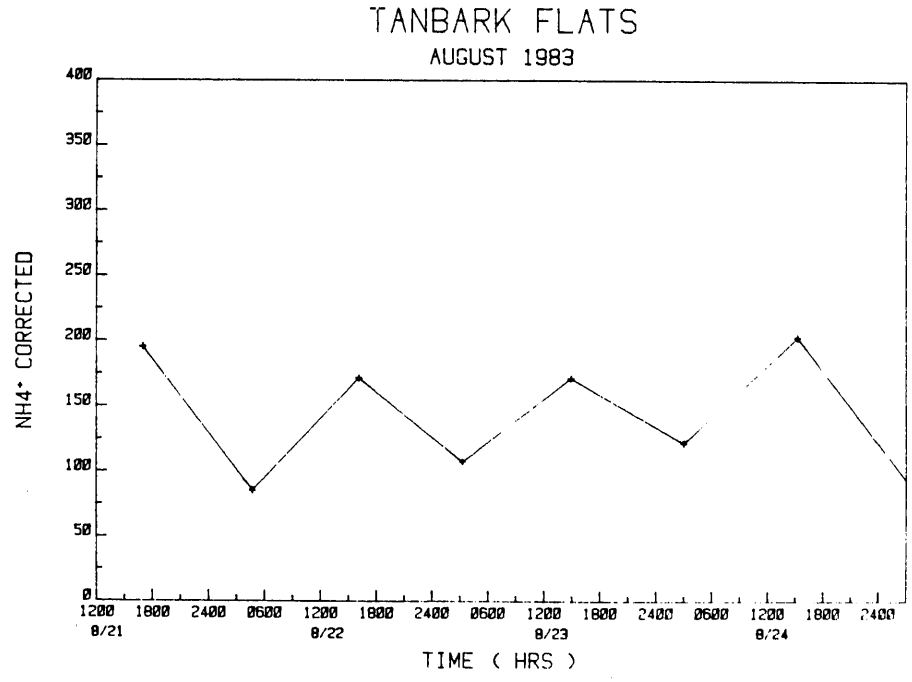

Figure 35. Fine particulate ammonium vs. time at Tanbark Flats.

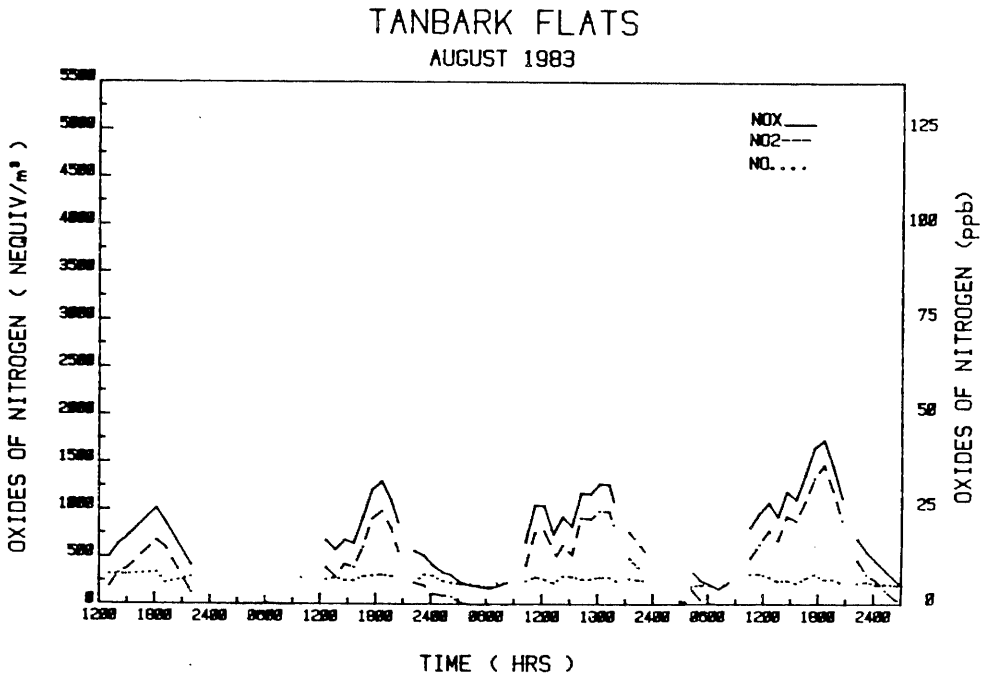

Figure 36. Oxides of nitrogen vs. time at Tanbark Flats.

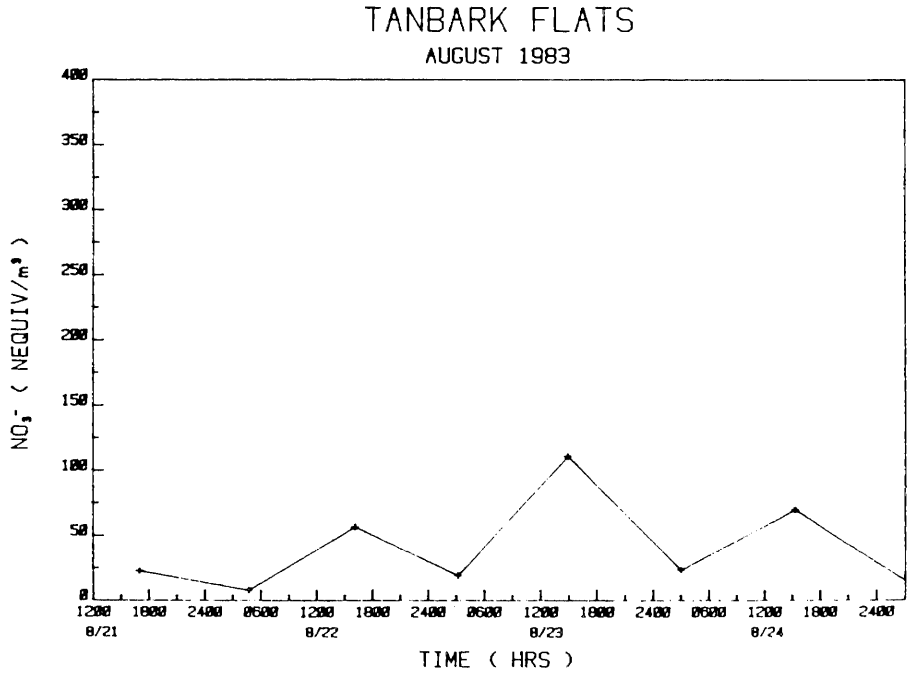

Figure 37. Fine particulate nitrate vs. time at Tanbark Flats.

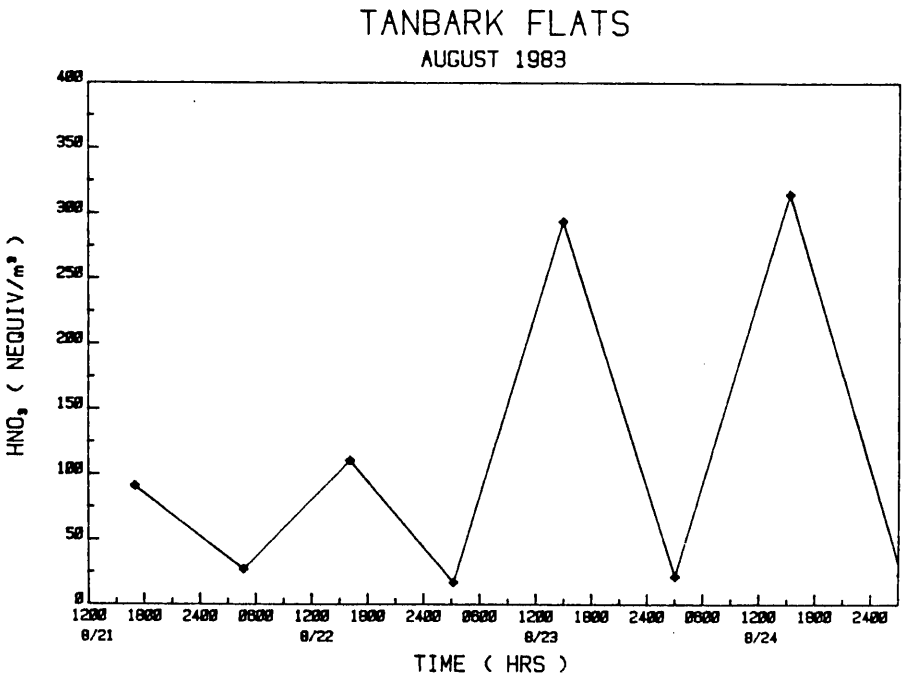

Figure 38. Nitric acid concentration vs. time at Tanbark Flats.

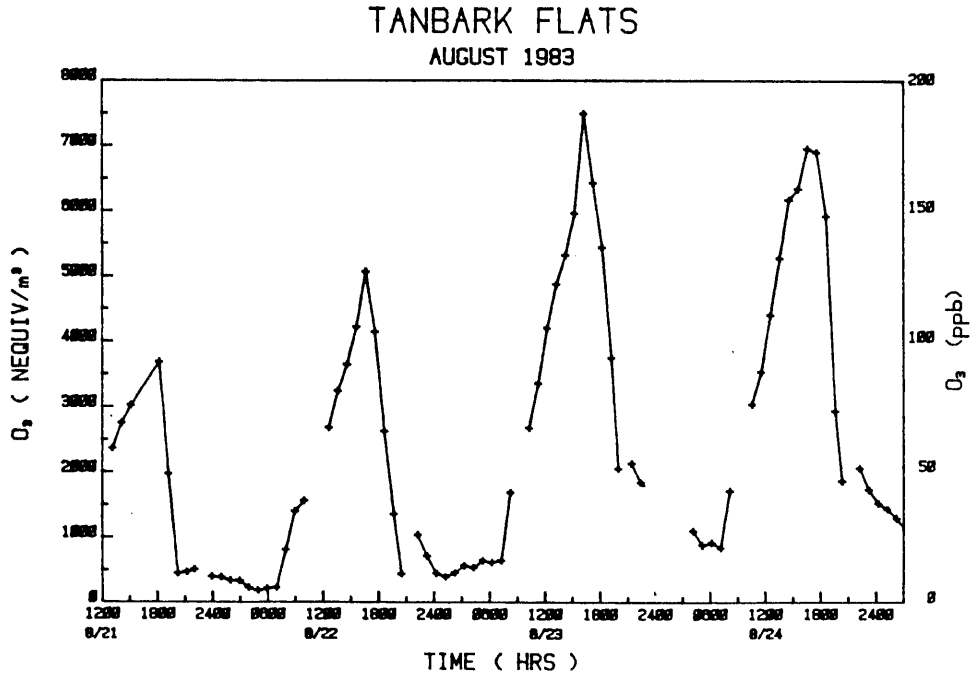

Figure 39. Ozone concentration vs. time at Tanbark Flats.

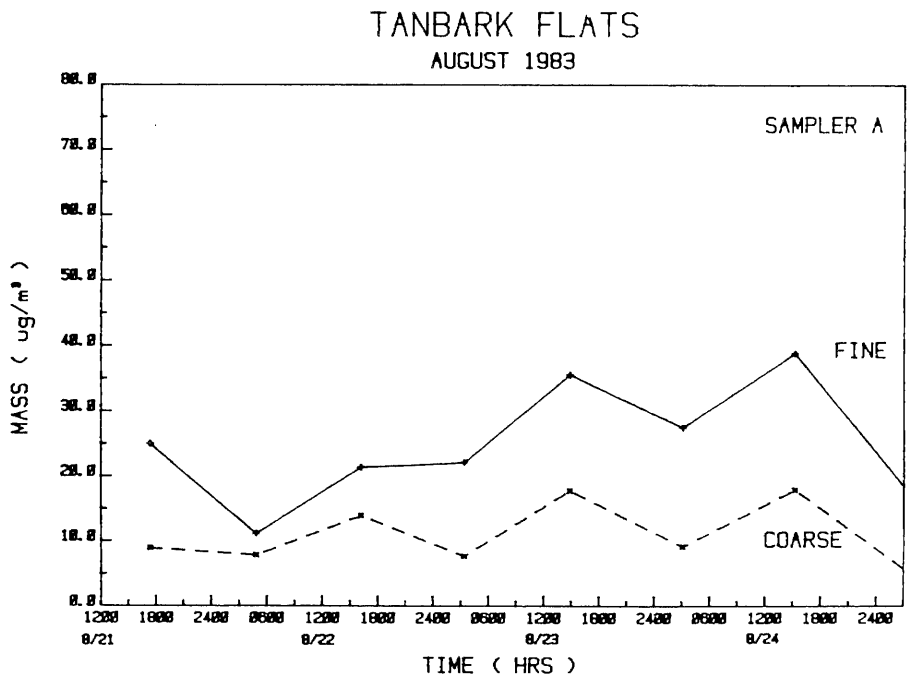

Figure 40. Fine and coarse particulate concentrations at Tanbark Flats.

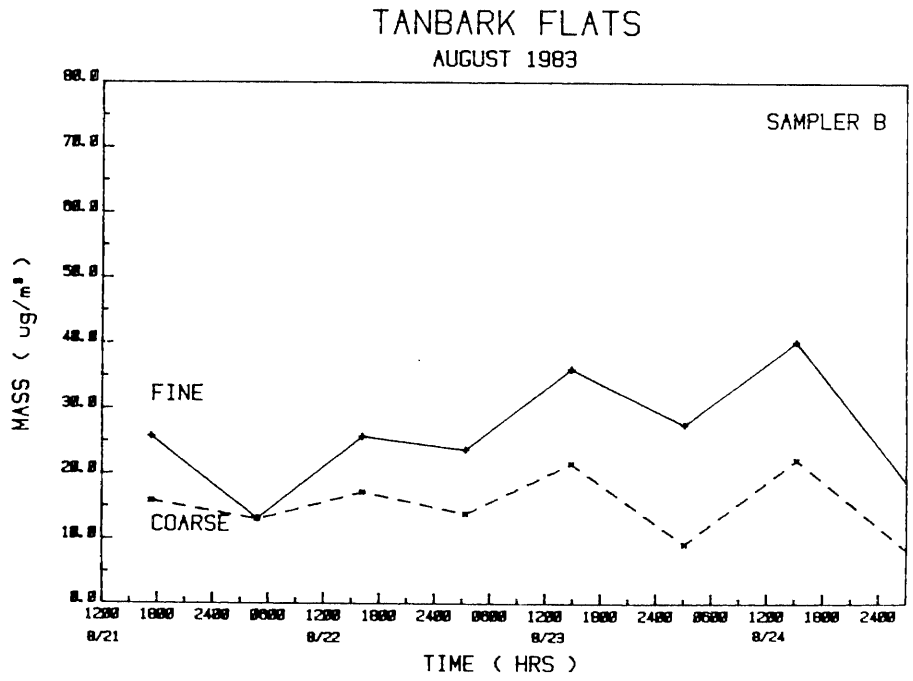

Figure 41. Same as Fig. 40 but for dichotomous sampler B.

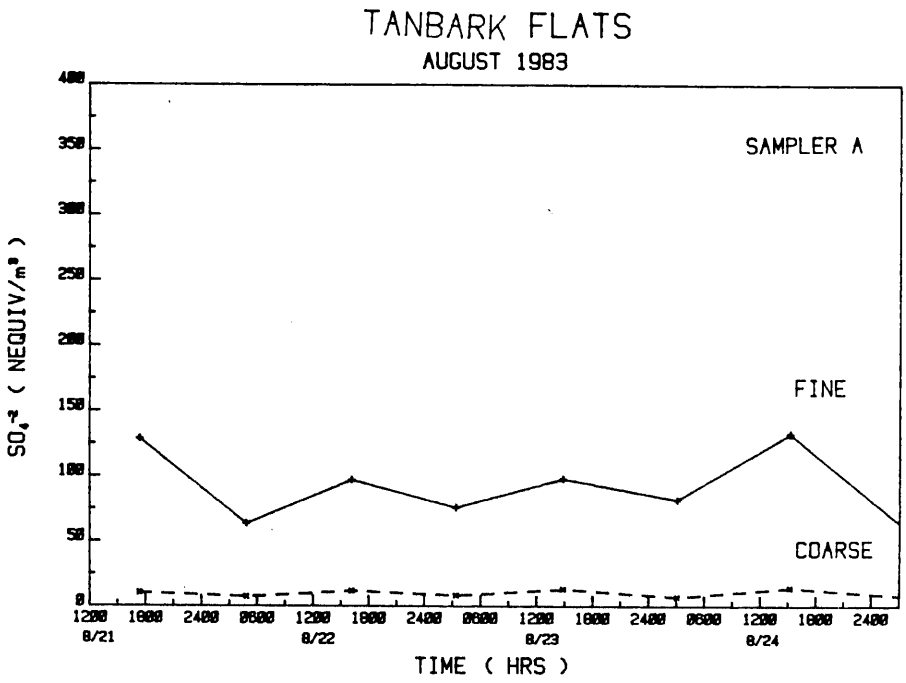

Figure 42. Fine and coarse sulfate concentrations at Tanbark Flats.

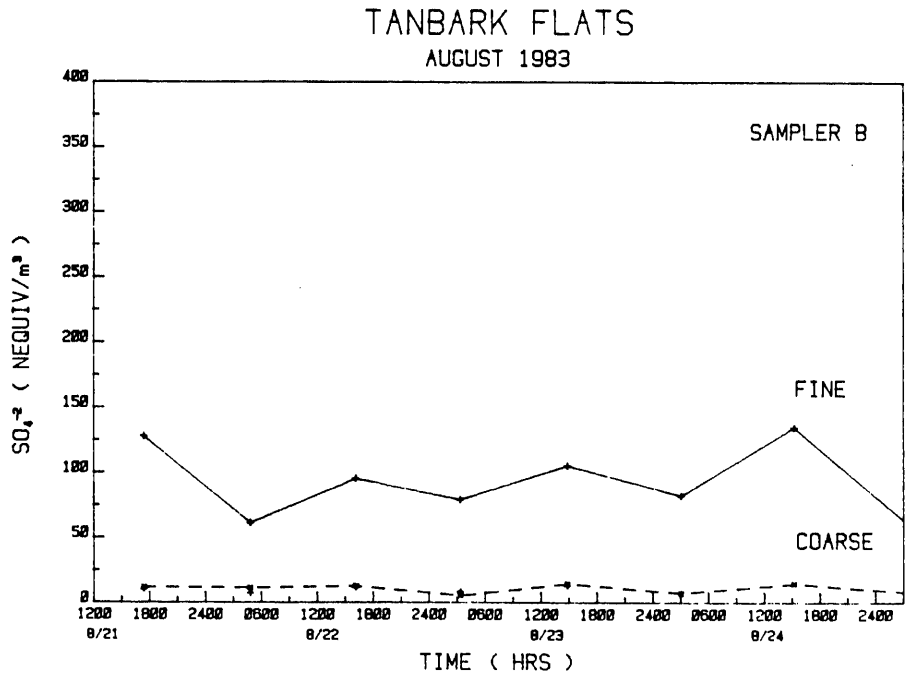

Figure 43. Same as Fig. 42 but for dichotomous sampler B.

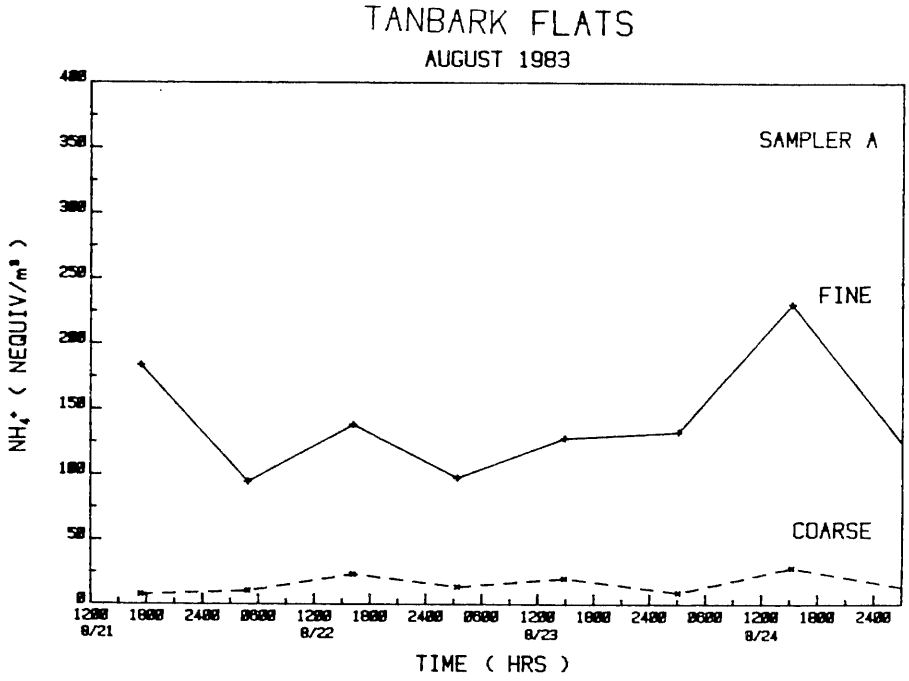

Figure 44. Fine and coarse ammonium concentrations at Tanbark Flats.

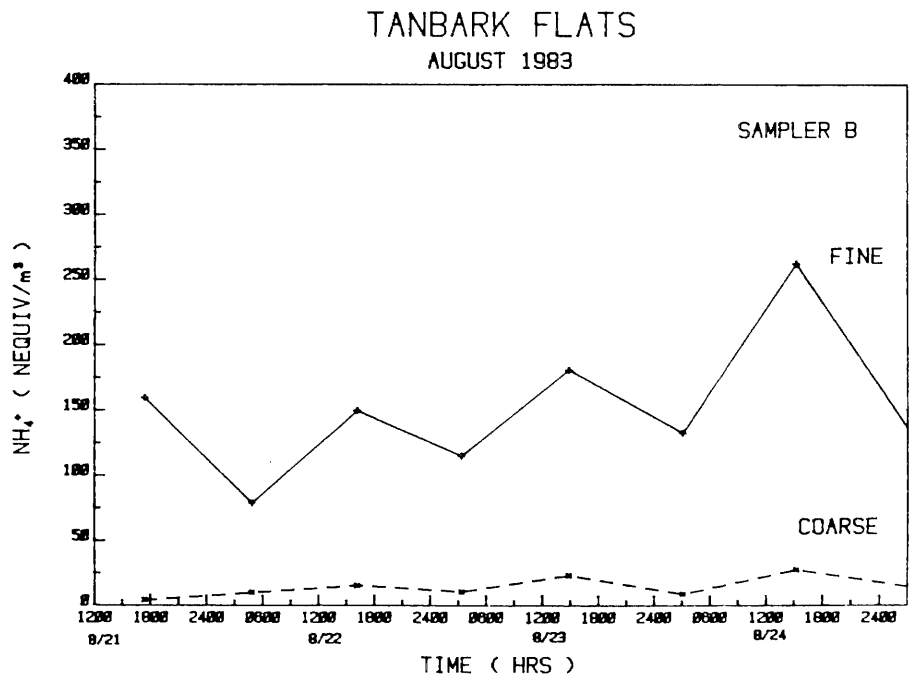

Figure 45. Same as Fig. 44 but for dichotomous sampler B.

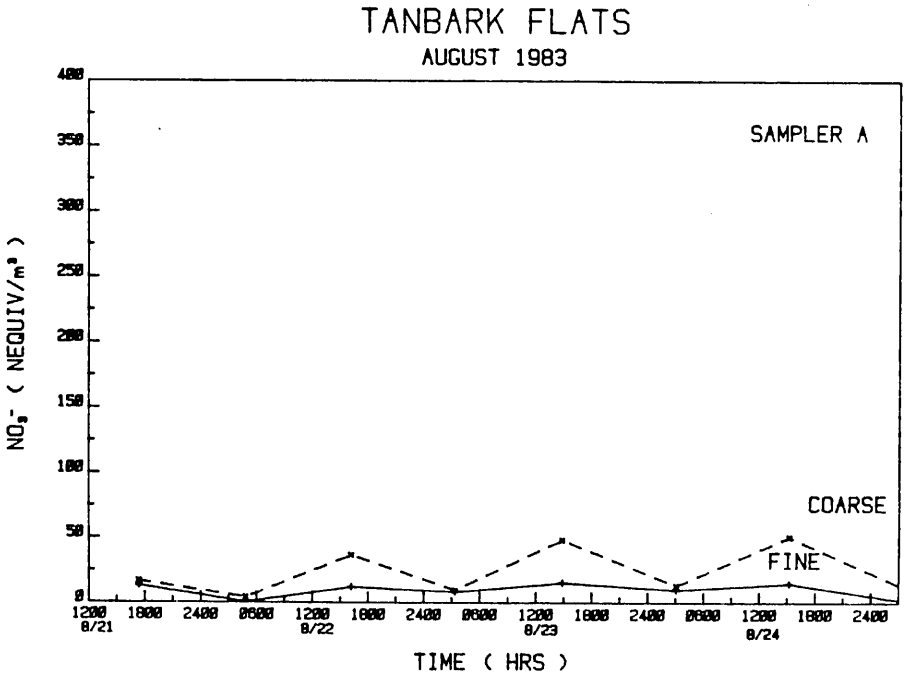

Figure 46. Fine and coarse nitrate concentrations at Tanbark Flats.

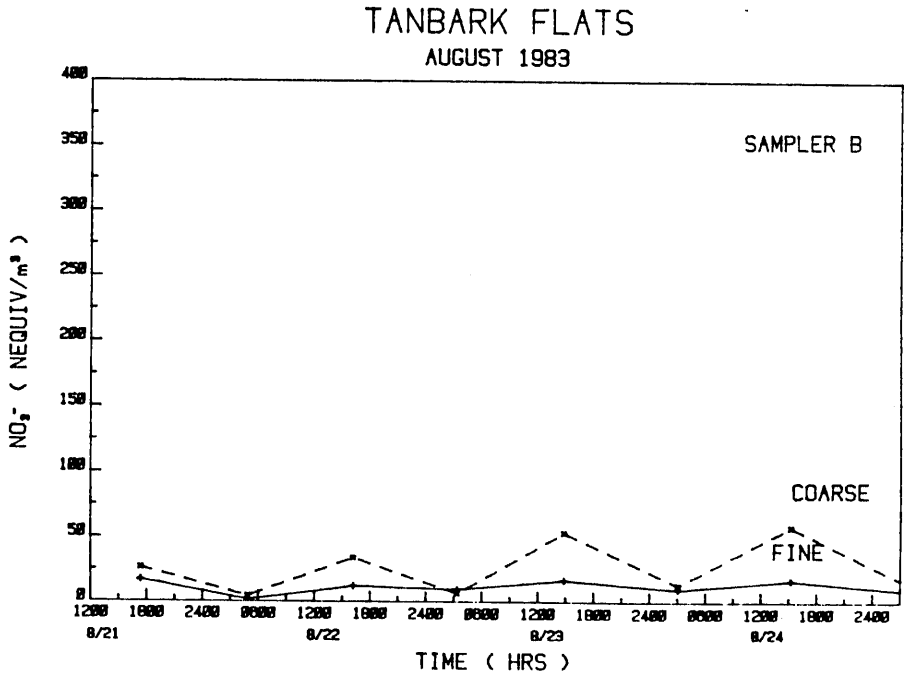

Figure 47. Same as Fig. 46 but for dichotomous sampler B.

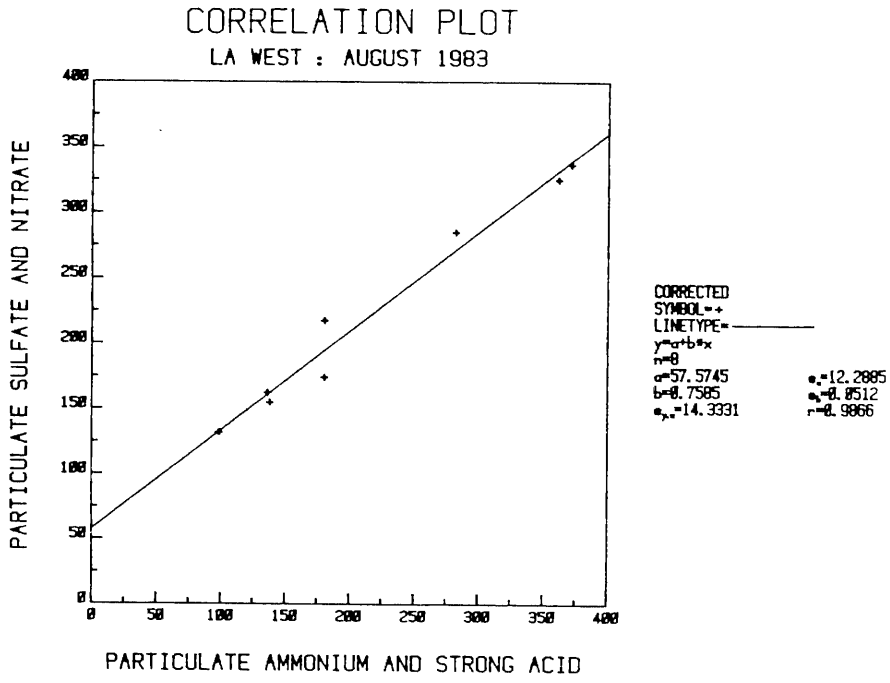

Figure 48. Anion vs. cation concentrations at West Los Angeles.

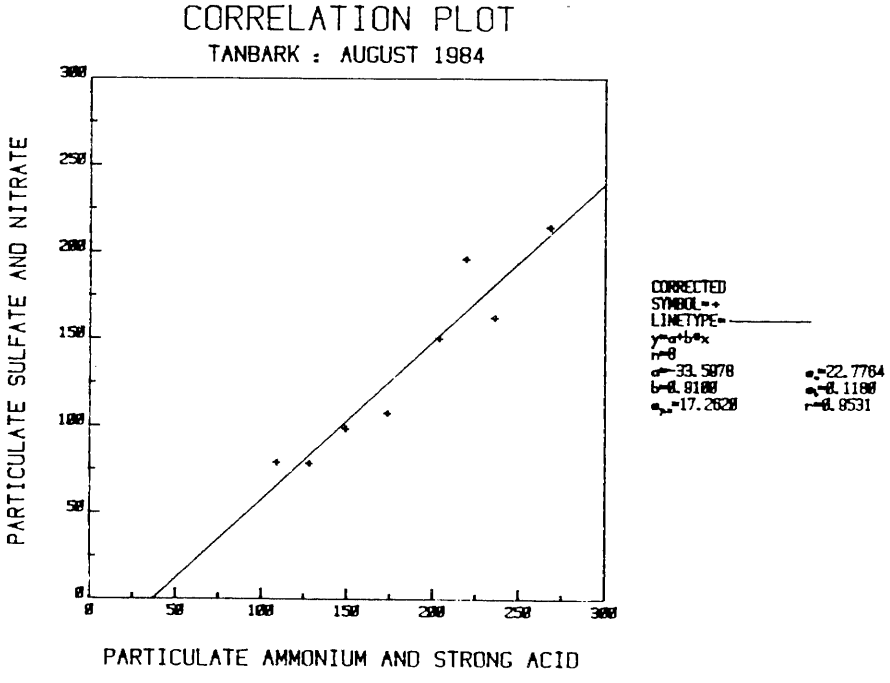

Figure 49. Anion vs. cation concentrations at Tanbark Flats.

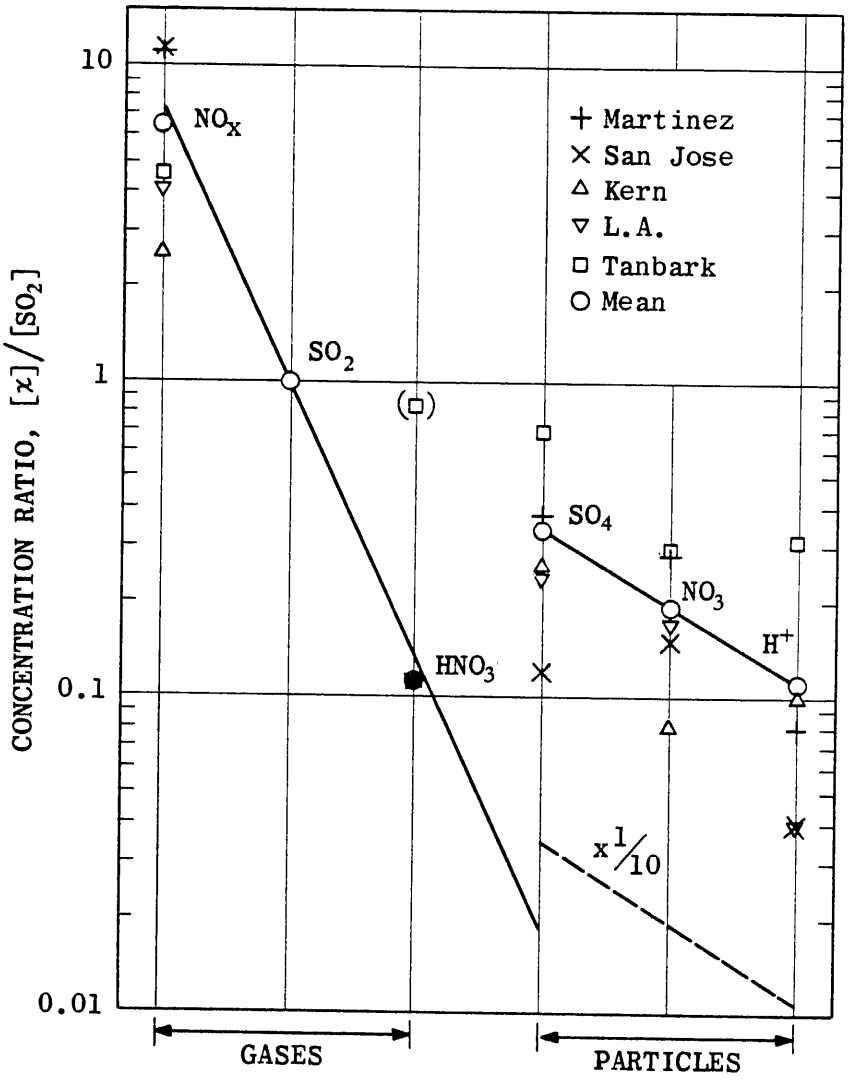

Figure 50. Ratio of concentrations (in equivalents / m^3) of acidic pollutants. The solid line connects the means over five California locations. Relative deposition fluxes are given very approximately by the solid line for gases and by the dashed line for particles.

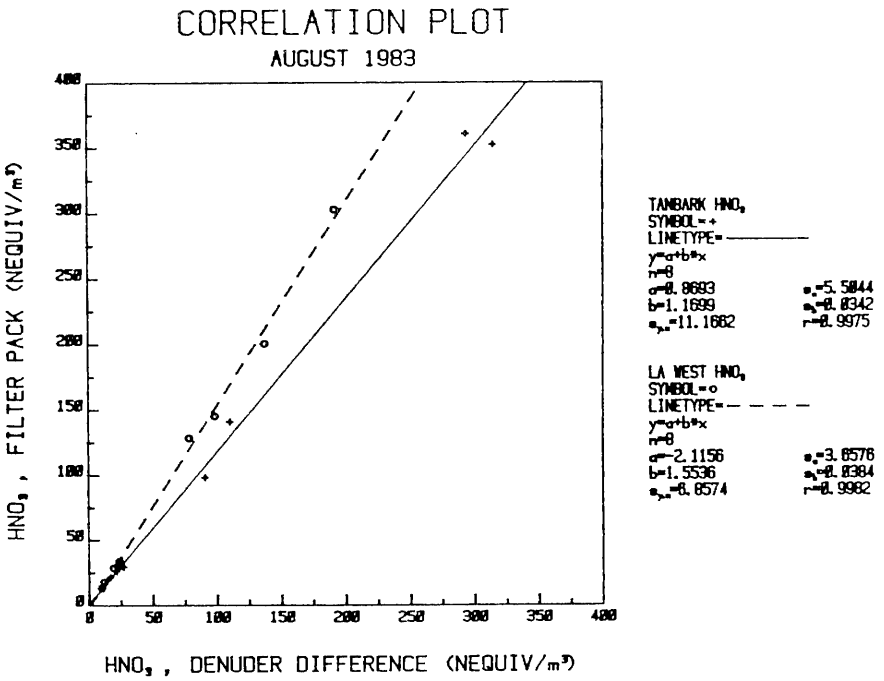

Figure 51. Nitric acid determined by filter pack (sampling train no. 3) vs. that from denuder difference, for Tanbark and L. A.

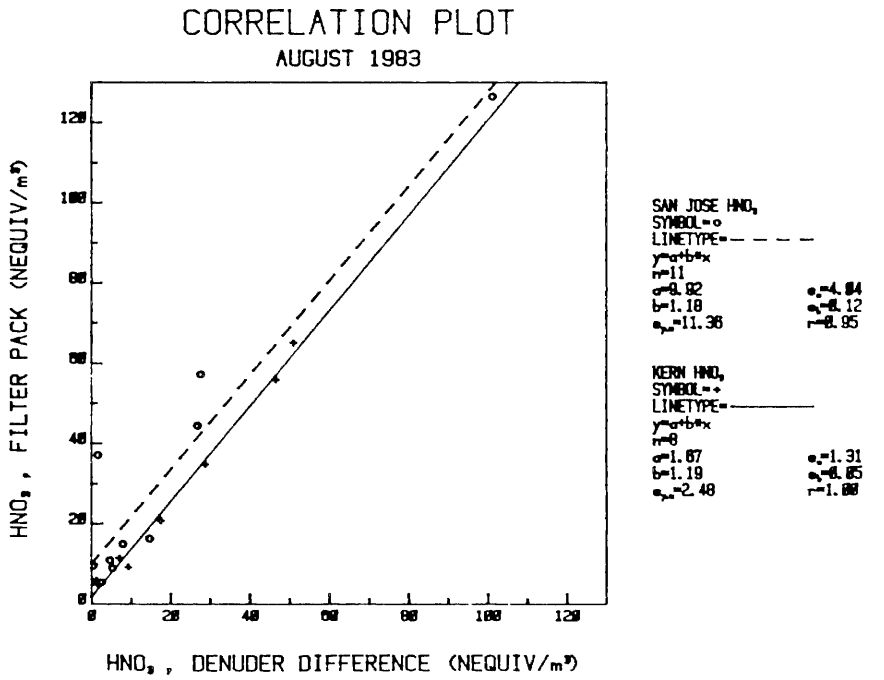

Figure 52. Same as Fig. 51 but for San Jose and the Kern River Canyon.

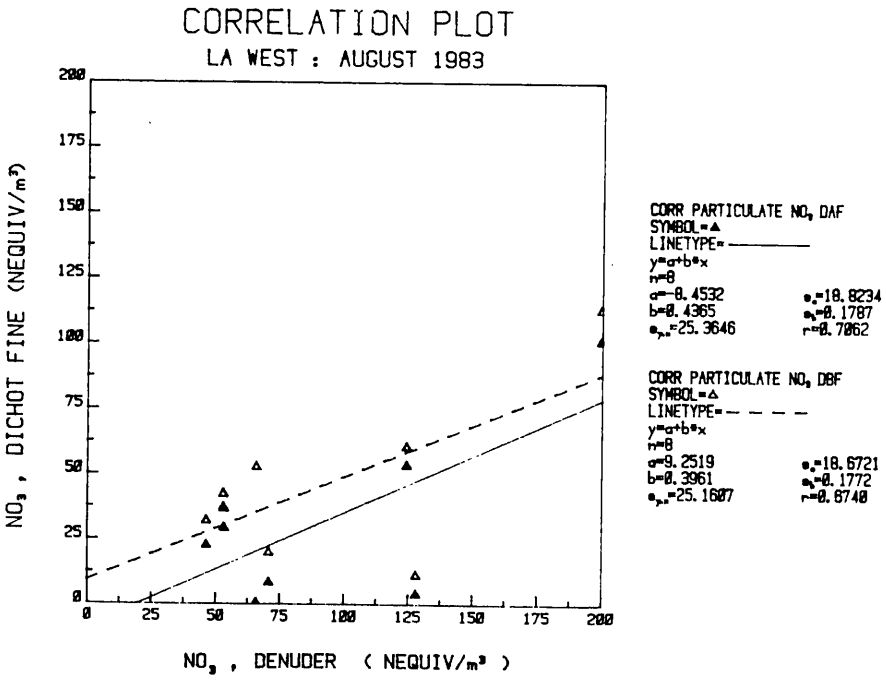

Figure 53. Fine nitrate particulate from the dichotomous samplers vs. that from the denuder sampling train (No. 2), at West Los Angeles.

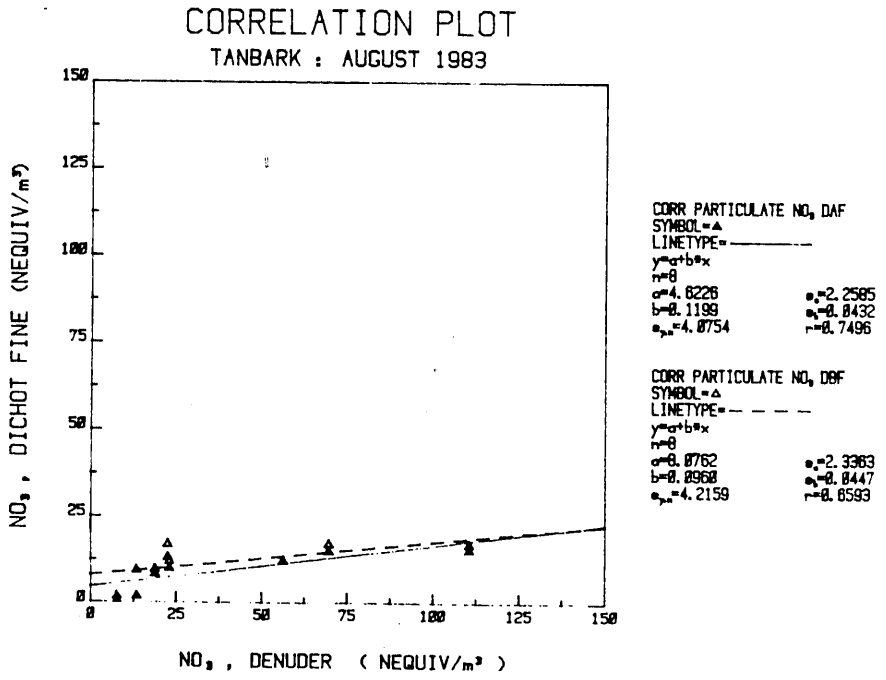

Figure 54. Same as Fig. 53 but for Tanbark Flats.

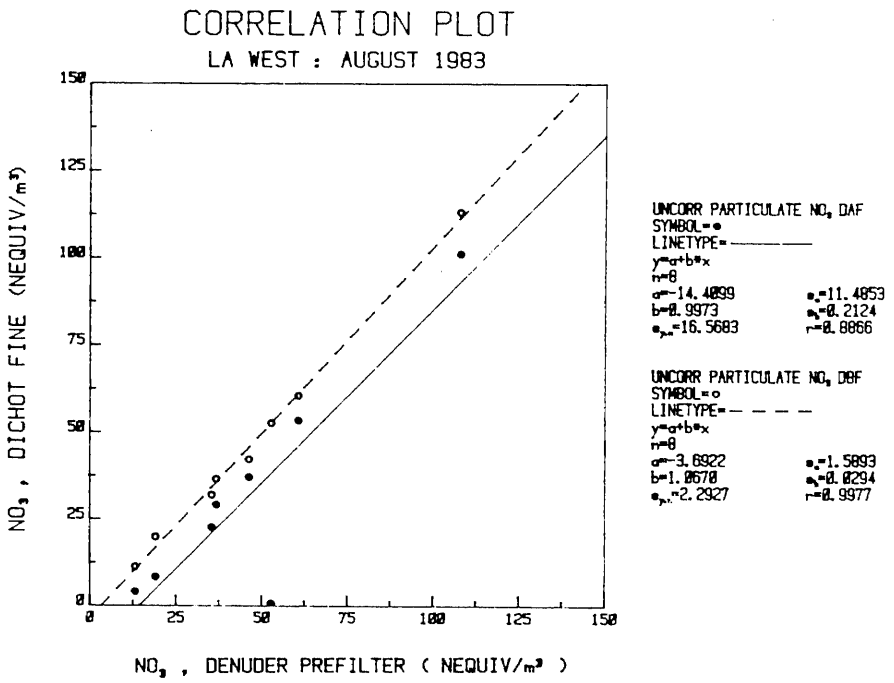

Figure 55. Fine nitrate from the dichotomous samplers vs. that from the prefilter of the denuder sampling train (No. 2), at West L. A.

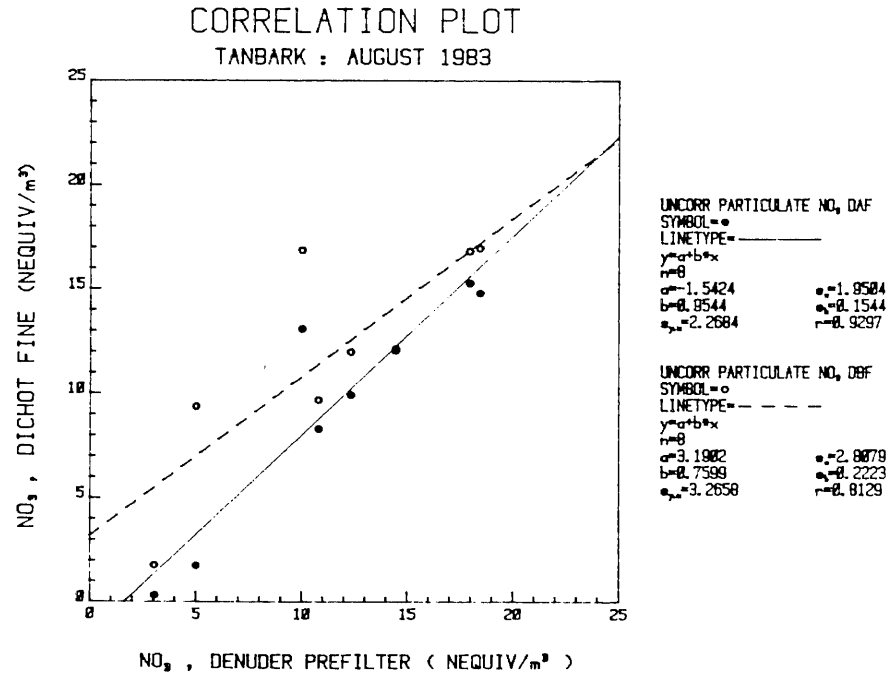

Figure 56. Same as Fig. 55 but for Tanbark Flats.

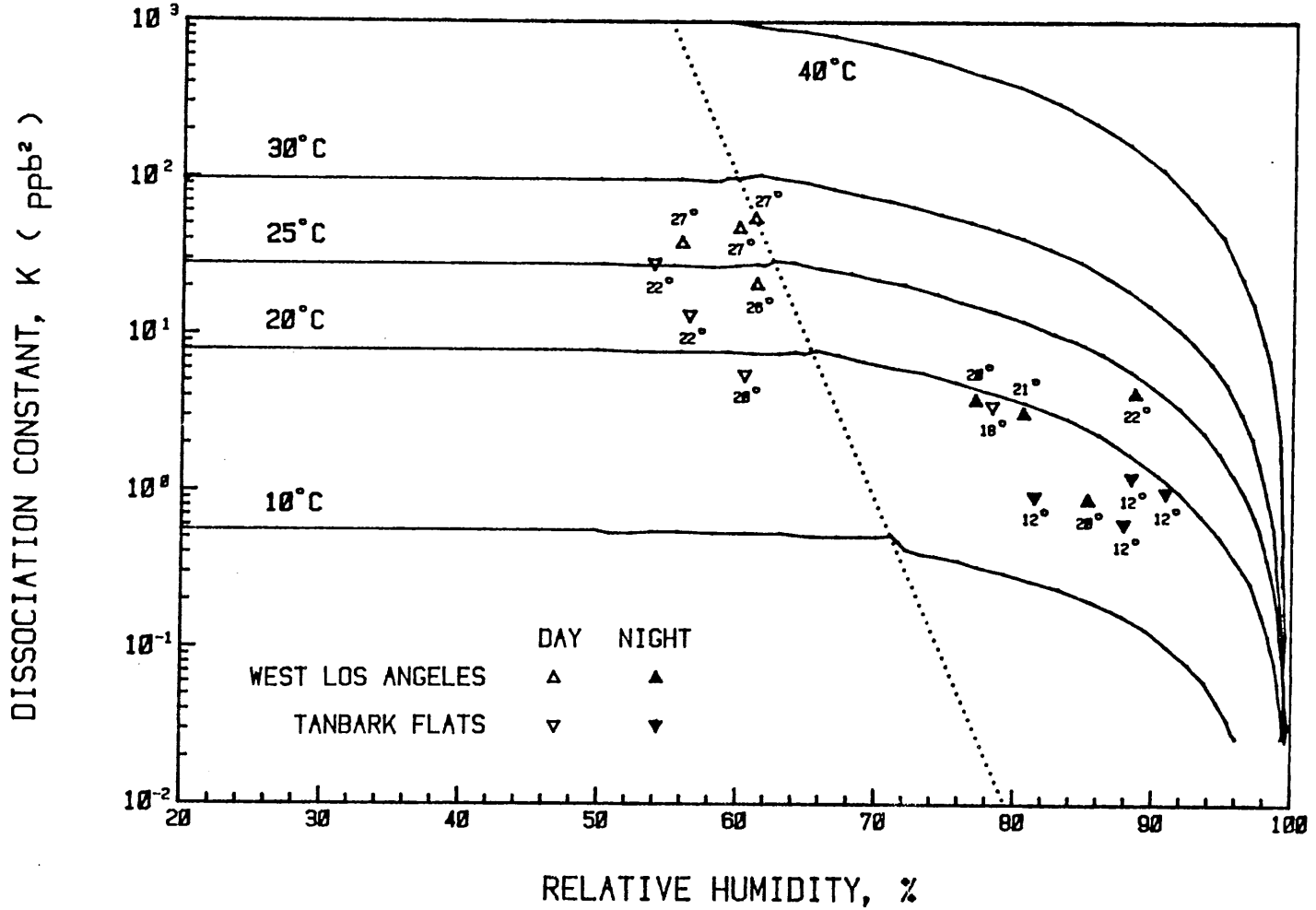

Figure 57. Dependence of the dissociation constant of ammonium nitrate on relative humidity and temperature, based on Stelson, et al., (Ref. 16), solid line. The dashed line is the deliquesence point. Data points are labelled with the ambient temperature.

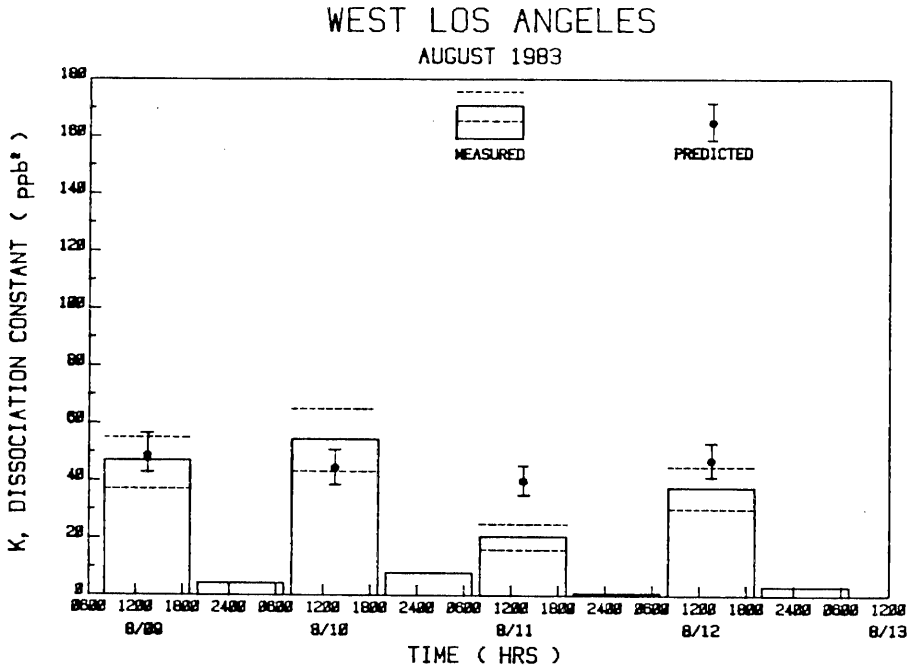

Figure 58. Comparison of the measured and predicted dissociation constant of ammonium nitrate at West Los Angeles.

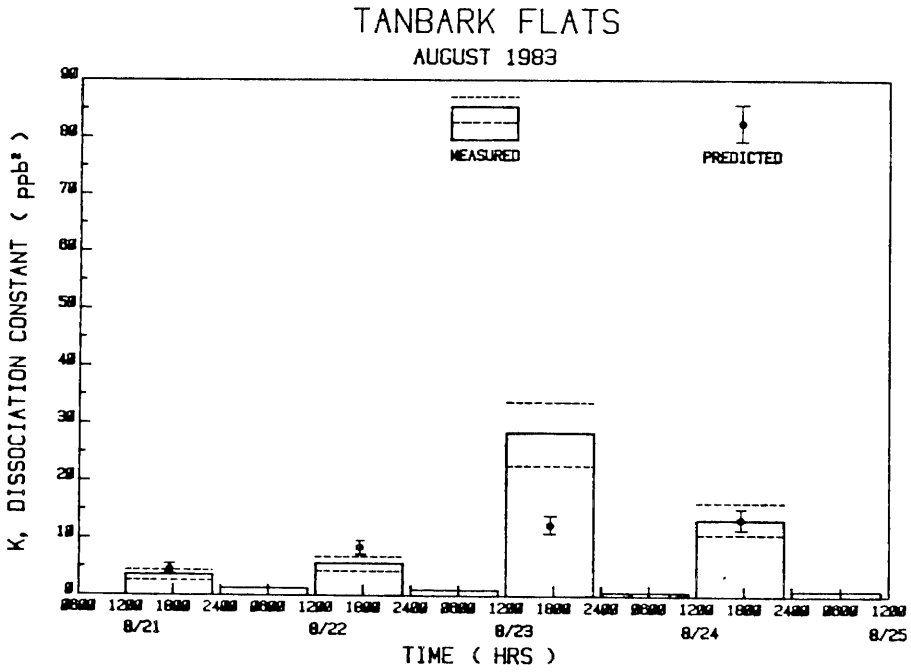

Figure 59. Same as Fig. 58 but for Tanbark Flats.

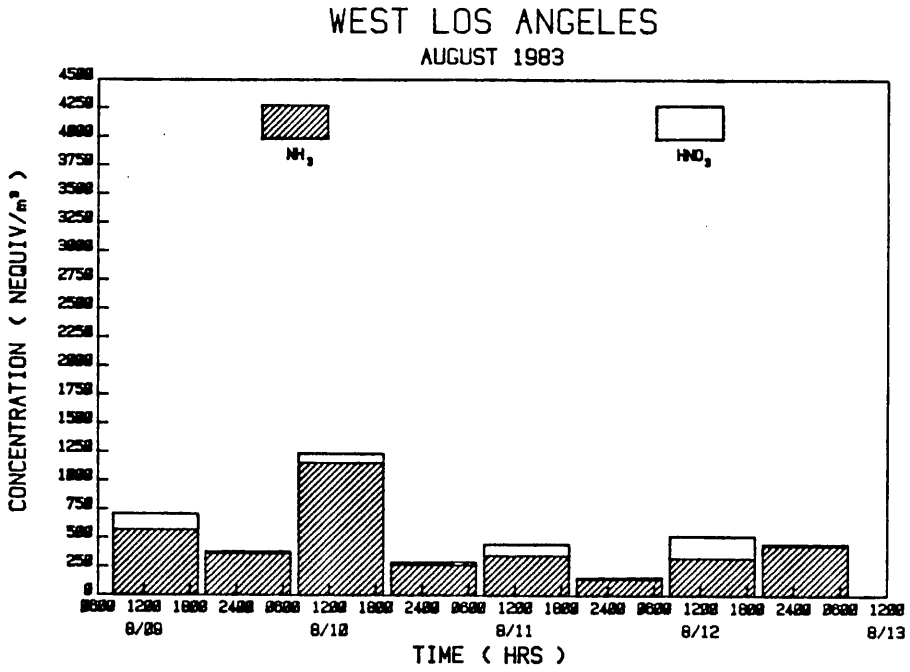

Figure 60. Observed concentrations of ammonia and nitric acid at West L. A.

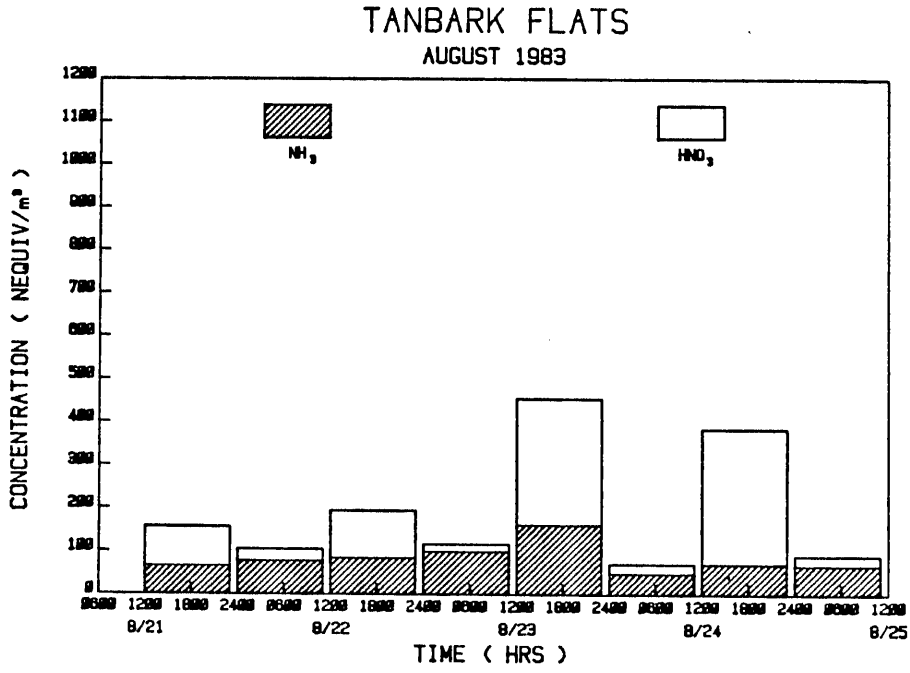

Figure 61. Same as Fig. 60 but for Tanbark Flats.

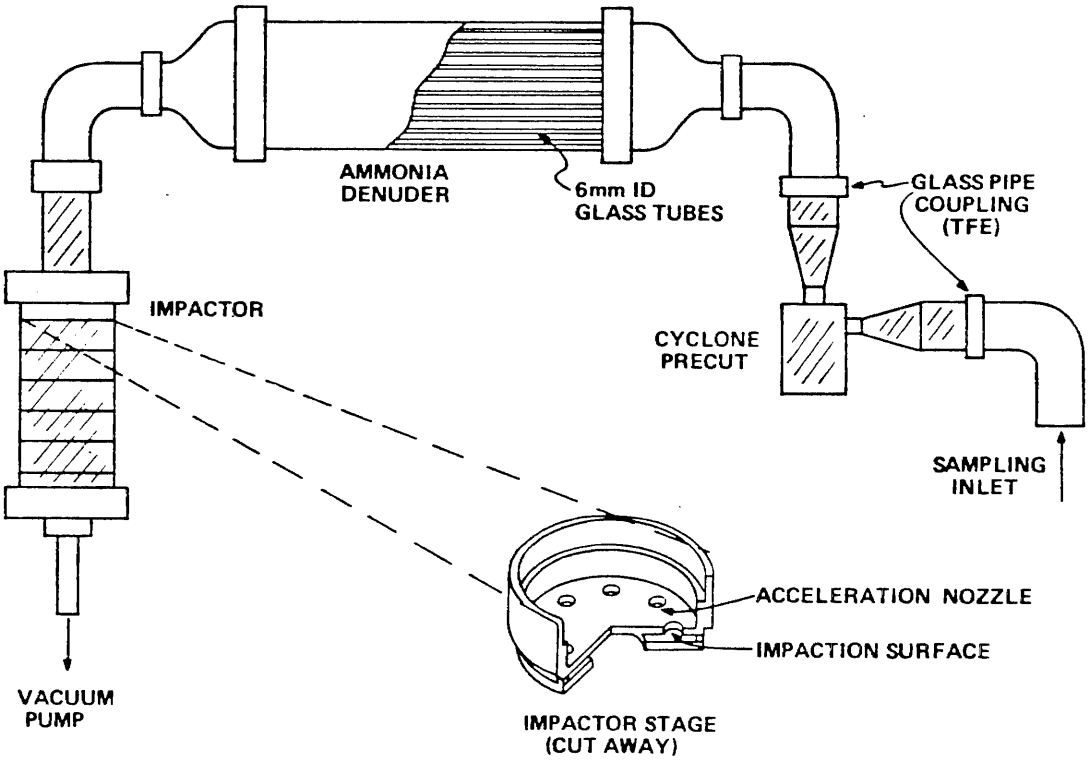

Figure 62. Sampling system for measurement of the size distribution of acidic particles.

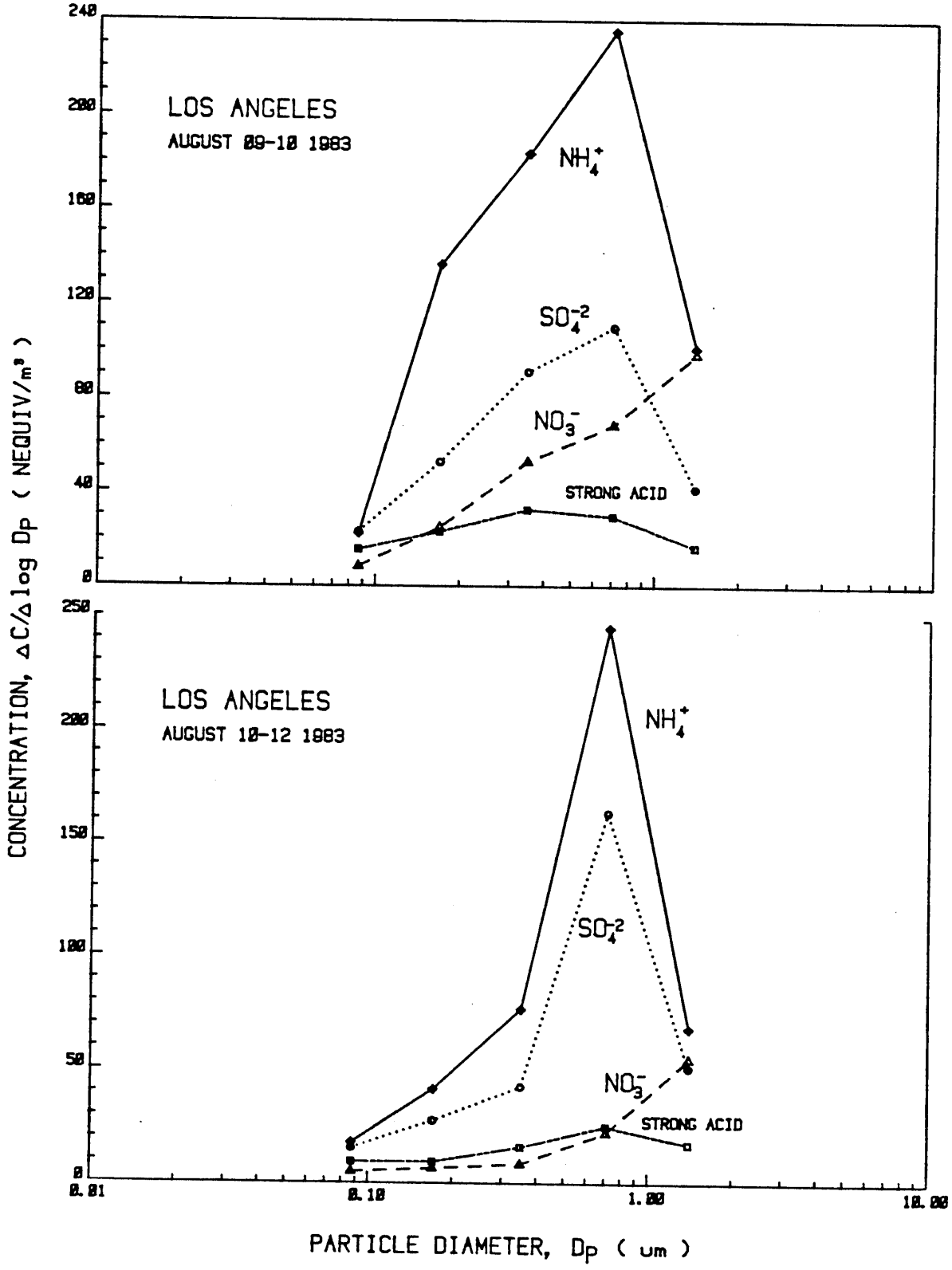

Figure 63. Particle size distributions at West Los Angeles from chemical analysis of deposits on cascade impactor stages.

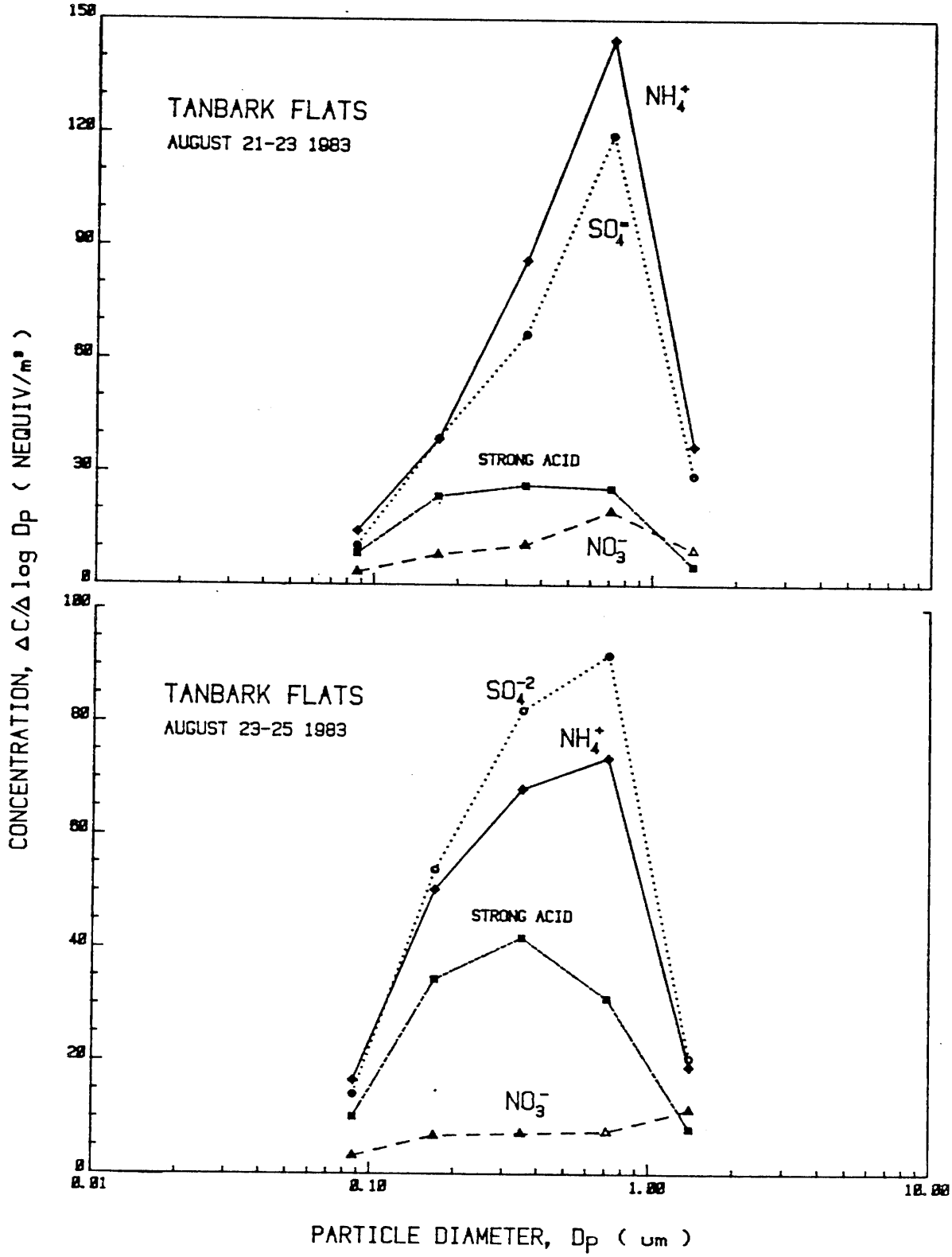

Figure 64. Particle size distributions by chemical species for Tanbark Flats.

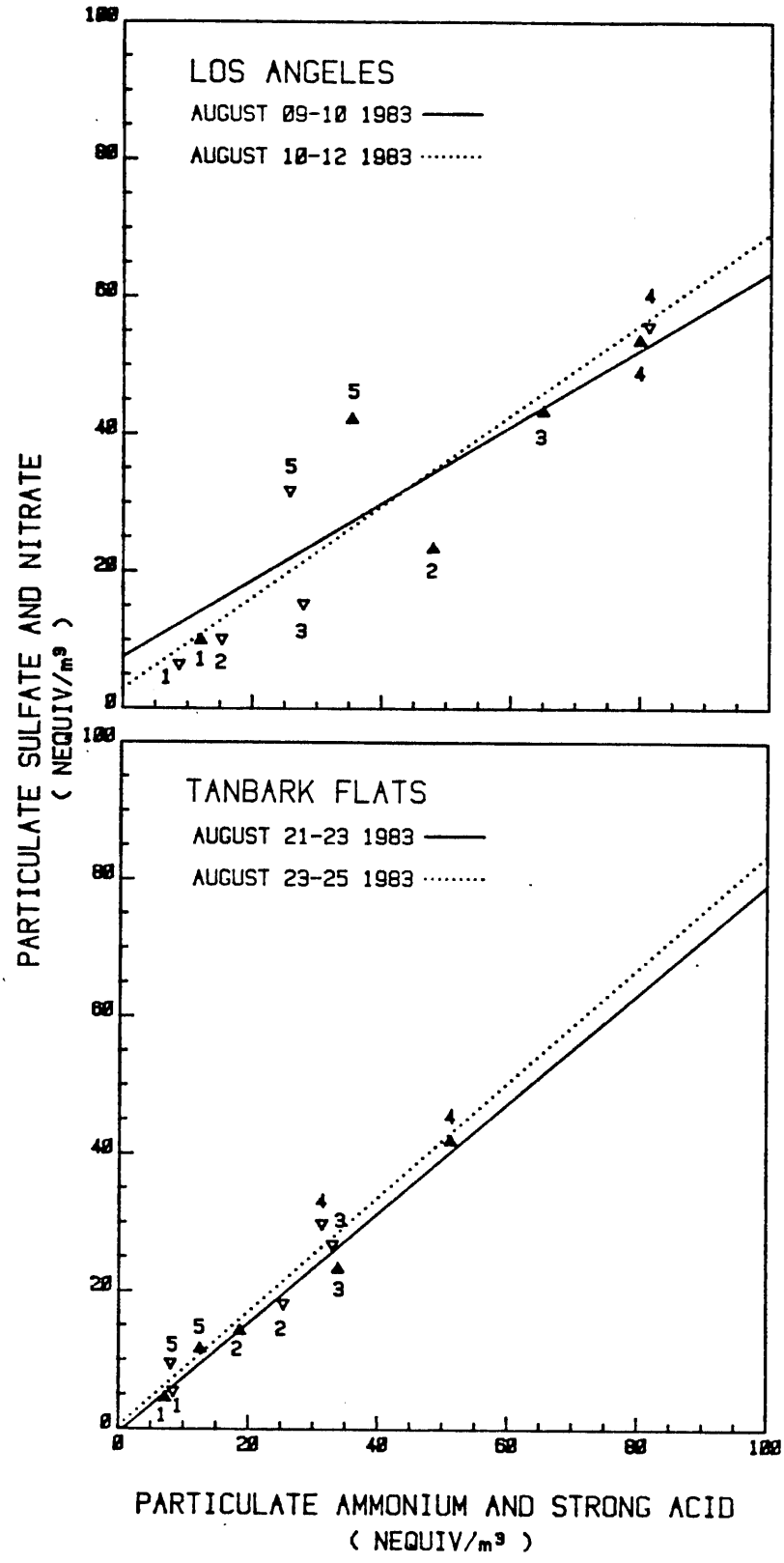

Figure 65. Anion vs. cation concentrations on impactor stages.

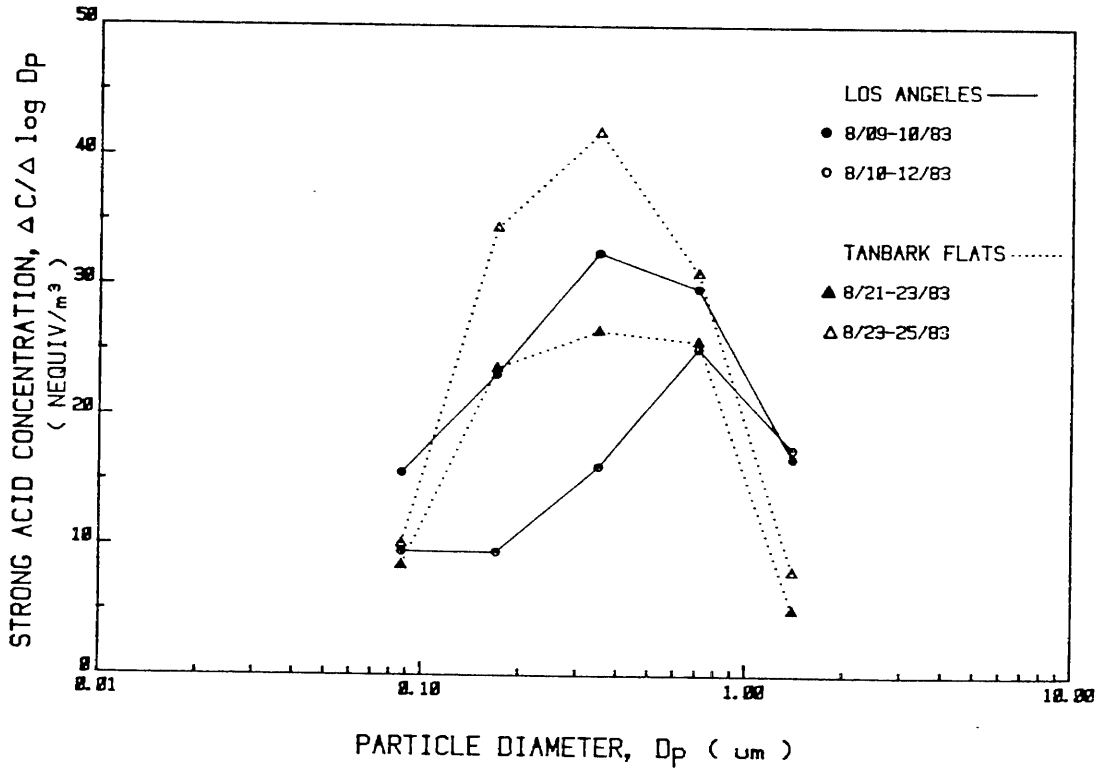

Figure 66. Size distributions for particulate strong acid.

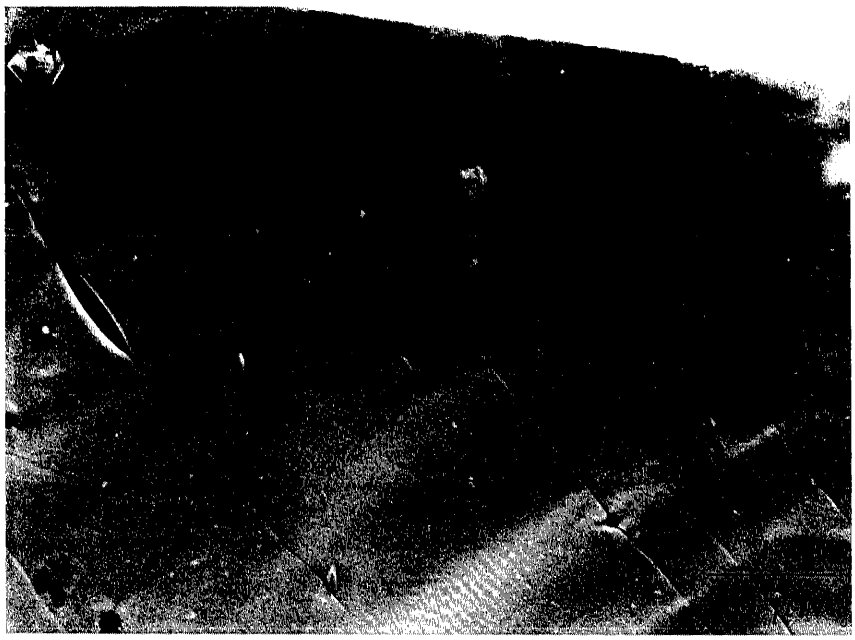

Figure 67. Scanning electron micrograph of iron film exposed to ambient air in western Los Angeles, showing acid-etched holes (dark circular spots).

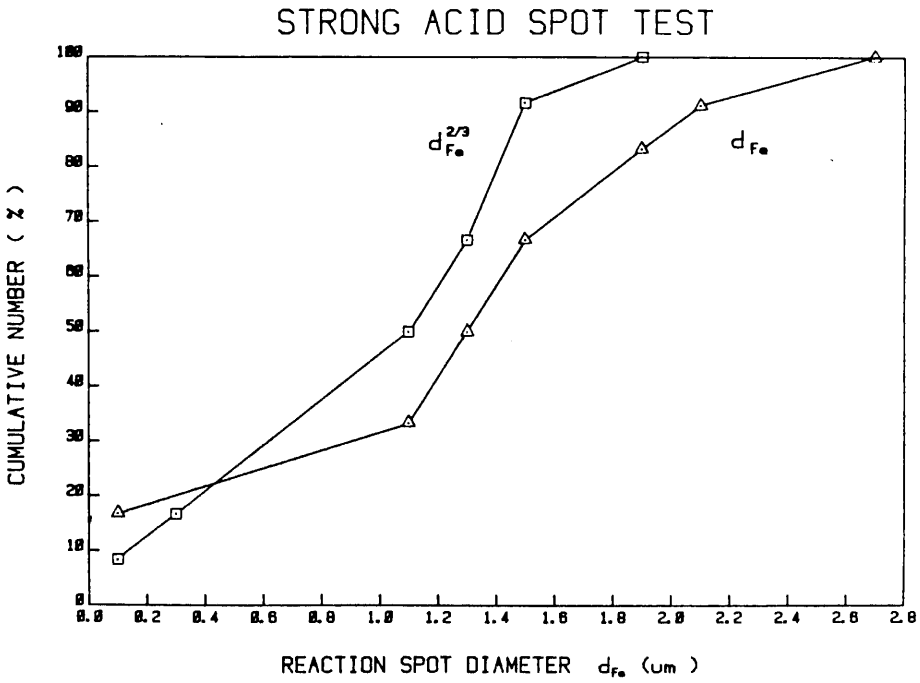

Figure 68. Size distribution of holes etched into an iron film exposed to ambient air in West Los Angeles. Hole diameter d is plotted and the corresponding airborne particle diameter, $d^{2/3}$.

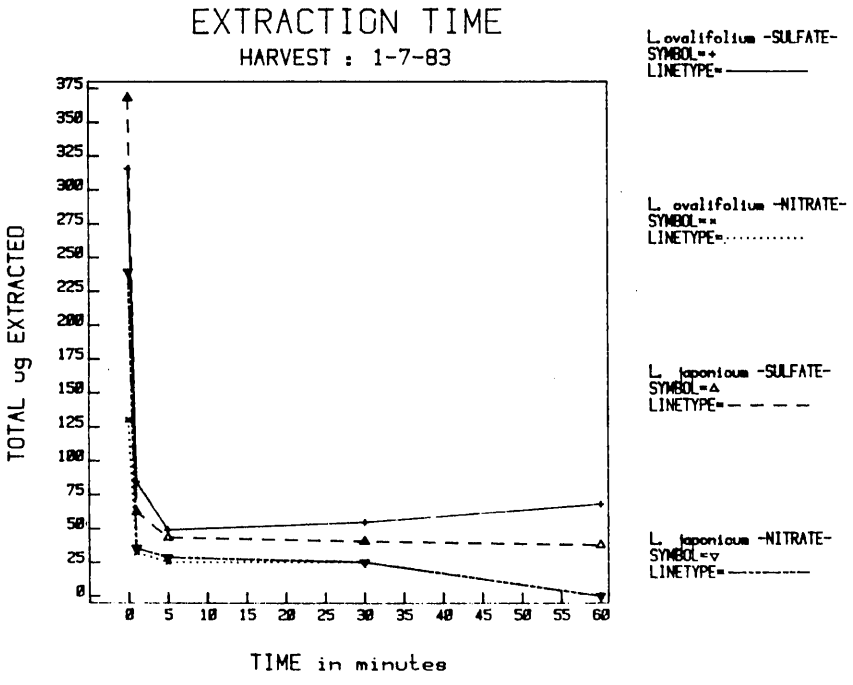

Figure 69. Data showing that most of the sulfate and nitrate on Ligustrum leaves is extracted in the first few minutes.

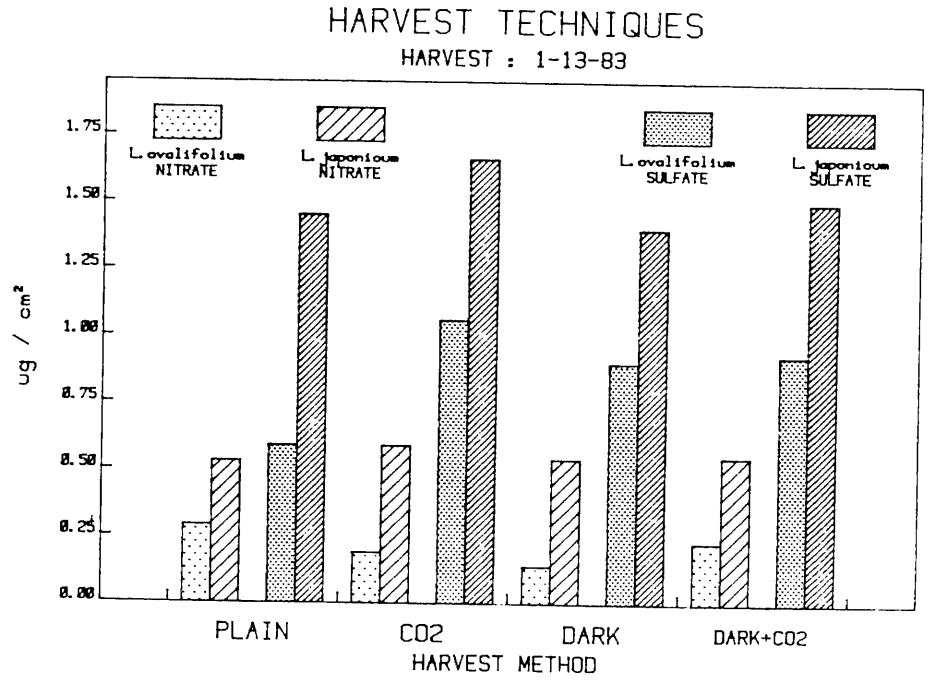

Figure 70. Data demonstrating that material is not extracted through stomata.

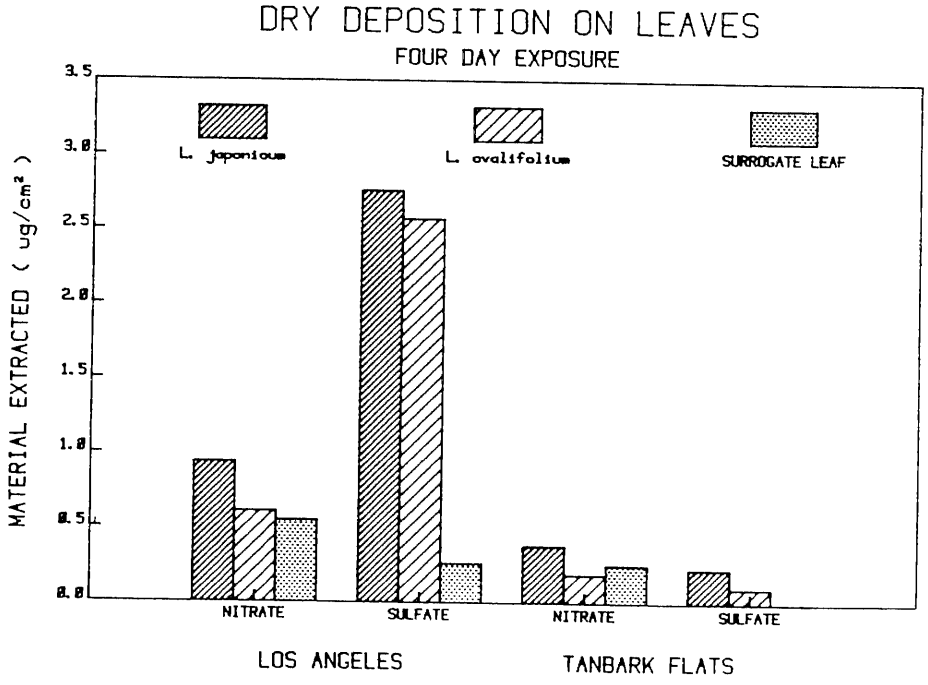

Figure 71. Deposits on Ligustrum leaves and surrogate surfaces.

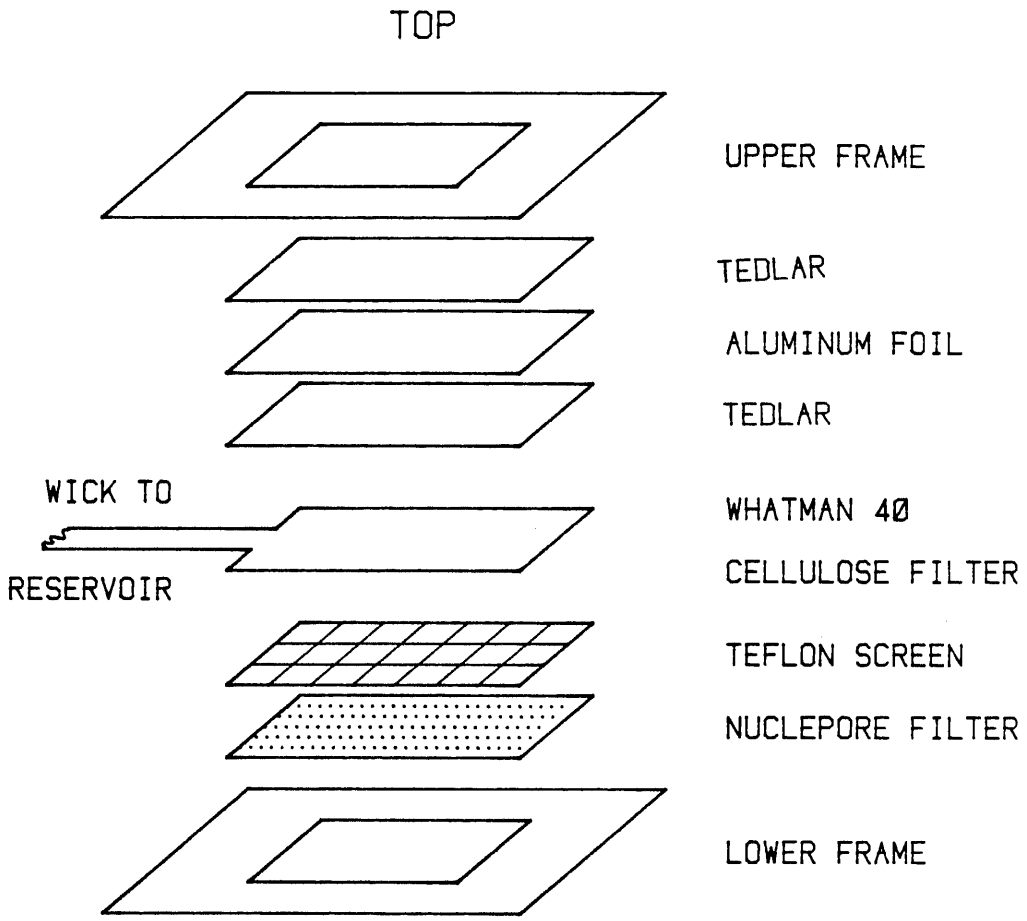

Figure 72. Construction of Nuclepore surrogate leaf.

PROPOSED
ACIDIC PARTICLE AND GAS SAMPLING SCHEME

1. Dichotomous Sampler with Modified Filter Holders

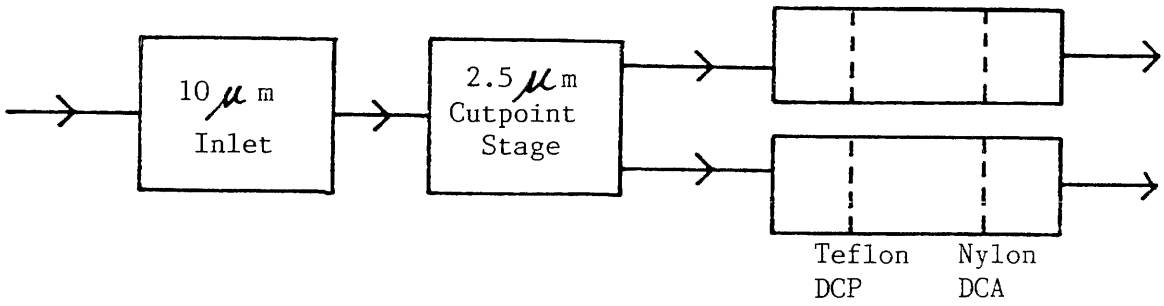

2. AIHL Cyclone Sampler

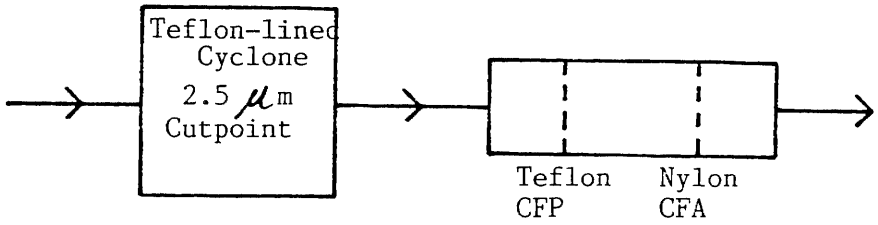

3. Bubbler

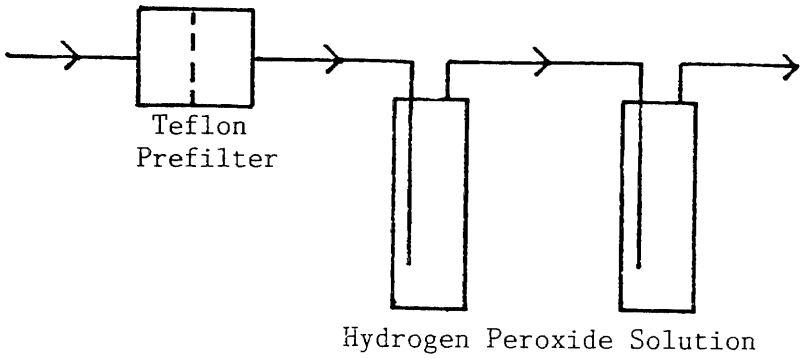

Species	Sample Analyzed Filter Code: (Sampler)(Fine/Coarse)(Pre/After Filter)
True Fine Particulate Nitrate	DFP + DFA
True Coarse Particulate Nitrate	DCP + DCA
Nitric Acid	(CFP + CFA) - (DFP + DFA)
Fine Particulate Sulfate	DFP or CFP
Particulate Strong Acid	DFP or CFP
Fine Particulate Ammonium	DFP or CFP (with volatility correction)
Sulfur Dioxide	Hydrogen Peroxide Solution

Figure 73. Preliminary sampler design for acidic particles and gases, based on present findings. Additional verification of the denuding action of the dichotomous sampler is necessary.